SYNTHESIS AND BIOLOGICAL EVALUATION OF DISPYRIN, SYNTHESIS AND DESIGN OF SELECTIVE M_4 MUSCARINIC MODULATORS, AND EXPLORATION OF THE TOTAL SYNTHESIS OF PIPERAZIMYCIN A

By

J. Phillip Kennedy

Dissertation

Submitted to the Faculty of the

Graduate School of Vanderbilt University

in partial fulfillment of the requirements

for the degree of

DOCTOR OF PHILOSOPHY

in

Chemistry

August, 2010

Nashville Tennessee

Approved:

Dr. Craig W. Lindsley

Dr. Gary A. Sulikowski

Dr. Lawrence J. Marnett

Dr. P. Jeffrey Conn

To my best

friend, Daniel

ACKNOWLEDMENTS

Throughout my undergraduate, professional, and graduate school career I have had the privilege to work with many great researchers from industry and academia. I would like to acknowledge my first mentor Dr. Grant Boldt, who patiently trained me during my undergraduate research and without whom I would not have learned many of the finer points of lab technique. Also included in my undergraduate training would be Dr. Doug Grotjahn who graciously accepted me into his lab even though I had no research experience.

I would also like to acknowledge Dr. Kim Janda of The Scripps Research Institute for the technician position that he provided between my undergraduate and graduate training. He gave me the opportunity to learn how a professional lab is run, and the opportunity to manage my own projects and experiments. During my time at TSRI I would like to thank Dr. Tobin Dickerson who helped me with any questions I had, and gave me productive input on all my projects.

The most important learning experience I have had to date has been during my graduate school training. I would like to thank every member of the Lindsley lab for input, advice and help. I am particularly grateful to have had such a wonderful research advisor, Dr. Craig Lindsley. His guidance and input allowed me to complete my graduate work and his humor and personality made the time at Vanderbilt enjoyable and fun.

I am very grateful to my committee members Dr. Gary Sulikowski, Dr. Larry Marnett, and Dr. Jeff Conn. I have learned greatly from them and I will strive to live up to their standards throughout my career. Their incredible intelligence and practical input gives me something to aspire too.

Finally, I would like to thank my parents for support throughout my graduate training. I would not have been able to survive graduate school without their help.

There have been many great researchers that I have had the privilege to work with, and I have learned from every person that I have encountered, the remainder of the acknowledgements go to these great people.

TABLE OF CONTENTS

Page

LIST OF TABLES

LIST OF FIGURES

LIST OF SCHEMES

LIST OF ABBREVIATIONS

^{o}C	Degrees celcius
ACH	Acetocholine
ACN	Acetonitrile
ADHD	Attention-Deficit Hyperactivity Disorder
Alloc	Allyl carbamate
AMDA	(*S*)-2-amino-8-methyl-4,6-nonadecadienoic acid
BBr_3	Boron tribromide
Boc	tert-Butyloxycarbonile
Boc_2O	Di-tert-butyldicarbonate
CBz	Carbobenzyloxy
CCl_4	Carbon tetrachloride
$CDCl_3$	Deuterated chloroform
CHO	Chinese hamster ovary
CNS	Central nervous system
CRC	Concentration response curve

Cs_2CO_3	Cesium carbonate
CYP_{450}	Cytochrome P450
DBAD	Di-tert-butyl azodicarboxylate
DCC	Dicyclohexylcarbodiimide
DCM	Dichloromethane
DIBAL-H	Diisobutylaluminum hydride
DIC	Diisopropylcarbodiimide
DIEA	*N*,*N* diisopropylethylamine
DIAD	Diisopropyl azodicarboxylate
DMF	*N*,*N* dimethylformamide
DMPK	Drug Metabolism/Pharmacokinetics
DMS	Dimethylsulfide
DMSO	Dimethyl sulfoxide
EC_{20}	Sub maximal effective concentration, 20% response
EC_{50}	Half maximal effective concentration
EtOAc	Ethyl acetate
EtOH	Ethanol

Et_2O	ethyl ether
GI_{50}	Half maximal growth inhibition
GPCR	G-protein coupled receptor
h	Hour
H_1	Histamine H_1 Receptor
H_2	Histamine H_2 Receptor
H_3	Histamine H_3 Receptor
H_4	Histamine H_4 Receptor
HAA	Hydroxyacetic acid
HATU	2-(7-Aza-1H-benzotriazole-1-yl)-1,1,3,3-tetramethyluronium hexafluorophosphate
HCl	Hydrogen chloride
hERG	Human ether-a-go-go related gene
HMPA	Hexamethylphosphoramide
HOAt	1-Hydroxy-7-azabenzotriazole
HOBt	Hydroxybenzotriazole
HPLC	High pressure liquid chromatography
HRMS	High resolution mass spectrometry

IC_{50}	Half maximal inhibitory concentration
Imid	Imidazole
K_2CO_3	Potassium carbonate
KHMDS	Potassium bis(trimethylsilyl)amide
KI	Potassium iodide
K_i	Dissociation constant
M	Molar
M_1	Muscarinic M_1 receptor
M_2	Muscarinic M_2 receptor
M_3	Muscarinic M_3 receptor
M_4	Muscarinic M_4 receptor
M_5	Muscarinic M_5 receptor
mAChR	Muscarinic acetocholine receptor
MAOS	Microwave-assisted organic synthesis
μM	Micromolar
MeOH	Methanol
$MgSO_4$	Magnesium sulfate

min	Minutes
mM	Millimolar
mw	Microwave
NAcc	Nucleus accumbens
NaOH	Sodium hydroxide
NCS	*N*-chlorosuccinimide
nM	Nanomolar
PAM	Positive allosteric modulator
PEG	Polyethylene glycol
P-gp	P-glycoprotein
Ph	Phenyl
PPh_3	Triphenylphosphine
rt	Room temperature
SAR	Structure-activity relationship
SAX	Strong anion exchange
SCX	Strong cation exchange
SEM	Standard error of the mean

TBAF	Tetra-*N*-butylammonium fluoride
TBDPS	tert-Butyldiphenylsilyl
TBS	tert-Butyldimethylsilyl
TCFH	*N*,*N*,*N*',*N*' tetramethylchloroformamidinium hexafluorophosphate
TEA	Triethylamine
Teoc	2-Trimethylsilylcarbamate
Tos	*p*-toluenesulfonyl
Troc	2,2,2-Trichloroethoxycarbonyl
TFA	Trifluoroacetic acid
TFFH	*N*,*N*,*N*',*N*' tetramethylfluoroformamidinium hexafluorophosphate
THF	Tetrahydrofuran
TLC	Thin layer chromatography
TMS	Trimethylsilyl
TsOH	*p*-toluenesulfonic acid
UV	ultraviolet light
VTA	Ventral tegmental area

CHAPTER I

SYNTHESIS AND BIOLOGICAL EVALUATION OF DISPYRIN

A large amount of the most common metabolites of marine sponges are bromopyrrole alkaloids (1). Sponges of the genus Agelas are found throughout the world's tropical reefs and have provided a wealth of bromopyrrole carboxamide containing alkaloids that can be derived biosynthetically from oroidin (2). Examples include the tetracyclic alkaloid (-)-dibromophakelin and the tetrasubstituted cyclobutane marine alkaloid (-)-sceptrin (3,4), **Figure 1**. In 2007, Crews and co-workers reported on the discovery of a new bromopyrrole alkaloid, dispyrin **1**, from the Carribean sponge Agelas dispar, **Figure 1** (5).

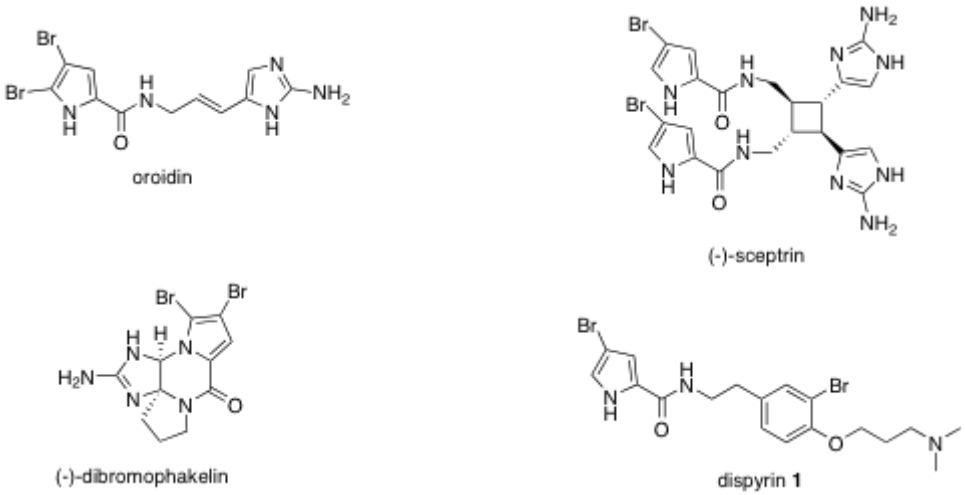

Figure 1. Examples of marine natural products from sponges *Agelas*.

Unlike many laboratories that rely on bio-fractionation, triaging natural product extracts or sponge/soil samples for antibacterial or anticancer activities, the Crews laboratory focused on discovering compounds with unique molecular architectures. Dispyrin is novel in that it contains a distinct bromopyrrole tyramine motif that has no precedent in marine natural products research. Crews also reported that unlike all bromopyrrole carboxamide alkaloids discovered from Agelas thus far, dispyrin has an independent biosynthetic pathway and is not biosynthetically derived from oroidin (5). Crews and co-workers did not ascribe any biological activity for dispyrin **1**, since our laboratory is interested in new biologically active compounds we initiated a program to synthesize dispyrin **1** and elucidate the molecular target(s) of this unique natural product with a bromopyrrole carboxamide alkaloid.

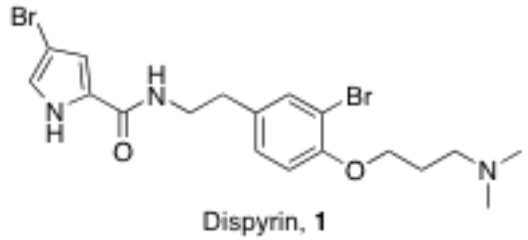

Dispyrin, **1**

Figure 2. Structure of the dispyrin **1**, a bromopyrrole alkaloid from *Agelas dispar*.

As outlined in **Scheme 1**, our retrosynthetic analysis of dispyrin **1** envisaged an amide coupling between 4-bromo-2-carboxypyrrole **2** and 3-bromo-

4-hydroxyphenethylamine **3**, followed by an alkylation or Mitsunobu reaction with *N,N*-dimethyl-3-chloropropyl amine or *N,N*-dimethyl-3-hydroxypropyl amine **4**, respectively. This expedited route should allow for the synthesis of gram quantities of dispyrin **1** to facilitate biological evaluation as well as an opportunity to readily prepare libraries of unnatural analogues (5).

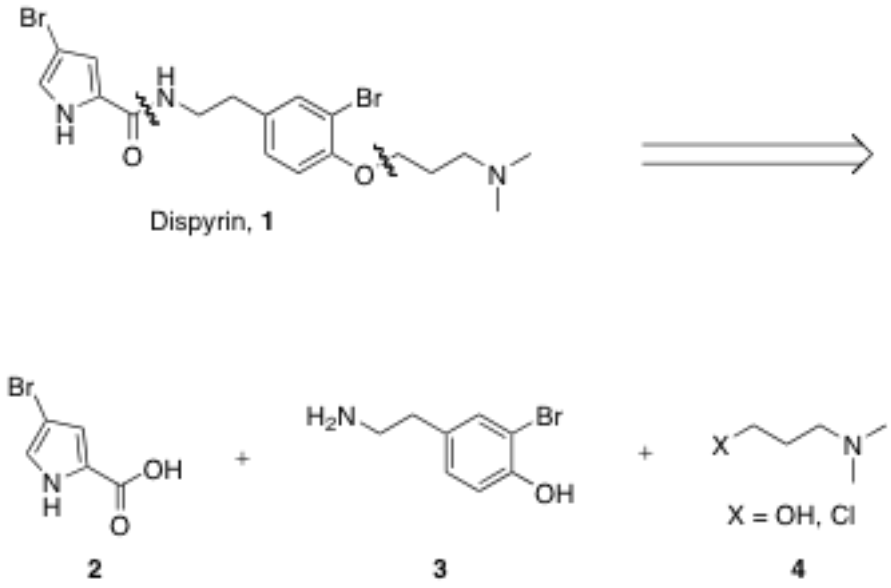

Scheme 1. Retrosynthetic analysis of dispyrin **1**.

As shown in **Scheme 2**, our synthesis began with commercially available acid **2**, which was coupled to 3-bromo-4-methoxyphenethylamine **5** to provide **6** in 93% yield. Subsequent deprotection of the methyl ether with BBr_3 afforded **7** in 92% yield. Multiple alkylation protocols were attempted, as well as Mitsunobu protocols, but all failed to deliver dispyrin **1** in reasonable yields. Ultimately,

phenol **7** was successfully alkylated with *N,N*-dimethyl-3-chloropropyl amine **4**, under a microwave-assisted protocol at 160°C for 20 minutes, to deliver dispyrin **1** in 80% isolated yield. Thus, the first total synthesis of dispyrin **1** was completed on a one-gram scale in three synthetic steps with an overall yield of 68.4% (7). In the original disclosure by Crews et al., spectroscopic data were reported for what was depicted as the free base of dispyrin **1**. The spectroscopic data (^{1}H, ^{13}C NMR and MS) we obtained for synthetic **1** were not in complete accordance with that reported for dispyrin **1** by Crews and co-workers (5).

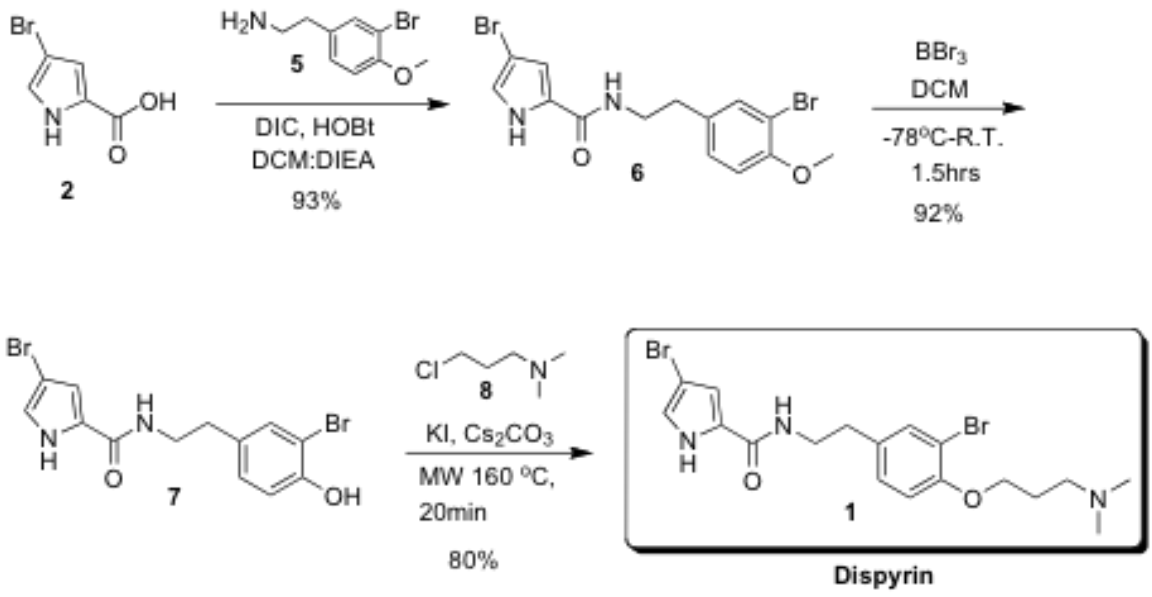

Scheme 2. Synthesis of dispyrin **1**.

We rationalized that the discrepancies observed could arise if the spectroscopic data reported for **1** were of the corresponding protonated salt form

of the distal dimethylamino moiety. To evaluate this possibility, we synthesized the corresponding HCl salt of our synthetic dispyrin **1**. As shown in **Scheme 3**, dispyrin **1** was dissolved in MeOH, and HCl gas was bubbled through the solution for 10 minutes. The reaction solution was concentrated and washed with dry Et_2O. The resulting white solid, the HCl salt of dispyrin **9**, provided spectroscopic data (^1H, ^{13}C NMR and MS) in complete accordance with that reported for dispyrin **1** by Crews and co-workers; thus, the original report of natural dispyrin **1** characterized a protonated salt form, such as **9**, and not the free-base **1** (5). The NMR spectroscopic comparison is summarized in **Table 1**.

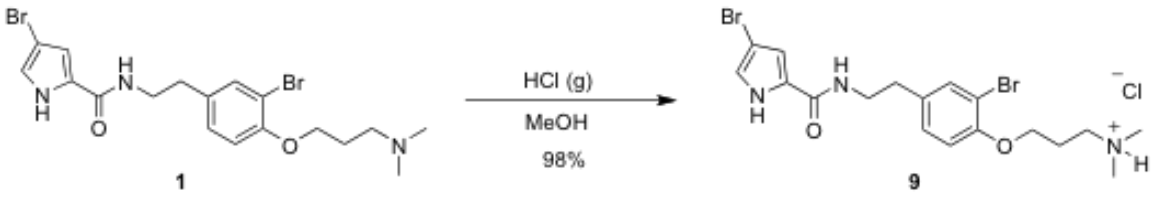

Scheme 3. Synthesis of the HCl salt of dispyrin **9**.

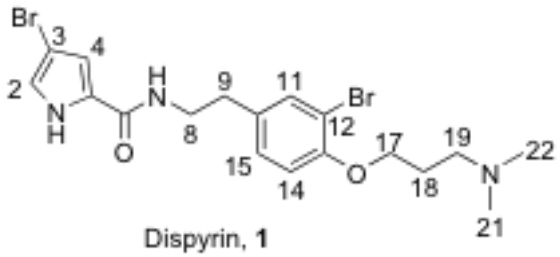

Dispyrin, **1**

	Dispyrin (Crews 500 MHz)		Dispyrin Freebase x HCl (400 MHz)	
position	δ_H (*J* in Hz)	δ_C	δ_H (*J* in Hz)	δ_C
2	6.86 d (2.0)	122.7	6.90 d (1.6)	122.8
3		96.2		97.5
4	6.68 d (2.0)	113.1	6.72 d (1.6)	113.3
5		127.6		127.6
6		163.5		162.6
8	3.46 t (7.5)	41.9	3.48 t (7.6)	42.0
9	2.77 t (7.5)	35.3	2.80 t (7.2)	35.6
10		135.3		135.3
11	7.44 d (2.0)	134.6	7.45 d (2.0)	134.6
12		113.1		112.9
13		155.0		154.7
14	6.96 d (8.0)	114.8	6.97 d (8.0)	114.8
15	7.16 dd (8.0, 2.0)	130.3	7.17 dd (8.0, 2.0)	130.4
17	4.14 t (5.5)	67.5	4.15 t (5.6)	67.5
18	2.24 m	25.6	2.25 m	25.7
19	3.35 t (7.0)	57.2	3.39 t (7.6)	57.2
21,20	2.93 s	43.8	2.96 s	43.8

Table 1. NMR comparison of Dispyrin reported by Crews et al. and synthetic Dispyrin x HCl, **9**.

With a large quantity of dispyrin **1** in hand, we embarked on the study to identify potential molecular target(s) for dispyrin **1**. With thousands of discrete molecular targets known, it was a challenge to develop a plan to evaluate dispyrin **1** against all potential biological targets; moreover, unlike traditional natural products research, we did not want to solely focus on antibacterial and

anticancer activity. After careful consideration, we pursued multiple screening avenues. In the pharmaceutical industry, medicinal chemists evaluate late stage preclinical candidates against large panels of discrete molecular targets in an attempt to identify ancillary pharmacology and potential problems. In a paradigm change, we took advantage of this approach, but employed the power of these large panels of G protein-coupled receptors (GPCRs), ion channels, transporters and kinases to potentially elucidate a molecular target(s) for dispyrin **1**. Utilizing panels of radioligand binding assays from several companies, dispyrin **1** was evaluated against >200 discrete molecular targets over the course of two months. The MDS Pharma Services panel identified multiple activities for dispyrin **1** (8). In the initial screen at a single 10 μM concentration, dispyrin **1**, was found to provide modest inhibition (50-60% at 10 μM) of calcium (L-type) and potassium (hERG) ion channels, but none with significant activity after full concentration-response-curves were obtained (no K_is or IC_{50}s <10 μM) (7,8).

Importantly, the MDS panel identified four G protein-coupled receptors (adrenergic α_{1D}, adrenergic α_{2A}, H_2 and H_3 receptors) against which **1** showed promising therapeutic potential (8-10). Amongst the adrenergic family of GPCRs, the α_{1D} and α_{2A} subtypes are well-documented targets for hypertension as they contribute to smooth muscle contraction and neural baroreflex control of blood pressure (11-12). A number of H2 receptor antagonists are on the market for the treatment of peptic ulcer disease, and the H_3 receptor is a well validated target for a number of CNS pathologies including depression, schizophrenia, ADHD, dementia and sleep disorders (13,14). As shown in **Table 2**, dispyrin **1** displayed

significant inhibition in a single point screen at 10 μM against these four GPCRs, which justified obtaining full dose-response curves. Dispyrin **1** showed nanomolar binding and inhibition of both the adrenergic $\alpha 1\Delta$ receptor (K_i = 275 nM, IC_{50} = 560 nM) and the α_{2A} receptor (K_i = 69 nM, IC_{50} = 180 nM), while affording low micromolar binding and inhibition of both the H_2 receptor (K_i = 1.02 □M, IC_{50} = 1.25 μM) and the □□ receptor (K_i= 1.04 μM, IC_{50} = 2.35 μM) (7,8). Thus, dispyrin **1** represents a new chemotype and a potential novel lead compound for these therapeutically important molecular targets, and a rare example of a marine natural product as a ligand for such GPCRs.

Target	% inhibition (10μM)	K_i (μM)	IC_{50} (μM)
Adren α_{1D}	91	0.275	0.560
Adren α_{2A}	97	0.069	0.185
H_2	91	1.02	1.25
H_3	91	1.04	2.35

Table 2. Biological evaluation of dispyrin **1**.

In order to evaluate functional activity, dispyrin **1** was also placed on the screening deck of the Vanderbilt Screening Center for GPCRs, Ion Channels and Transporters, a member of the Molecular Library Screening Center Network which employs cell-based functional assays (15). Thus far, dispyrin **1** has yet to

be identified as a hit, but it will remain on the Vanderbilt screening deck and will be evaluated in ~20 assays/year.

In summary thus far, we have completed the first total synthesis of dispyrin **1** on a 1 gram scale, demonstrated that the spectroscopic data reported for the natural product **1** were that of a protonated salt form, such as **9** and not the free base (as reported), and that dispyrin is a potent ligand for therapeutically important GPCRs (the adrenergic α_{1D}, adrenergic α_{2A}, H_2 and H_3 receptors).

Based on these data, we initiated a natural product guided synthesis effort, employing iterative parallel synthesis (18) for molecular editing, aimed at improving H_3 inhibition and binding; moreover, we wanted to validate the marine natural product dispyrin **1** as a viable lead molecule due to the novel scaffold providing intellectual property in extremely crowded chemical space.

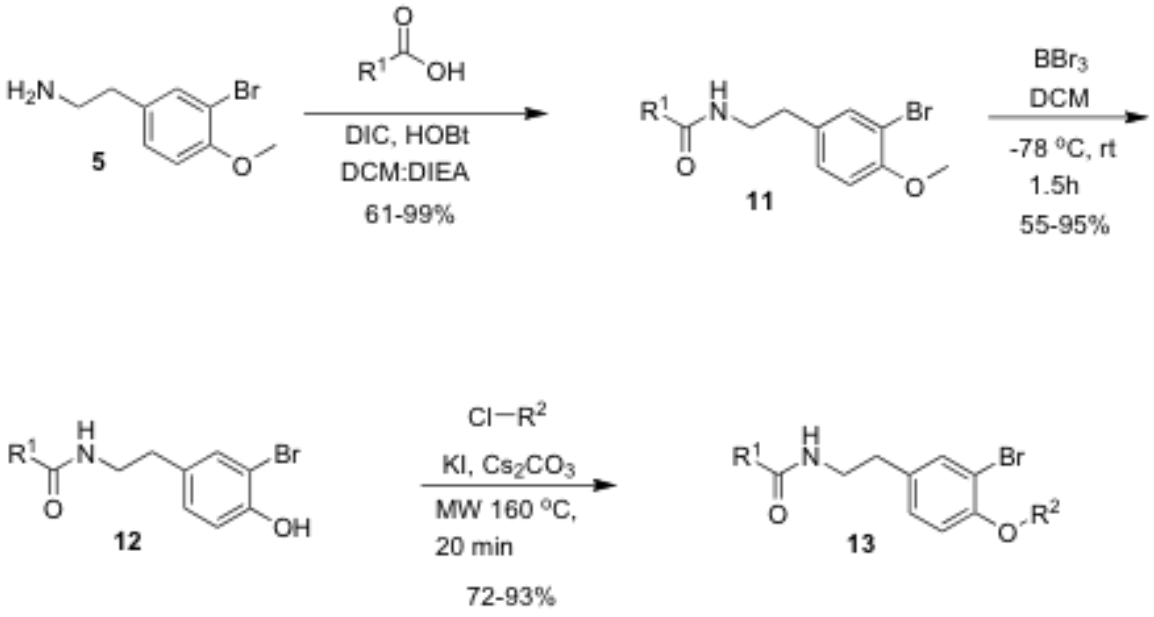

Scheme 4. First-Generation Library Synthesis.

The first generation 25-member library was based on a 5 x 5 two-dimensional matrix design wherein the core was held constant and the amide R^1 and aminoalkyl moieties R^2 varied, **Scheme 4**. The library synthesis began with a simple DIC amide coupling employing commercially available 3-bromo-4-methoxyphenylethylamine **5** with one of five heterocyclic carboxylic acids designated R^1. These five scaffolds were then treated with BBr_3 to remove the methyl ether generating the free phenols **12**. Each of the five phenols **12** was then alklyated with one of five aminoalkyl chlorides to install R^2 under microwave-assisted conditions to afford 25 unnatural dispyrin analogs **13** which were the purified to >98% by mass directed HPLC (18).

This first generation library was highly informative. In general, all R^1s and R^2s afforded modestly potent (K_is and IC_{50}s in the low micromolar range) H_3 antagonists. Potent H_3 antagonists (K_is < 200 nM, IC_{50}s < 430 nM) resulted for all of the heterocyclic amides R^1 in combination with the ethyl pyrrolidinyl R^2 (**13c**, **13h**, **13m**, **13r** and **13w**). In contrast, the ethyl morpholino congeners (**13d**, **13i**, **13n**, **13s** and **13x**) were uniformly weak (K_is > 12 μM, IC_{50}s > 29 μM). The most potent H_3 antagonist from the first generation library was **13r** (R^1 = 4-bromo-thiophene, R^2 = ethyl pyrrolidine) with a K_i of 80 nM and an IC_{50} of 180 nM – a 13-fold improvement over the parent natural product dispyrin **1** (IC_{50} = 2.35 μM, K_i = 1.04 μM). Based on these data, the next library maintained R^1 = 4-bromo-thiophene and surveyed functionalized pyrrolidines at R^2.

Compound	R^1	R^2	H_3 K_i (μM)	H_3 IC_{50} (μM)
13a	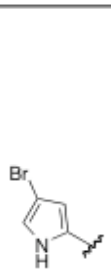		1.04	2.35
13b		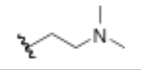	1.61	3.72
13c		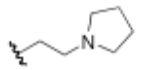	0.19	0.43
13d		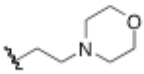	12.9	29.1
13e		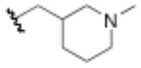	1.33	2.94
13f			1.36	2.92
13g		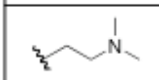	1.55	3.43
13h		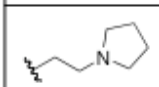	0.15	.38
13i		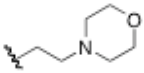	26.4	59.2
13j		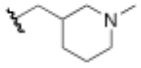	1.52	3.63

Compound	R^1	R^2	H_3 K_i (μM)	H_3 IC_{50} (μM)
13k	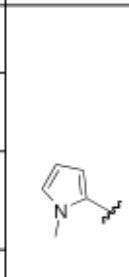		1.76	3.99
13l		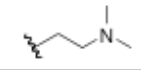	2.13	4.54
13m		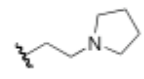	0.13	0.31
13n		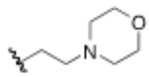	17.6	39.6
13o		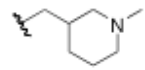	1.65	3.62
13p	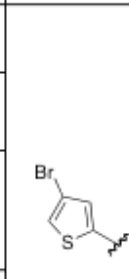		1.61	3.61
13q		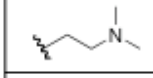	0.67	1.52
13r		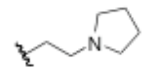	0.08	0.18
13s		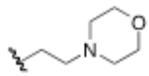	13.5	30.4
13t		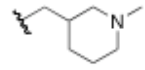	1.25	3.73
13u	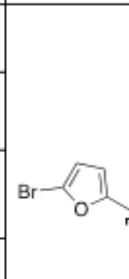		2.29	4.81
13v		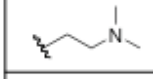	2.72	5.93
13w		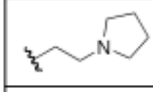	0.17	0.39
13x		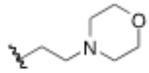	32.5	73.2
13y		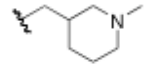	2.11	4.56

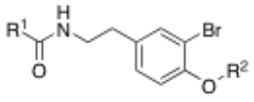

Table 3. Structures and activities of dispyrin analogs **13**.

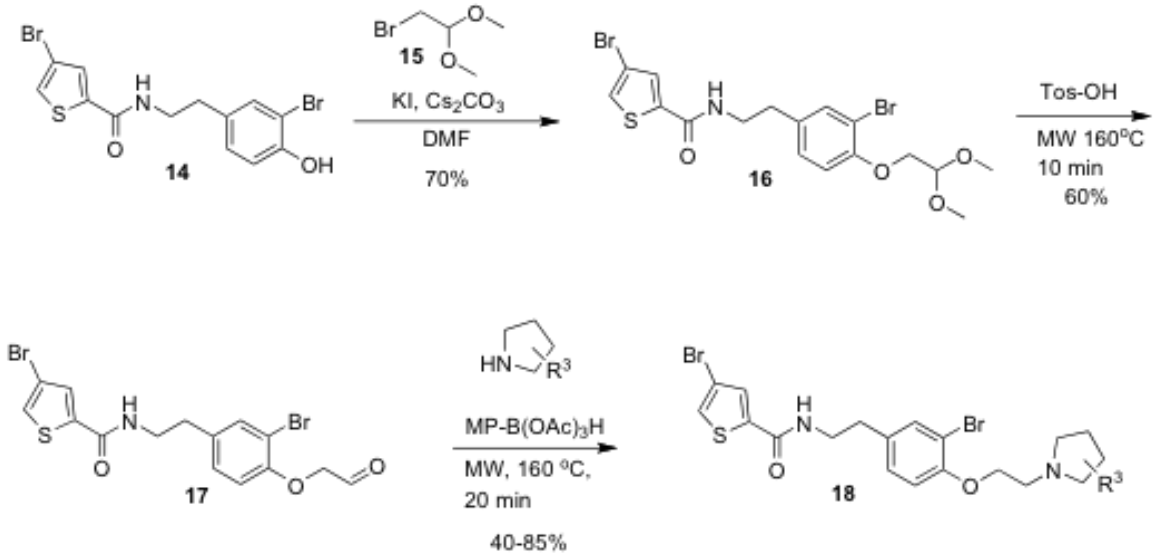

Scheme 5. Second Generation Library Synthesis.

Following **Scheme 4**, a large quantity of **14** was prepared. Then, the phenol was alkylated with 2-bromo-1,1-dimethoxy ethane **15** to provide **16**, which was then converted to the corresponding aldehyde **17** by treatment with tosylic acid via microwave irradiation. Finally, reductive amination employing a functionalized pyrrolidine and MP-B(OAc)$_3$H provided analogs **18**, which were purified to >98% by mass-directed preparative HPLC (18). As shown in **Table 4**, analogs **18** were weaker H_3 antagonists than **13r**, and there was no evidence of enantioselective inhibition (**18a** vs. **18b**). Incorporation of β-fluorine atoms such as in **18c** and **18d**, which lower the pKa on the pyrrolidine nitrogen from 11 to 9, afforded diminished H_3 inhibition (13).

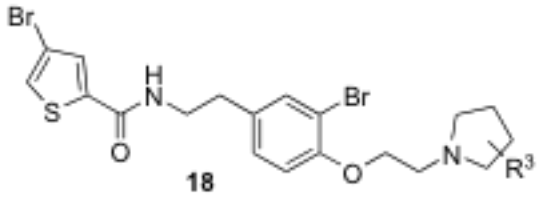

18

Compound	R^3	H_3 K_i (μM)	H_3 IC_{50} (μM)
18a	(*S*)-2-Me	0.31	0.71
18b	(*R*)-2-Me	0.33	0.75
18c	(*S*)-3-F	1.10	2.11
18d	(*R*)-3-F	1.15	2.52

Table 4. Structures and activities of dispyrin pyrrolidine analogs **18**.

We then prepared two singleton compounds following the synthetic route depicted in **Scheme 4** with the appropriate substitutions, wherein the bromine in **13r** was replaced with a chlorine **19** and a truncated version **20**, **Figure 2**. A 2-fold diminution in potency was noted for **19**, relative to **13r**, and the truncated benzyl version lost over 13-fold compared to **13r**; however, this highlighted that the heavy bromine atom was not required for H_3 inhibition.

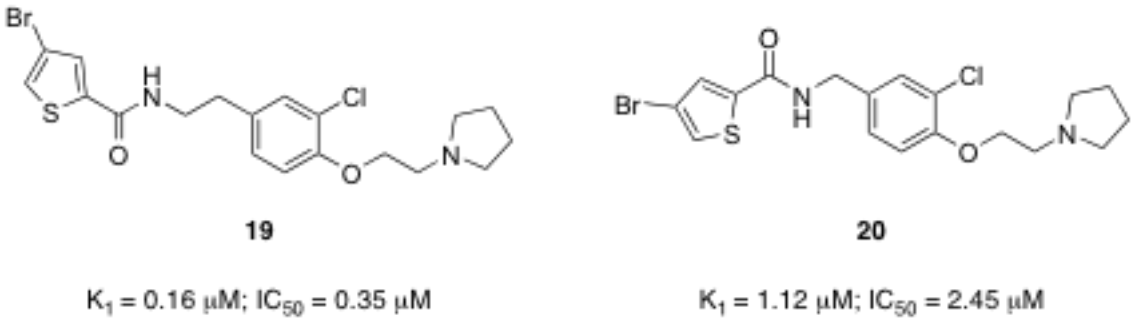

Figure 3. Chlorinated version and chlorinated truncated version of bromothiophene analogues, **14r**.

The final library iteration was directed at surveying a wider range of alternative amides (heterocycles and functionalized aromatic moieties) while holding the preferred ethyl pyrrolidine ether and bromotyramine core constant. The synthesis began with **5** and conversion to the phthalimide congener **21** using MAOS. Standard BBr_3 deprotection provided **22**, which was alkylated with chloroethyl pyrrolidine **23** to deliver **24**. Hydrolysis of the phthalimide with hydrazine afforded **25**, followed by amide coupling with a diverse collection of aryl and heteroaryl carboxylic acids generated library **26** shown in **Scheme 6**, these library members were purified to >98% purity by mass-directed preparative HPLC (18).

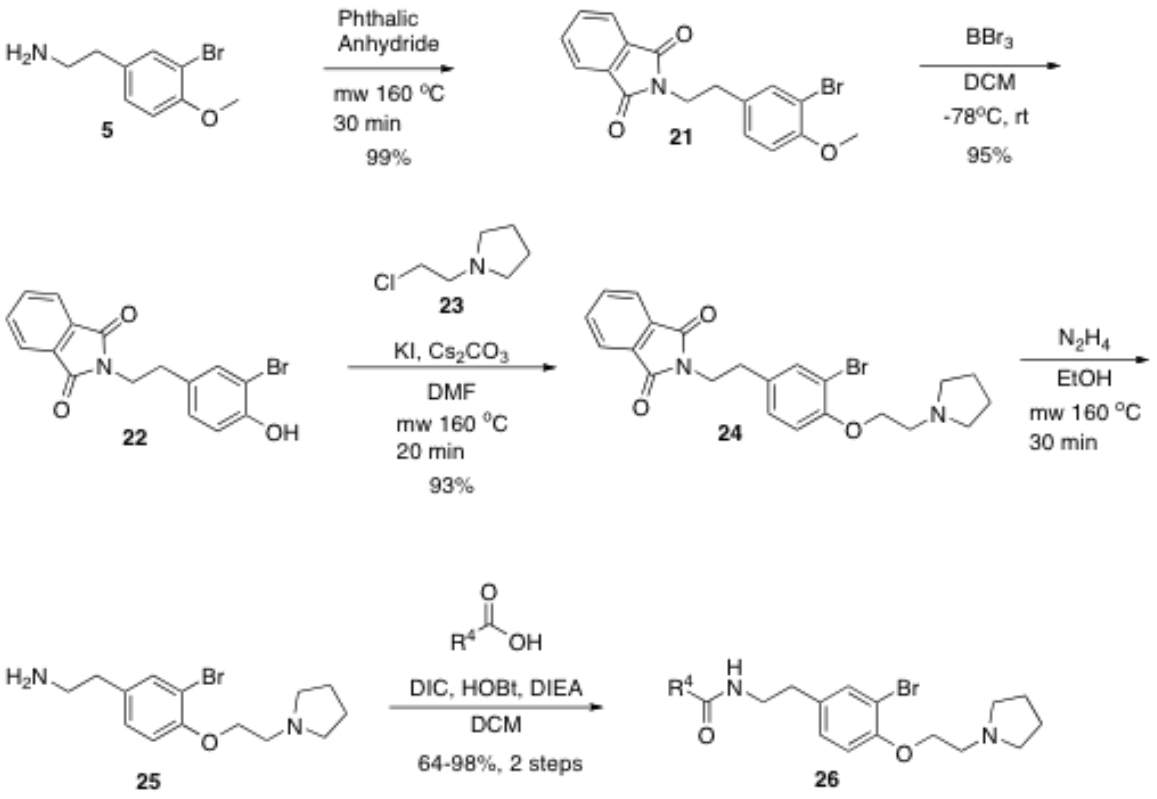

Scheme 6. Third-generation library synthesis.

This third generation library was uniformly active, providing H_3 antagonists in the sub-micromolar range, **Table 5**. Six-member heterocycles, such as pyridine **26a**, were active, as were aryl amides with halogens (Cl and Br) or trifluoromethyl groups in the 3-position (**26f**-**26h**). Five-member heterocycles (**26b**-**26e**) proved optimal, with a 5-oxazole **26b** (K_i = 32 nM, IC_{50} = 83 nM) and 2-thiazole **26d** (K_i = 32 nM, IC_{50} = 72 nM) affording the most potent H_3 antagonists of the unnatural dispyrin analogs. For example, **26d** improved the H_3 K_i and IC_{50} ~33-fold over the natural product dispyrin, and required only three

iterations of molecular editing and 40 analogs. Moreover, as dispyrin **1** represented a novel chemotype, we were able to obtain composition of matter patents for the dispyrin analogs as H_3 antagonists within an incredibly crowded intellectual property landscape (20). This effort highlights the value of employing natural products as leads for therapeutically relevant targets.

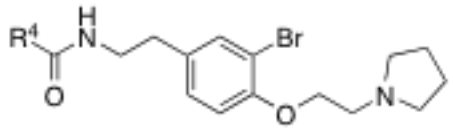

26

Compound	R^4	H_3 K_i (μM)	H_3 IC_{50} (μM)
26a	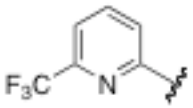	0.27	0.56
26b	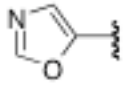	0.03	0.08
26c	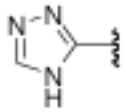	0.43	0.97
26d	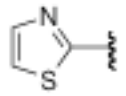	0.03	0.07
26e	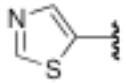	0.12	0.26
26f	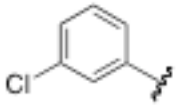	0.25	0.55
26g	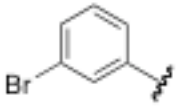	0.21	0.45
26h	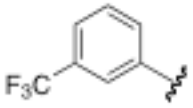	0.41	0.98

Table 5. Structures and activities of third-generation dispyrin acid analogs **26**.

During the course of the total synthesis of dispyrin we have completed the first total synthesis of dispyrin **1** on a 1 g scale and demonstrated that the

spectroscopic data reported for the natural product **1** were that of a protonated salt form, such as **2**, and not the free base (as reported), and that dispyrin is a potent ligand for therapeutically important GPCRs (the adrenergic α_{1D}, adrenergic α_{2A}, H_2, and H_3 receptors) **Figure 4**.

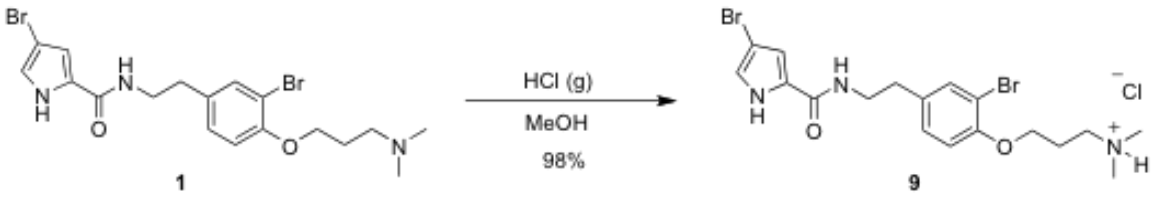

Figure 4. Structure of dispyrin **1** and the protonated form **9**.

We employed a natural product guided synthesis effort in molecular editing, employing itertative parallel synthesis, quickly optimized the weak H_3 antagonsim of the marine natural product dispyrin **1** over 30-fold to afford unnatural analogs **26d** and **26e** with low nanomolar potency and binding, **Figure 5**.

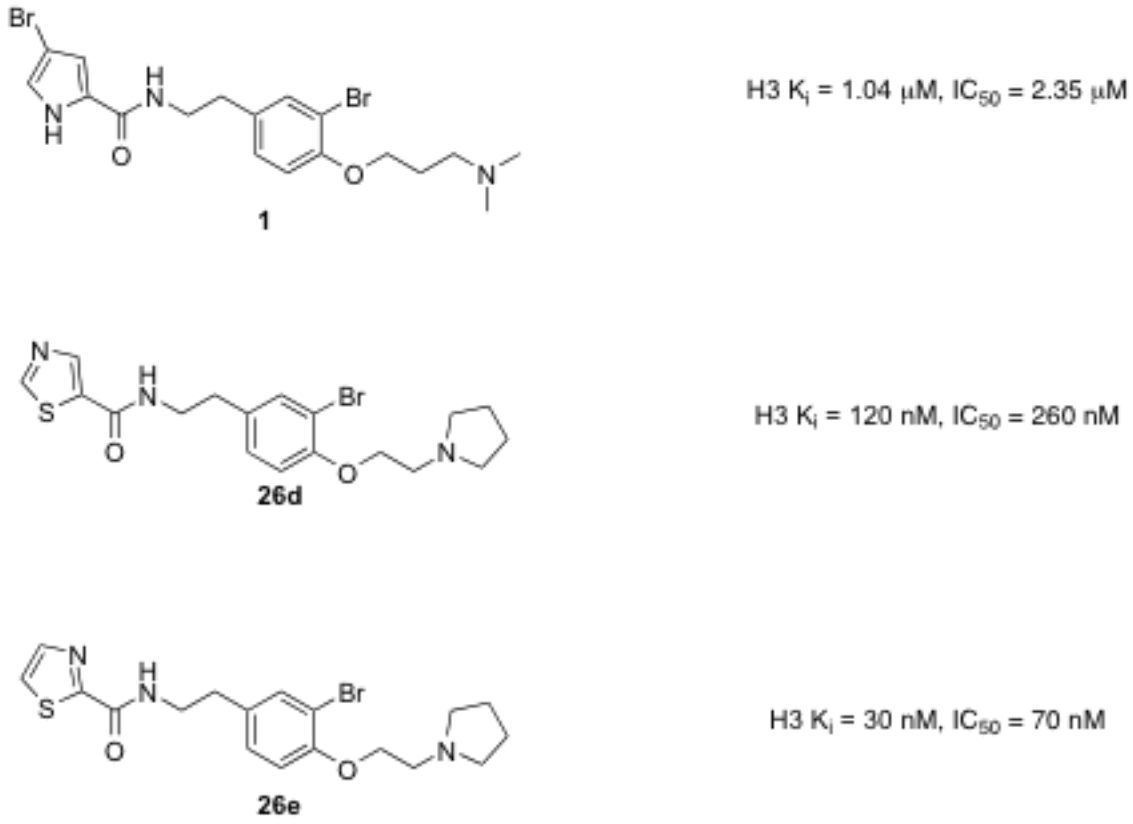

Figure 5. Summary of structures and binding potencies of dispyrin **1** and the two best library compounds **26d** and **26e.**

By employing a novel natural product scaffold for lead optimization, we were able to establish an intellectual property position in an incredibly crowded intellectual property landscape. Although the role of natural products drug discovery efforts within the pharmaceutical industry is being significantly reduced, despite overwhelming success, the biological activity of dispyrin and its analogs argue further that natural products are viable drug leads and have the potential to offer patenting advantages.

Experimental Procedures for the Synthesis of Dispyrin-

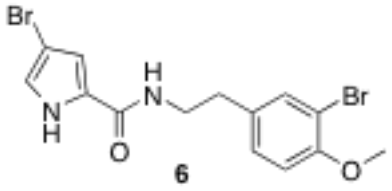

6

4-bromo-*N*-(3-bromo-4-methoxyphenethyl)-1*H*-pyrrole-2-carboxamide 6:

To a stirred solution of acid **2** (1.00 g, 5.3 mmol), HOBt (1.50 g, 11.0 mmol), and amine **5** (1.21 g, 5.3 mmol) in 9:1 CH_2Cl_2:DIEA at 25 ^oC was added DIC (1.33 g, 10.6 mmol) and the mixture was stirred overnight. After quenching with 250 mL water, the reaction was added to a 500 mL separatory funnel and extracted 3 x 200 mL CH_2Cl_2. The organic layers were combined, and washed with 500 mL saturated aqueous brine solution. The organic layer was dried over $MgSO_4$, and concentrated *in vacuo* to yield the crude coupled product. The crude material was then subjected to flash chromatography (EtOAc:Hexanes 1:1) to give pure **6** as a white solid (1.98 g, 4.9 mmol, 93 % yield). ^1H NMR (400 MHz, DMSO-d_6) δ 8.13 (t, *J* = 5.6 Hz, 1H), 7.43 (d, *J* = 2.0 Hz, 1H), 7.17 (dd, *J* = 1.6, 8.4 Hz, 1H), 7.00 (d, *J* = 8.4 Hz, 1H), 6.96 (m, 1H), 6.82 (s, 1H), 3.80 (s, 3H), 3.40 (q, *J* = 6.8 Hz, 2H), 2.74 (t, *J* = 7.2 Hz, 2H). ^{13}C NMR (100 MHz, DMSO-d_6) δ 159.5, 153.7, 133.3, 132.9, 129.1, 126.9, 121.1, 112.5, 111.3, 110.4, 94.9, 56.1, 40.1, 33.8. HRMS (Q-TOF): *m/z* calc for $C_{14}H_{14}Br_2N_2O_2$ [M + H]: 400.9500; found 400.9517.

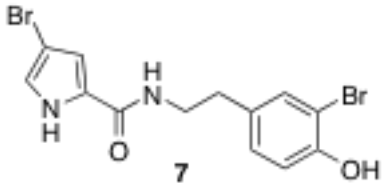

7

4-bromo-*N*-(3-bromo-4-hydroxyphenethyl)-1*H*-pyrrole-2-carboxamide 7:

To a stirred solution of coupled material **6** (1.00 g, 2.5 mmol) in anhydrous CH_2Cl_2 under argon at -78 ^oC was added BBr_3 (10 mL, 10 mmol, 1.0 M solution in CH_2Cl_2) over 20 minutes. The solution was stirred at -78 ^oC for 30 minutes and then allowed to warm to 25 ^oC for 1.5 hours. The reaction was slowly quenched with saturated aqueous $NaHCO_3$ until slightly basic by pH paper. This solution was added to a 1 L separatory funnel containing 500 mL water and extracted with 3 x 300 mL CH_2Cl_2. The combined organic layers were washed with 500 mL saturated aqueous brine solution. The organic layer was dried over $MgSO_4$, and concentrated *in vacuo* to yield the deprotected product **7** (0.89 g, 2.3 mmol, 92 % yield). This material was used without further purification. ^1H NMR (400 MHz, DMSO-d_6) δ 9.98 (br s, 1H) 8.11 (t, *J* = 5.2 Hz, 1H), 7.33 (d, *J* = 1.6 Hz, 1H), 7.02 (dd, *J* = 2.0, 8.4 Hz, 1H), 6.95 (m, 1H), 6.85 (d, *J* = 8.0 Hz, 1H), 6.80 (d, *J* = 2.0 Hz, 1H), 3.37 (m, 2H), 2.68 (t, *J* = 6.8 Hz, 2H). ^{13}C NMR (100 MHz, DMSO-d_6) δ 159.5, 152.3, 132.7, 131.6, 128.9, 126.9, 121.0, 116.2, 111.3, 109.0, 94.9, 40.2, 33.9. HRMS (Q-TOF): *m/z* calc for $C_{13}H_{12}Br_2N_2O_2$ [M + H]: 386.9344; found 386.9359.

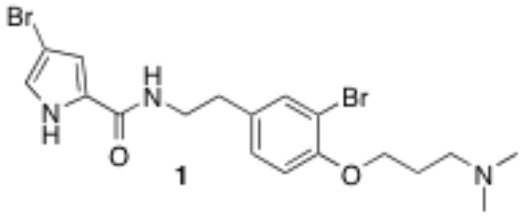

1

(4-bromo-*N*-(3-bromo-4-(3-(dimethylamino)propoxy)phenethyl)-1*H*-pyrrole-2-carboxamide), Dispyrin 1:

In a 5 mL microwave vial containing **7** (100 mg, 0.26 mmol), amine 16 (49 mg, 0.31 mmol), KI (129 mg, 0.78 mmol), and Cs_2CO_3 (254 mg, 0.78 mmol) was added anhydrous DMF, 4 mL. This was heated under microwave conditions at 160 ^oC for 20 minutes. The reaction was filtered, concentrated *in vacuo* and purified via mass directed HPLC to obtain pure dispyrin as the TFA salt. This material was dissolved in a minimal amount of MeOH, and added to a 12 mL SCX solid phase extractor column, which was washed with 2 column volumes MeOH. The material was removed from the column by eluting with 2 column volumes 2 M NH_3 in MeOH. This was again concentrated *in vacuo* to obtain pure dispyrin **1** as the free base (98 mg, 0.21 mmol, 80 % yield). ^1H NMR (400 MHz, MeOH-d_4) δ 7.42 (d, *J* = 2.0 Hz, 1H), 7.14 (dd, *J* = 2.0, 8.4 Hz, 1H), 6.93 (d, *J* = 8.4 Hz, 1H), 6.89 (d, *J* = 1.2 Hz, 1H), 6.70 (d, *J* = 1.6 Hz, 1H), 5.48 (s, 1H), 4.05 (t, *J* = 6.0 Hz, 2H), 3.47 (t, *J* = 7.6 Hz, 2H), 2.78 (t, *J* = 7.2 Hz, 2H), 2.61 (t, *J* = 7.6 Hz, 2H), 2.30 (s, 6H), 1.99 (m, 2H). ^{13}C NMR (100 MHz, MeOH-d_4) δ 162.5, 155.2, 134.5, 130.1, 127.6, 122.7, 114.6, 113.1, 112.9, 97.4, 68.2, 57.4, 49.0, 45.4, 42.0, 35.6, 28.0. HRMS (Q-TOF): *m/z* calc for $C_{18}H_{23}Br_2N_3O_2$ [M + H]: 472.0235; found 472.0243.

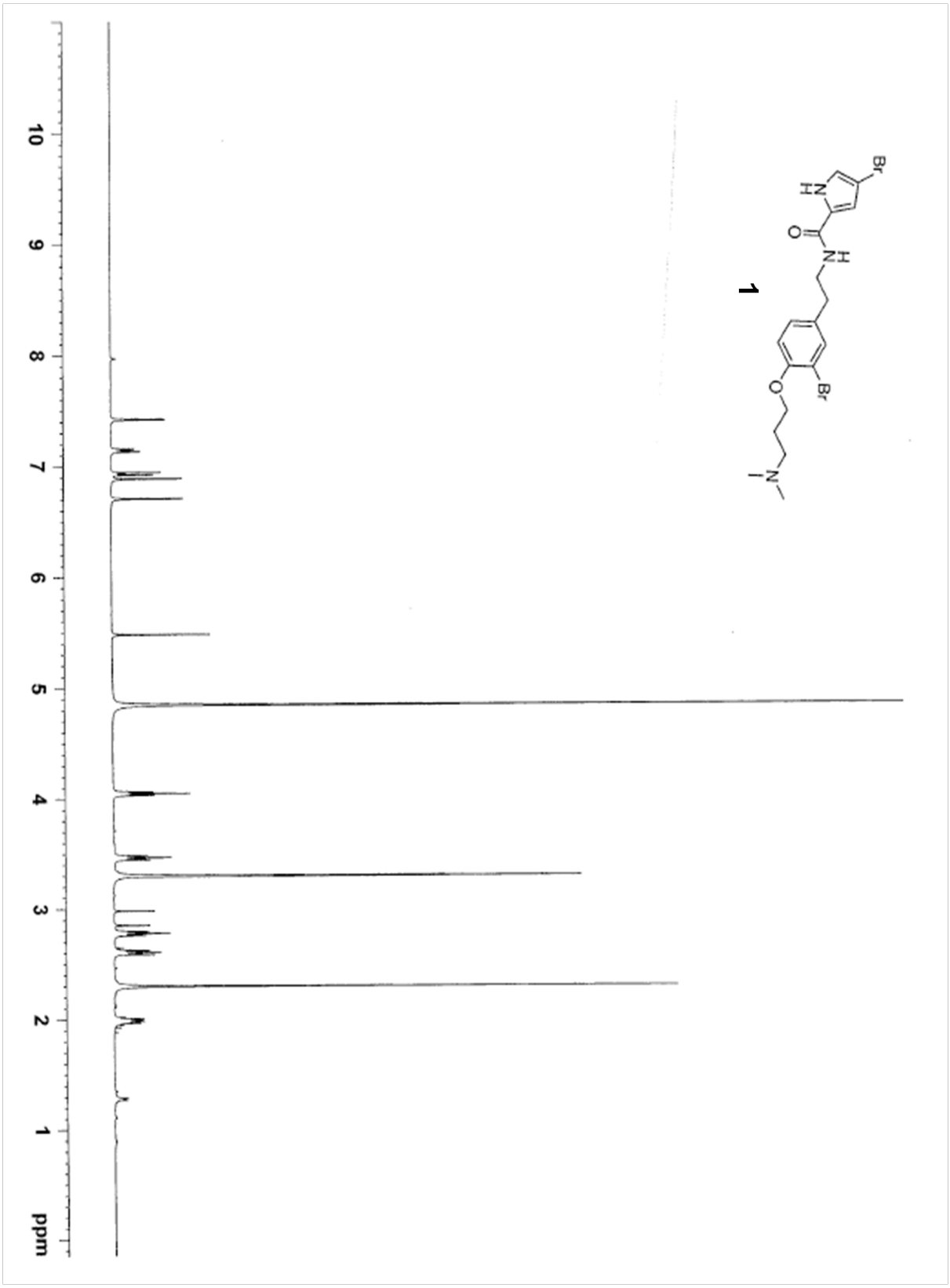
1
Br
Br
10
9
8
7
6
5
4
3
2
1
ppm

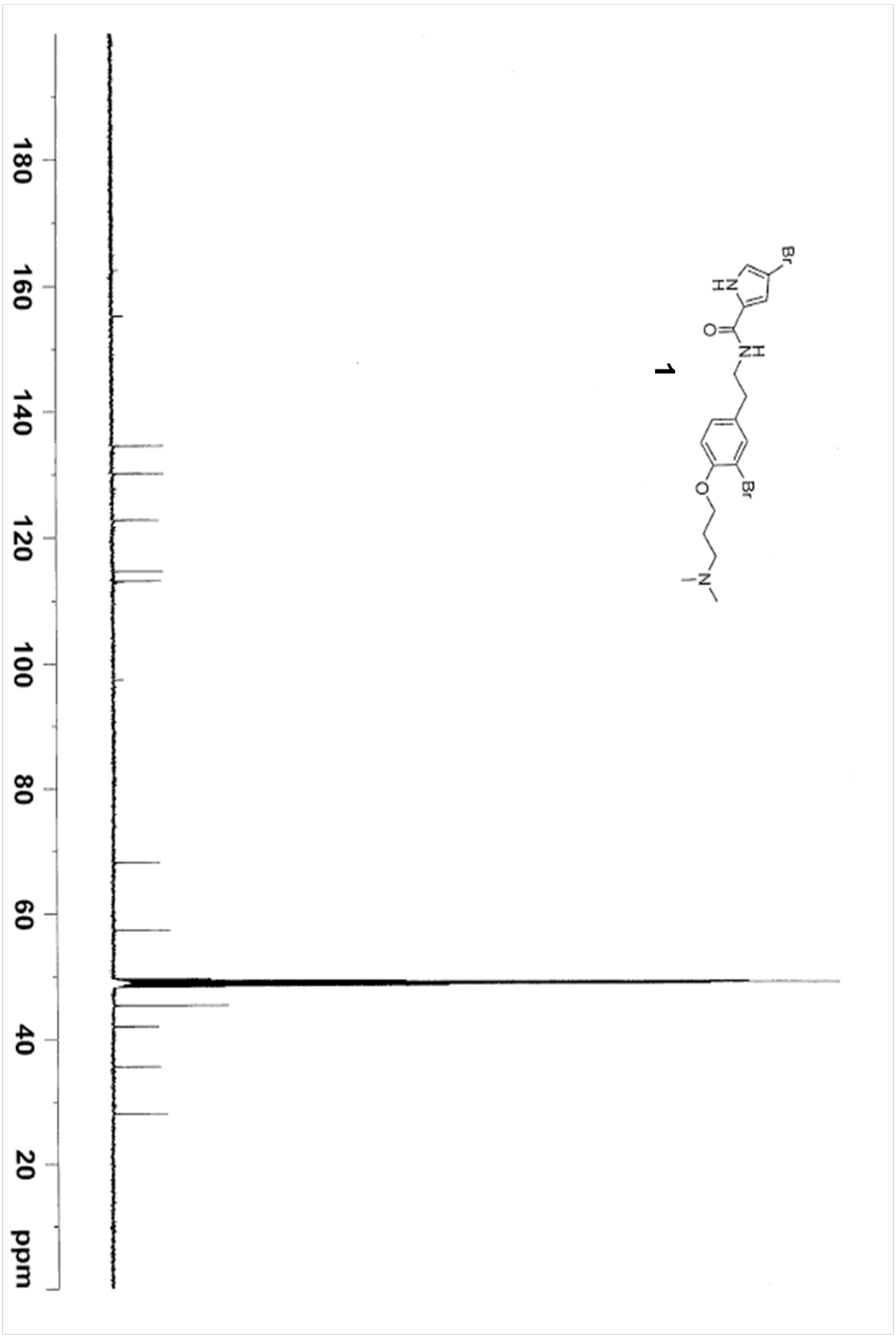
180
160
140
120
100
80
60
40
20
ppm
1
Br
H
N
O
H
N
Br
O
N

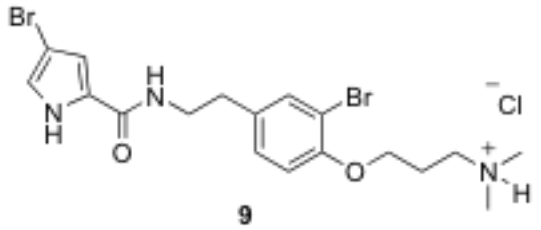

9

(4-bromo-*N*-(3-bromo-4-(3-(dimethylamino)propoxy)phenethyl)-1*H*-pyrrole-2-carboxamide) Hydrochloride, 9:

Dispyrin (**1**) (400 mg, 845 mmol) was dissolved in MeOH (20 mL). HCl gas was bubbled slowly through the solution for 10 min. The solvent was removed *in situ* and washed with anhydrous ether (3 x 20 mL) too afford Dispyrin HCl as a white solid (420 mg, 98 %). ^{1}H-nmr (400 MHz, MeOH-d_4) ™ 7.45 (d, *J* = 2.0 Hz, 1H), 7.17 (dd, *J* = 2.0, 8.0 Hz, 1H), 6.97 (d, *J* = 8.0 Hz, 1H), 6.90 (d, *J* = 1.6 Hz, 1H), 6.72 (d, *J* = 1.6 Hz, 1H), 4.15 (t, *J* = 5.6 Hz, 2H), 3.48 (t, *J* = 7.6 Hz, 2H), 3.39 (t, *J* = 7.6 Hz, 2H), 2.96 (s, 6H), 2.80 (t, *J* = 7.2 Hz, 2H), 2.25 (m, 2H). ^{13}C-nmr (100 MHz, MeOH-d_4) ™ 162.6, 154.7, 135.3, 134.6, 130.4, 127.6, 122.8, 114.8, 113.3, 112.9, 97.5, 67.5, 57.2, 43.8, 42.0, 35.6, 25.7. HRMS (Q-TOF): *m/z* calc for $C_{18}H_{24}Br_2N_3O_2$ [M + H^+]: 472.0234; found 472.0235.

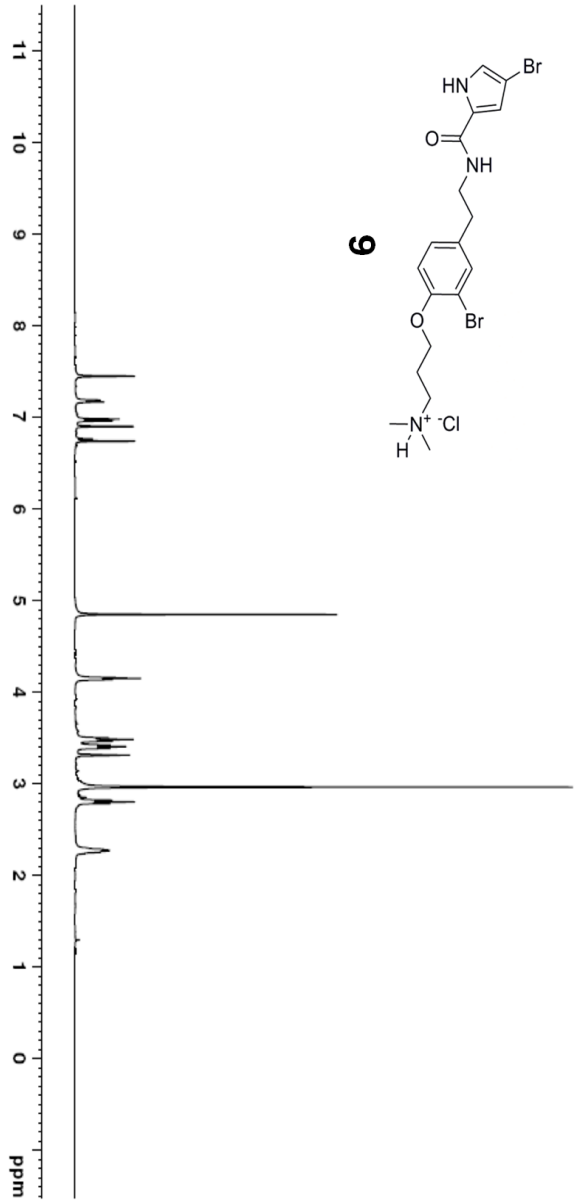
11
10
9
8
7
6
5
4
3
2
1
0
ppm
6
HN
Br
O
NH
O
Br
N+
H
Cl-

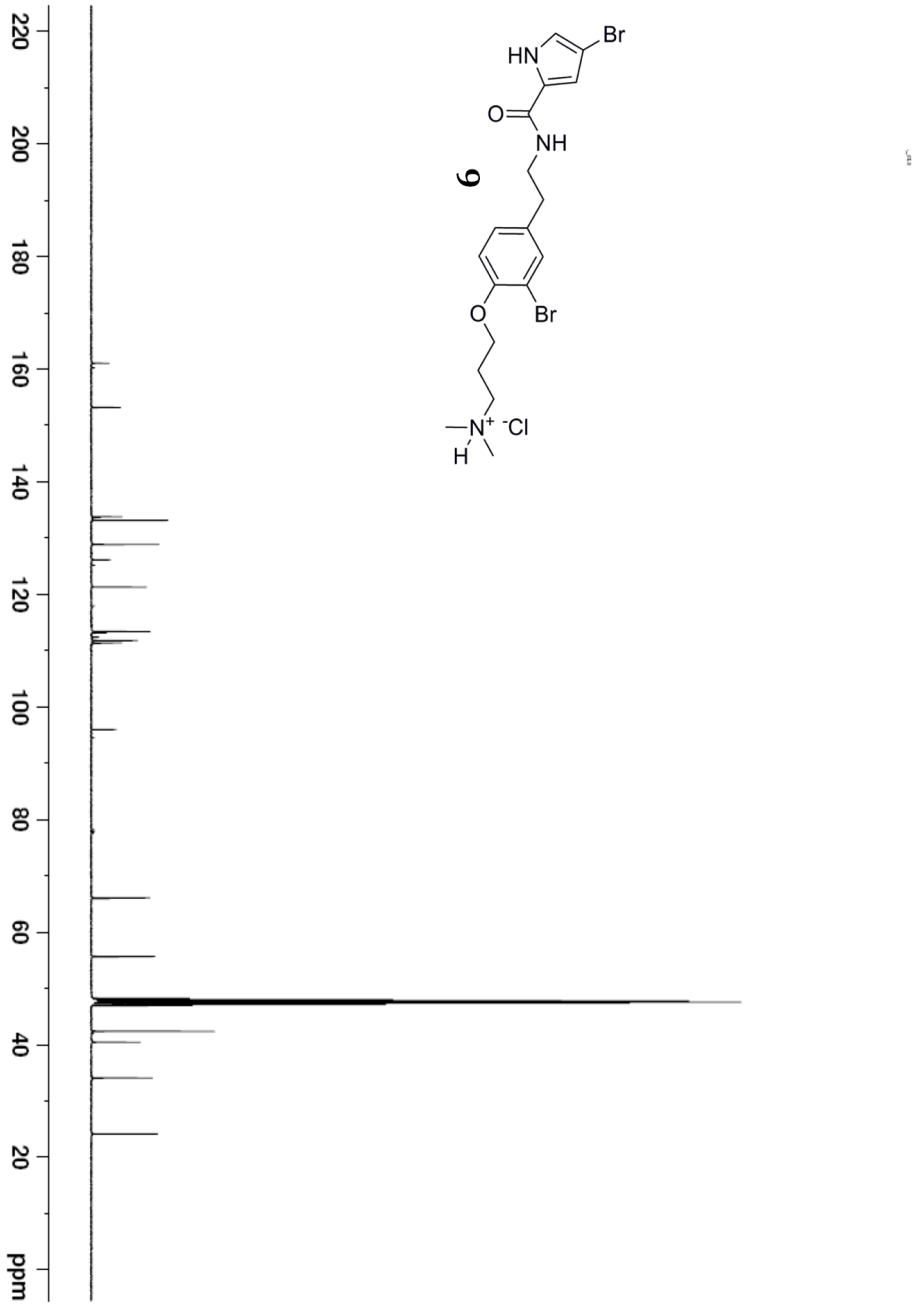
220
200
180
160
140
120
100
80
60
40
20
ppm
HN
Br
O
NH
O
Br
N+
H
Cl
9

General Synthetic Scheme 1.

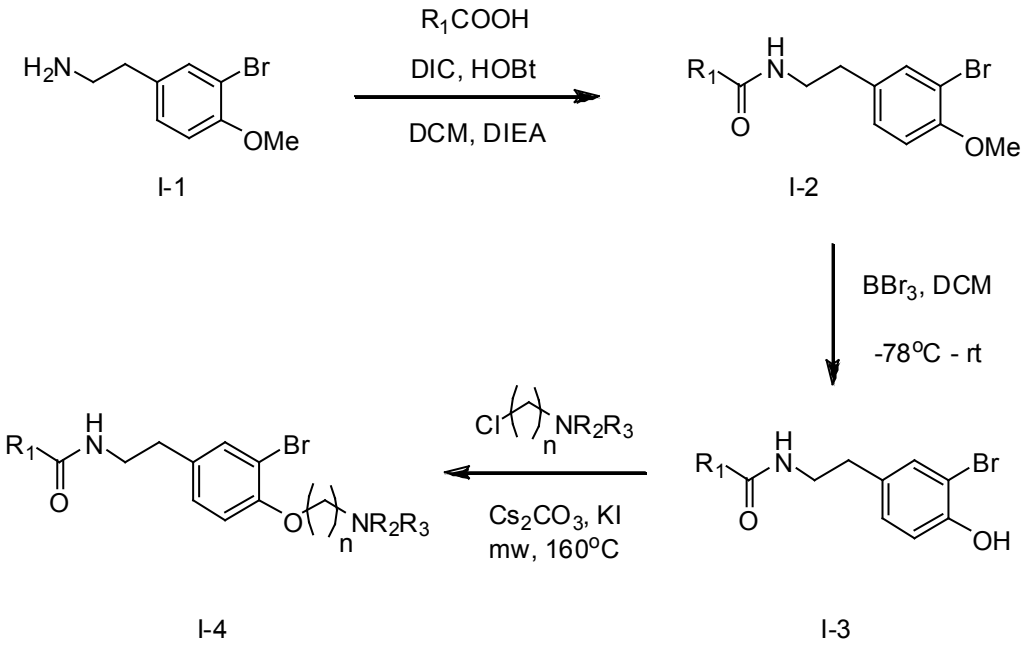

General Coupling Procedure for Library Synthesis:

To a stirred solution of acid R_1COOH (1 equivalent), HOBt (2.1 equivalents), and amine **I-1** (1 equivalent) in 9:1 CH_2Cl_2:DIEA at 25 ^oC was added DIC (2 equivalents) and the mixture was stirred overnight. After quenching with water, the reaction was added to a separatory funnel and washed 3x with CH_2Cl_2. The organic layers were combined, and washed with saturated aqueous brine solution. The organic layer was dried over $MgSO_4$, and concentrated *in vacuo* to yield **I-2**. The crude material was then subjected to flash chromatography to give pure **I-2** as a white solid (79-93 % yield).

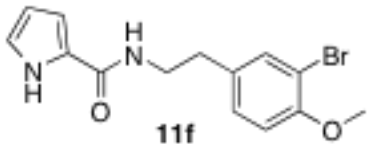

11f

***N*-(3-bromo-4-methoxyphenethyl)-1*H*-pyrrole-2-carboxamide 11f**:

^{1}H NMR (400 MHz, DMSO-d_6) δ 9.31 (br s, 1H), 7.42 (d, *J* = 2.0, 1H), 7.12 (dd, *J* = 2.0, 8.4 Hz, 1H), 6.92 (m, 1H), 6.84 (d, *J* = 8.4 Hz, 1H), 6.44 (s, 1H), 6.22 (m, 1H), 5.85 (m, 1H), 3.89 (s, 3H), 3.63 (q, *J* = 6.8 Hz, 2H), 2.82 (t, *J* = 7.2 Hz, 2H). ^{13}C NMR (100 MHz, DMSO-d_6) δ 161.4, 154.5, 133.4, 231.4, 128.7, 125.7, 121.8, 112.0, 111.6, 109.0, 77.3, 76.9, 76.7, 56.2, 40.5, 34.7. HRMS (Q-TOF): *m/z* calc for $C_{14}H_{15}BrN_2O_2$ [M + H]: 323.0395; found 323.0408. 84.7 % yield.

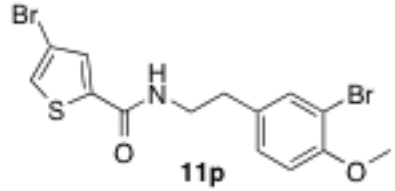

11p

4-bromo-*N*-(3-bromo-4-methoxyphenethyl)thiophene-2-carboxamide 11p:

^{1}H NMR (400 MHz, DMSO-d_6) δ 7.41 (d, *J* = 2.0 Hz, 1H), 7.37 (s, 1H), 7.27 (s, 1H), 7.12 (dd, *J* = 2.0, 8.4 Hz, 1H), 6.86 (d, *J* = 8.0 Hz, 1H), 5.93 (m, 1H), 3.89 (s, 3H), 3.63 (q, *J* = 6.8 Hz, 2H), 2.84 (t, *J* = 7.2 Hz, 2H), 2.17 (s, 1H). ^{13}C NMR (100 MHz, DMSO-d_6) δ 159.8, 153.8, 141.1, 133.0, 132.9, 129.7, 129.1, 128.5,

112.5, 110.3, 108.6, 56.1, 40.7, 33.5. HRMS (Q-TOF): *m/z* calc for $C_{14}H_{13}Br_2NO_2S$ [M + H]: 417.9112; found 417.9120. 79 % yield.

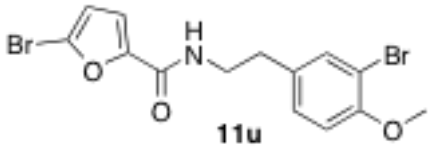

11u

5-bromo-*N*-(3-bromo-4-methoxyphenethyl)furan-2-carboxamide 11u:

^{1}H NMR (400 MHz, DMSO-d_6) δ 7.42 (d, *J* = 2.0 Hz, 1H), 7.13 (dd, *J* = 2.0, 8.0 Hz, 1H), 7.06 (d, *J* = 3.6 Hz, 1H), 6.85 (d, *J* = 8.4 Hz, 1H), 6.43 (d, *J* = 3.2 Hz, 1H), 6.32 (br s, 1H), 3.88 (s, 3H), 3.62 (m, 2H), 2.83 (t, *J* = 7.2 Hz, 2H). ^{13}C NMR (100 MHz, DMSO-d_6) δ 156.6, 153.8, 149.7, 133.0, 132.9, 129.1, 124.2, 115.6, 113.9, 112.5, 110.3, 56.1, 40.0, 33.6. HRMS (Q-TOF): *m/z* calc for $C_{14}H_{13}Br_2NO_3$ [M + H]: 401.9340; found 401.9350. 91 % yield.

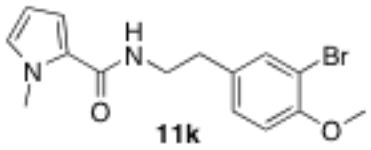

11k

***N*-(3-bromo-4-methoxyphenethyl)-1-methyl-1*H*-pyrrole-2-carboxamide 11k**:

^{1}H NMR(400 MHz, DMSO-d_6) δ 8.01 (t, *J* = 5.2 Hz, 1H), 7.43 (d, *J* = 1.2 Hz, 1H), 7.18 (d, *J* = 6.8 Hz, 1H), 7.01 (d, *J* = 8.4 Hz, 1H), 6.86 (s, 1H), 6.70 (d, *J* = 2.0 Hz, 1H), 5.98 (t, *J* = 3.2 Hz, 1H), 3.81 (d, *J* = 3.2 Hz, 6H), 3.36 (m, 2H). ^{13}C NMR (100 MHz, DMSO-d_6) δ 161.3, 153.7, 133.45, 132.9, 129.1, 127.5, 125.7, 112.5,

112.5, 111.9, 110.3, 106.5, 56.1, 40.0, 36.0, 33.9. HRMS (Q-TOF): *m/z* calc for $C_{15}H_{17}BrN_2O_2$ [M + H]: 337.0552; found 337.0563. 82 % yield.

General Deprotection Procedure for Library Synthesis:

To a stirred solution of coupled material **I-2** (1 equivalent) in anhydrous CH_2Cl_2 under argon at -78 ^oC was added BBr_3 (4 equivalents of 1.0 M solution in CH_2Cl_2) over 20 minutes. The solution was stirred at -78 ^oC for 30 minutes and then allowed to warm to 25 ^oC for 1.5 hours. The reaction was slowly quenched with saturated aqueous $NaHCO_3$ until slightly basic by pH paper. This solution was added to a separatory funnel containing water and extracted 3x with CH_2Cl_2. The combined organic layers were washed with saturated aqueous brine solution. The organic layer was dried over $MgSO_4$, and concentrated *in vacuo* to yield the deprotected product **I-3** (82-92 % yield). This material was used without further purification.

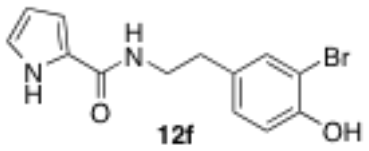

12f

***N*-(3-bromo-4-hydroxyphenethyl)-1*H*-pyrrole-2-carboxamide 12f**:

^1H NMR (400 MHz, DMSO-d_6) δ 11.36 (s, 1H), 7.99 (br s, 1H), 7.32, (d, *J* = 2.0 Hz, 1H), 7.10 (dd, *J* = 2.0, 8.0 Hz, 1H), 6.84 (d, *J* = 8.4 Hz, 1H), 6.81 (br s, 1H),

6.70 (br s, 1H), 6.04 (m, 1H), 3.34 (q, *J* = 6.8 Hz, 2H), 2.68 (t, *J* = 7.2 Hz, 2H). ^{13}C NMR (100 MHz, DMSO-d_6) δ 160.5, 152.2, 132.7, 131.8, 128.8, 126.3, 121.1, 116.2, 109.6, 108.9, 108.4, 40.2, 39.9, 39.7, 39.5, 39.3, 39.1, 34.0. HRMS (Q-TOF): *m/z* calc for $C_{13}H_{13}BrN_2O_2$ [M + H]: 309.0239; found 309.0241. 92 % yield.

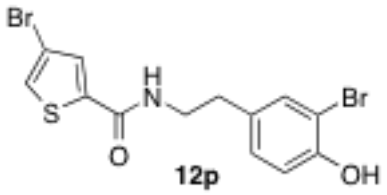

12p

4-bromo-*N*-(3-bromo-4-hydroxyphenethyl)thiophene-2-carboxamide 12p:

^{1}H NMR (400 MHz, DMSO-d_6) δ 9.99 (br s, 1H) 8.62 (t, *J* = 5.6 Hz, 1H), 7.87 (d, *J* = 1.2 Hz, 1H), 7.73 (d, *J* = 1.2 Hz, 1H), 7.32 (d, *J* = 1.6 Hz, 1H), 7.00 (dd, *J* = 2.0, 8.4 Hz, 1H), 6.84 (d, *J* = 8.4, 1H), 3.38 (q, *J* = 6.8 Hz, 3H), 2.69 (t, *J* = 7.2, 2H). ^{13}C NMR (100 MHz, DMSO-d_6) δ 159.7, 152.3, 141.2, 132.7, 131.4, 129.7, 128.9, 128.5, 116.2, 109.0, 108.1, 40.8, 33.58. HRMS (Q-TOF): *m/z* calc for $C_{13}H_{11}Br_2NO_2S$ [M + H]: 403.8955; found 403.8967. 82.2 % yield.

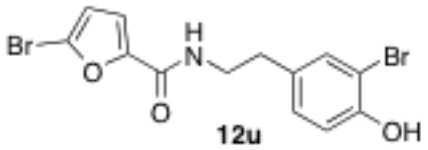

12u

5-bromo-*N*-(3-bromo-4-hydroxyphenethyl)furan-2-carboxamide 12u:

^{1}H NMR (400 MHz, DMSO-d_6) δ 9.98 (br s, 1H), 8.44 (t, *J* = 5.6 Hz, 1H), 7.30 (d, *J* = 1.6 Hz, 1H), 7.08 (d, *J* = 3.6 Hz, 1H), 7.00 (dd, *J* = 2.0, 8.4 Hz, 1H), 6.84 (d, *J* = 8.4 Hz, 1H), 6.72 (d, *J* = 3.6 Hz, 1H), 3.35 (q, *J* = 6.8 Hz, 2H), 2.68 (t, *J* = 7.2 Hz, 2H). ^{13}C NMR (100 MHz, DMSO-d_6) δ 156.4, 152.1, 149.6, 132.5, 131.2, 128.7, 124.0, 116.0, 115.4, 113.7, 108.8, 39.9, 33.5. HRMS (Q-TOF): *m/z* calc for $C_{13}H_{11}Br_2NO_3$ [M + H]: 387.9184; found 387.9198. 84.2 % yield.

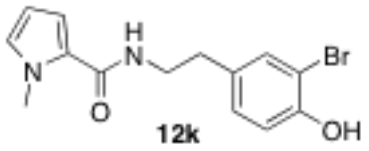

12k

***N*-(3-bromo-4-hydroxyphenethyl)-1-methyl-1*H*-pyrrole-2-carboxamide 12k**:

^{1}H NMR (400 MHz, DMSO-d_6) δ 9.97 (s, 1H), 7.98 (t, *J* = 5.6 Hz, 1H), 7.31 (d, *J* = 1.6 Hz, 1H), 7.00 (dd, *J* = 1.6, 8.0 Hz, 1H), 6.85 (m, 2H), 6.68 (m, 1H), 5.97 (m, 1H), 3.79 (s, 3H), 3.31 (q, *J* = 7.6 Hz, 2H), 2.69 (t, *J* = 7.6 Hz, 2H). ^{13}C NMR (100 MHz, DMSO-d_6) δ 161.7, 152.6, 133.1, 132.2, 129.3, 127.8, 126.1, 116.6, 112.3, 109.4, 106.9, 40.6, 36.4, 34.4. HRMS (Q-TOF): *m/z* calc for $C_{14}H_{15}BrN_2O_2$ [M + H]: 323.0395; found 323.0398. 88.7 % yield.

General Alkylation Procedure for Library Synthesis:

In a 5 mL microwave vial containing **I-3** (1 equivalent), alkyl halide (1.2 equivalents), KI (3 equivalents), and Cs_2CO_3 (3 equivalents) was added anhydrous DMF, 4 mL. This was heated under microwave conditions at 160 ^oC for 20-60 minutes. The reaction was filtered, concentrated *in vacuo* and purified via mass directed HPLC to obtain pure **I-4** as the TFA salt (15-85% yield).

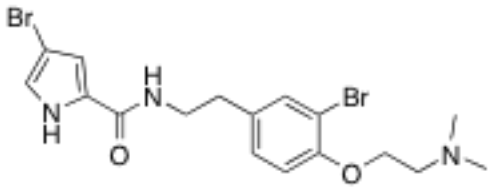

13b

4-bromo-*N*-(3-bromo-4-(2-(dimethylamino)ethoxy)phenethyl)-1*H*-pyrrole-2-carboxamide 13b:

^1H NMR (400 MHz, DMSO-d_6) δ 9.98 (br s, 1H), 8.14 (t, *J* = 4 Hz, 1H), 7.50 (d, *J* = 2.0 Hz, 1H), 7.22 (dd, *J* = 1.6, 8.4 Hz, 1H), 7.1 (d, *J* = 8.4 Hz, 1H), 6.96 (m, 1H), 6.81 (m,1H), 4.37 (t, *J* = 4.8 Hz, 2H), 3.55 (m, 2H), 3.41 (q, *J* = 6.4 Hz, 2H), 2.92 (s, 6H), 2.77 (m, 2H). ^{13}C NMR (100 MHz, DMSO-d_6) δ 159.9, 152.6, 134.5, 133.3, 129.4, 127.9, 121.2, 114.0, 111.4, 110.8, 95.0, 63.1, 55.6, 43.5, 40.4, 33.9. HRMS (Q-TOF): *m/z* calc for $C_{17}H_{21}Br_2N_3O_2$ [M + H]: 458.0079; found 458.0076.

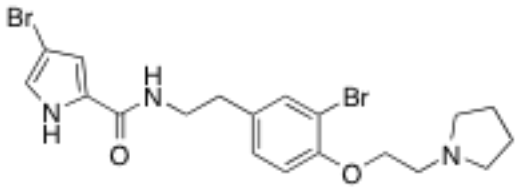

13c

4-bromo-*N*-(3-bromo-4-(2-(pyrrolidin-1-yl)ethoxy)phenethyl)-1*H*-pyrrole-2-carboxamide 13c:

^{1}H NMR (400 MHz, DMSO-d_6) δ 10.06 (br s, 1H), 8.14 (t, *J* = 5.2 Hz, 1H), 7.50 (d, *J* = 2.0 Hz, 1H), 7.22 (dd, *J* = 1.6, 8.4 Hz, 1H), 7.09 (d, *J* = 8.4 Hz, 1H), 6.95 (m, 1H), 6.81 (m, 1H), 4.34 (t, *J* = 4.4 Hz, 2H), 3.64 (m, 4H), 3.41 (q, *J* = 6.4 Hz, 2H), 3.18 (m, 2H), 2.76 (t, *J* = 6.8 Hz, 2H), 2.04 (m, 2H), 1.87 (m, 2H). ^{13}C NMR (100 MHz, DMSO-d_6) δ 159.5, 152.3, 134.4, 133.1, 129.2, 126.9, 121.1, 113.8, 111.3, 110.6, 94.8, 64.8, 54.4, 52.8, 40.0, 33.7, 22.5. HRMS (Q-TOF): *m/z* calc for $C_{19}H_{23}Br_2N_3O_2$ [M + H]: 484.0235; found 484.0226.

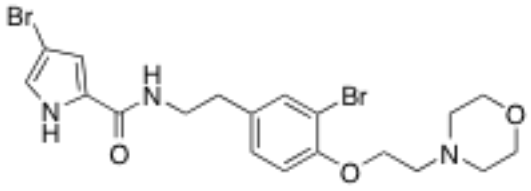

13d

4-bromo-*N*-(3-bromo-4-(2-morpholinoethoxy)phenethyl)-1*H*-pyrrole-2-carboxamide 13d:

^{1}H-nmr (400 MHz, DMSO-d_6) δ 10.30 (br s, 1H), 8.14 (t, *J* = 5.6 Hz, 1H), 7.50 (d, *J* = 1.6 Hz, 1H), 7.22 (dd, *J* = 1.6, 8.4 Hz, 1H), 7.10 (d, *J* = 8.4 Hz, 1H), 6.95 (m,

1H), 6.80 (m, 1H), 4.40 (t, *J* = 4.8 Hz, 2H), 3.98 (m, 2H), 3.70 (m, 2H), 3.59 (m, 2H) 3.41 (q, *J* = 6.8 Hz, 2H), 3.29 (m, 2H), 2.76 (t, *J* = 7.2 Hz, 2H). ^{13}C-nmr (100 MHz, DMSO-d_6) δ 159.5, 152.2, 134.4, 133.1, 129.2, 128.7, 121.1, 113.9, 111.3, 110.7, 94.84, 63.9, 63.4, 55.0, 52.2, 40.0, 33.8. HRMS (Q-TOF): *m/z* calc for $C_{19}H_{23}Br_2N_3O_3$ [M + H^+]: 500.0184; found 500.0161.

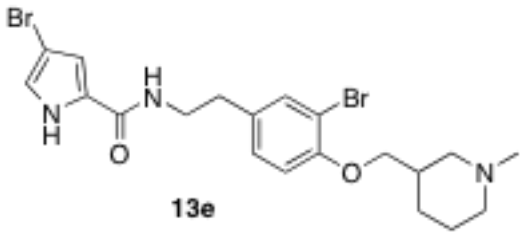

13e

4-bromo-*N*-(3-bromo-4-((1-methylpiperidin-3-yl)methoxy)phenethyl)-1*H*-pyrrole-2-carboxamide 13e:

^{1}H NMR (400 MHz, DMSO-d_6) δ 9.71 (br s, 1H), 8.14 (t, *J* = 5.2 Hz, 1H), 7.46 (d, *J* = 2.0 Hz, 1H), 7.18 (dd, *J* = 1.6, 8.4 Hz, 1H), 7.03 (d, *J* = 8.4 Hz, 1H), 6.95 (m, 1H), 6.81 (m, 1H), 3.99 (m, 1H), 3.89 (m, 1H), 3.51 (m, 1H), 3.40 (m, 3H), 2.80 (m, 4H), 2.74 (t, *J* = 6.8 Hz, 2H), 2.25 (m, 1H), 1.88 (m, 2H), 1.68 (m, 2H), 1.30 (m, 1H). ^{13}C NMR (100 MHz, DMSO-d_6) δ 159.5, 152.7, 133.9, 132.9, 129.2, 126.9, 121.1, 113.9, 111.3, 110.9, 94.8, 70.3, 55.7, 53.7, 43.1, 40.0, 34.3, 33.7, 23.9, 22.1. HRMS (Q-TOF): *m/z* calc for $C_{20}H_{25}Br_2N_3O_2$ [M + H]: 498.0392; found 498.0407.

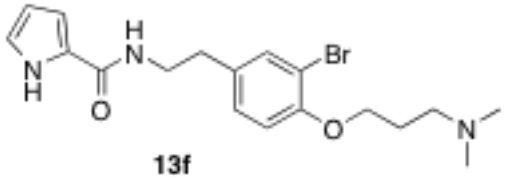

13f

***N*-(3-bromo-4-(3-(dimethylamino)propoxy)phenethyl)-1*H*-pyrrole-2-carboxamide 13f**:

^{1}H NMR (400 MHz, DMSO-d_6) δ 9.72 (br s, 1H), 8.03 (t, *J* = 5.2 Hz, 1H), 7.46 (d, *J* = 2.0 Hz, 1H), 7.20 (dd, *J* = 1.6, 8.4 Hz, 1H), 7.03 (d, *J* = 8.4 Hz, 1H), 6.82 (s, 1H), 6.72 (s, 1H), 6.05 (m, 1H), 4.07 (t, *J* = 6.0 Hz, 2H), 3.40 (q, *J* = 6.4 Hz, 2H), 3.23 (m, 2H), 3.10 (s, 1H), 2.82 (s, 6H), 2.76 (t, *J* = 6.8 Hz, 2H), 2.12 (m, 2H). ^{13}C NMR (100 MHz, DMSO-d_6) δ 160.6, 152.7, 133.9, 132.9, 129.1, 126.3, 121.1, 113.8, 110.9, 109.7, 108.4, 66.0, 54.3, 42.3, 40.0, 33.9, 23.8. HRMS (Q-TOF): *m/z* calc for $C_{18}H_{24}BrN_3O_2$ [M + H]: 394.1130; found 394.1121.

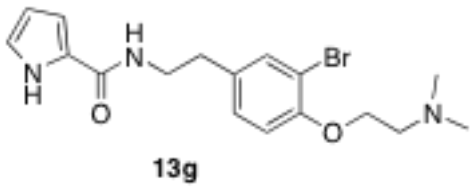

13g

***N*-(3-bromo-4-(2-(dimethylamino)ethoxy)phenethyl)-1*H*-pyrrole-2-carboxamide 13g**:

^{1}H NMR (400 MHz, DMSO-d_6) δ 10.10 (br s, 1H), 8.04 (t, *J* = 5.2 Hz, 1H), 7.50 (d, *J* = 2.0 Hz, 1H), 7.22 (dd, *J* = 1.6, 8.4 Hz, 1H), 7.09 (d, *J* = 8.4 Hz, 1H), 6.82 (s, 1H), 6.72 (s, 1H), 6.06 (m, 1H), 4.38 (t, *J* = 4.8 Hz, 2H), 3.55 (m, 2H), 3.41 (q,

J = 6.0 Hz, 2H), 3.21 (s, 1H), 2.92 (s, 6H), 2.77 (t, *J* = 6.0 Hz, 2H). ^{13}C NMR (100 MHz, DMSO-d_6) δ 160.6, 152.2, 134.5, 133.1, 129.2, 126.3, 121.1, 113.8, 110.7, 109.7, 108.5, 63.9, 55.5, 43.3, 39.9, 33.9. HRMS (Q-TOF): *m/z* calc for $C_{17}H_{22}BrN_3O_2$ [M + H]: 380.0974; found 380.0989.

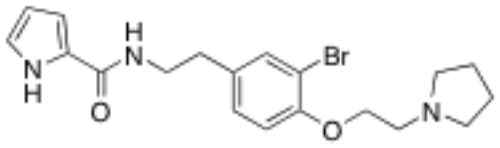

13h

***N*-(3-bromo-4-(2-(pyrrolidin-1-yl)ethoxy)phenethyl)-1*H*-pyrrole-2-carboxamide 13h:**

^{1}H NMR (400 MHz, DMSO-d_6) δ 10.10 (br s, 1H), 8.03 (t, *J* = 4.4 Hz, 1H), 7.50 (d, *J* = 2.0 Hz, 1H), 7.22 (dd, *J* = 1.6, 8.4 Hz, 1H), 7.09 (d, *J* = 8.4 Hz, 1H), 6.82 (s, 1H), 6.72 (s, 1H), 6.06 (m, 1H), 4.34 (t, *J* = 4.4 Hz, 2H), 3.64 (m, 4H), 3.41 (q, *J* = 6.0 Hz, 2H), 3.19 (m, 2H), 2.77 (t, *J* = 7.2 Hz, 2H), 2.04 (m, 2H), 1.86 (m, 2H). ^{13}C NMR (100 MHz, DMSO-d_6) δ 160.6, 152.3, 134.5, 133.1, 129.2, 126.3, 121.1, 113.8, 110.7, 109.7, 108.5, 64.8, 54.4, 52.8, 39.9, 33.9, 22.5. HRMS (Q-TOF): *m/z* calc for $C_{19}H_{24}BrN_3O_2$ [M + H]: 406.1130; found 406.1123.

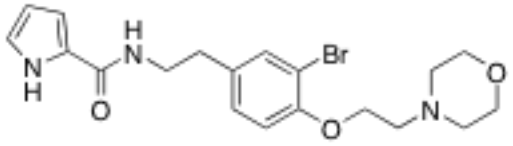

13i

***N*-(3-bromo-4-(2-morpholinoethoxy)phenethyl)-1*H*-pyrrole-2-carboxamide 13i:**

^{1}H-nmr (400 MHz, DMSO-d_6) δ 10.60 (br s, 1H), 8.04 (t, *J* = 5.6 Hz, 1H), 7.50 (d, *J* = 2.0 Hz, 1H), 7.32 (dd, *J* = 1.6, 8.8 Hz, 1H), 7.09 (d, *J* = 8.4 Hz, 1H), 6.82 (s, 1H), 6.72 (s, 1H), 6.06 (m, 1H), 4.41 (t, *J* = 4.4 Hz, 2H), 3.99 (m, 2H), 3.74 (m, 2H), 3.61 (t, *J* = 4.0 Hz, 2H), 3.58 (m, 2H), 3.41 (q, *J* = 6.0 Hz, 2H), 3.34 (m, 2H), 2.77 (t, *J* = 6.0 Hz, 2H). ^{13}C-nmr (100 MHz, DMSO-d_6) δ 160.6, 152.2, 134.6, 133.1, 129.2, 126.3, 121.2, 113.9, 110.7, 109.8, 108.5, 63.9, 63.4, 55.0, 52.2, 39.9, 33.9. HRMS (Q-TOF): *m/z* calc for $C_{19}H_{24}BrN_3O_3$ [M + H^+]: 422.1079; found 422.1086.

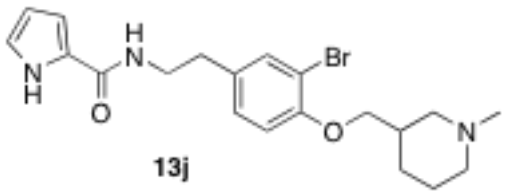

13j

***N*-(3-bromo-4-((1-methylpiperidin-3-yl)methoxy)phenethyl)-1*H*-pyrrole-2-carboxamide 13j**:

^{1}H NMR (400 MHz, DMSO-d_6) δ 9.90 (br s, 1H), 8.04 (t, *J* = 5.2 Hz, 1H), 7.46 (d, *J* = 2.0 Hz, 1H), 7.18 (dd, *J* = 1.6, 8.4 Hz, 1H), 7.02 (d, *J* = 8.4 Hz, 1H), 6.82 (s,

1H), 6.73 (s, 1H), 6.06 (m, 1H), 3.97 (m, 1H), 3.89 (m, 1H), 3.55 (m, 1H), 3.40 (m, 3H), 2.81 (m, 4H), 2.75 (t, *J* = 6.8 Hz, 2H), 2.37 (m, 1H), 1.88 (m, 2H), 1.74 (m, 2H), 1.37 (m, 1H). ^{13}C NMR (100 MHz, DMSO-d_6) δ 160.6, 152.7, 134.0, 132.9, 129.1, 126.3, 121.1, 113.9, 110.9, 109.8, 108.5, 70.3, 55.7, 53.6, 43.1, 40.0, 34.2, 34.0, 23.9, 22.1. HRMS (Q-TOF): *m/z* calc for $C_{20}H_{26}BrN_3O_2$ [M + H]: 420.1287; found 420.1303.

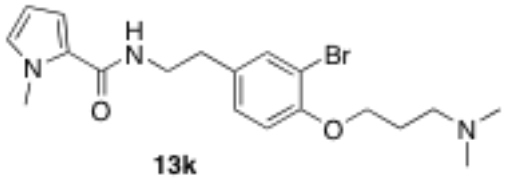

13k

***N*-(3-bromo-4-(3-(dimethylamino)propoxy)phenethyl)-1-methyl-1*H*-pyrrole-2-carboxamide 13k**:

^{1}H NMR (400 MHz, DMSO- d_6) δ 9.56 (br s, 1H), 8.00 (t, *J* = 5.6 Hz, 1H), 7.46 (d, *J* = 2.0 Hz, 1H), 7.20 (dd, *J* = 2.0, 8.4 Hz, 1H), 7.05 (d, *J* = 8.4 Hz, 1H), 6.86 (s, 1H), 6.69 (m, 1H), 5.98 (t, *J* = 2.4 Hz, 1H), 4.08 (t, *J* = 6.0 Hz, 2H), 3.80 (s, 3H), 3.35 (q, *J* = 6.4 Hz, 2H), 3.22 (m, 2H), 3.82 (s, 6H), 2.74 (t, *J* = 7.2 Hz, 2H), 2.12 (m, 2H). ^{13}C NMR (100 MHz, DMSO-d_6) δ 161.3, 152.7, 134.0, 132.9, 129.1, 127.5, 125.6, 113.8, 111.9, 110.8, 106.5, 66.0, 54.4, 42.4, 36.0, 33.9, 23.8. HRMS (Q-TOF): *m/z* calc for $C_{19}H_{26}BrN_3O_2$ [M + H]: 408.1287; found 408.1292.

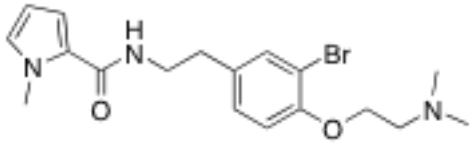

13l

***N*-(3-bromo-4-(2-(dimethylamino)ethoxy)phenethyl)-1-methyl-1*H*-pyrrole-2-carboxamide 13l**:

^{1}H NMR (400 MHz, DMSO- d_6) δ 10.17 (br s, 1H), 8.03 (t, *J* = 5.6 Hz, 1H), 7.49 (d, *J* = 2.9 Hz, 1H), 7.23, (dd, *J* = 2.0, 8.4 Hz, 1H), 7.11 (d, *J* = 8.4 Hz, 1H), 6.86 (s, 1H), 6.70 (m, 1H), 5.99 (t, *J* = 2.8 Hz, 1H), 4.38 (t, *J* = 5.2 Hz, 2H), 3.80 (s, 3H), 3.56 (m, 2H), 3.37 (q, *J* = 6.8 Hz, 2H), 2.93 (s, 6H), 2.76 (t, *J* = 7.2 Hz, 2H). ^{13}C NMR (100 MHz, DMSO-d_6) δ 161.3, 152.2, 134.6, 133.1, 129.2, 127.5, 125.7, 113.9, 112.0, 110.7, 106.5, 64.0, 55.5, 43.3, 40.0, 36.0, 33.9. HRMS (Q-TOF): *m/z* calc for $C_{18}H_{24}BrN_3O_2$ [M + H]: 394.1130; found 394.1133.

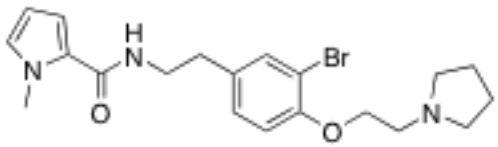

13m

***N*-(3-bromo-4-(2-(pyrrolidin-1-yl)ethoxy)phenethyl)-1-methyl-1*H*-pyrrole-2-carboxamide 13m**:

^{1}H NMR (400 MHz, DMSO- d_6) δ 10.27 (br s, 1H), 8.03 (t, *J* = 5.6 Hz, 1H), 7.49 (d, *J* = 2.0 Hz, 1H), 7.22 (dd, *J* = 2.0, 8.4 Hz, 1H), 7.09 (d, *J* = 8.4 Hz, 1H), 6.86 (s, 1H), 6.70 (m, 1H), 5.99 (t, *J* = 2.8 Hz, 1H), 4.35 (t, *J* = 4.8 Hz, 2H), 3.80 (s,

3H), 3.65 (m, 4H), 3.37 (q, *J* = 6.8 Hz, 2H), 3.20 (m, 2H), 2.76 (t, *J* = 6.8 Hz, 2H), 2.04 (m, 2H), 1.89 (m, 2H). ^{13}C NMR (100 MHz, DMSO-d_6) δ 161.3, 152.3, 134.5, 133.1, 129.2, 127.5, 125.7, 113.8, 112.0, 110.6, 106.5, 64.8, 54.4, 52.8, 40.0, 36.0, 33.9, 22.5. HRMS (Q-TOF): *m/z* calc for $C_{20}H_{26}BrN_3O_2$ [M + H]: 420.1287; found 420.1272.

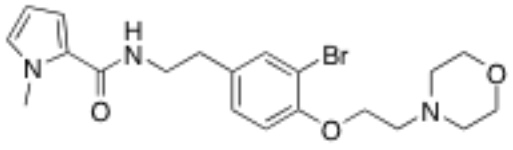

13n

***N*-(3-bromo-4-(2-morpholinoethoxy)phenethyl)-1-methyl-1*H*-pyrrole-2-carboxamide 13n:**

^{1}H-NMR (400 MHz, DMSO- d_6) δ 10.72 (br s, 1H), 8.04 (t, *J* = 5.6 Hz, 1H), 7.49 (d, *J* = 2.0 Hz, 1H), 7.23 (dd, *J* = 2.0, 8.4 Hz, 1H), 7.09 (d, *J* = 8.4 Hz, 1H), 6.86 (s, 1H), 6.71 (m, 1H), 5.98 (t, *J* = 2.8 Hz, 1H), 4.42 (t, *J* = 4.8 Hz, 2H), 3.98 (m, 2H), 3.80 (s, 3H), 3.76 (m, 2H), 3.62 (t, *J* = 4.4 Hz, 2H), 3.57 (m, 2H), 3.67 (q, *J* = 6.8 Hz, 2H), 2.76 (t, *J* = 7.2 Hz, 2H). ^{13}C-NMR (100 MHz, DMSO-d_6) δ 161.3, 152.2, 134.6, 133.1, 129.2, 127.5, 125.7, 113.9, 112.0, 110.7, 106.5, 63.9, 63.4, 55.0, 52.2, 40.0, 36.0, 33.9. HRMS (Q-TOF): *m/z* calc for $C_{20}H_{26}BrN_3O_3$ [M + H^+]: 436.1236; found 436.1237.

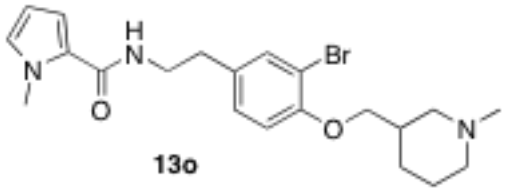

13o

***N*-(3-bromo-4-((1-methylpiperidin-3-yl)methoxy)phenethyl)-1-methyl-1*H*-pyrrole-2-carboxamide 13o**:

^{1}H NMR (400 MHz, DMSO- d_6) δ 9.89 (br s, 1H), 8.02 (t, *J* = 5.2 Hz, 1H), 7.45 (d, *J* = 2.0 Hz, 1H), 7.19 (dd, *J* = 2.0, 8.4 Hz, 1H), 7.03 (d, *J* = 8.4 Hz, 1H), 6.86 (s, 1H), 6.70 (m, 1H), 5.99 (t, *J* = 2.8 Hz, 1H), 4.00 (m, 1H), 3.89 (m, 1H), 3.80 (s, 3H), 3.52 (m, 1H), 3.44 (m, 1H), 3.35 (q, *J* = 6.8 Hz, 2H), 2.82 (m, 4H), 2.74 (t, *J* = 7.2 Hz, 2H), 2.27 (m, 1H), 1.89 (m, 2H), 1.68 (m, 2H), 1.29 (m, 1H). ^{13}C NMR (100 MHz, DMSO-d_6) δ 161.3, 152.7, 134.1, 132.9, 129.1, 127.5, 125.7, 113.9, 112.0, 110.9, 106.5, 70.3, 55.7, 53.6, 43.1, 40.0, 36.0, 34.2, 33.9, 23.9, 22.1. HRMS (Q-TOF): *m/z* calc for $C_{21}H_{28}BrN_3O_2$ [M + H]: 434.1443; found 434.1458.

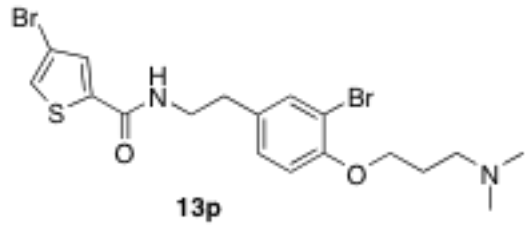

13p

4-bromo-*N*-(3-bromo-4-(3-(dimethylamino)propoxy)phenethyl)thiophene-2-carboxamide 13p:

^{1}H NMR (400 MHz, DMSO-d_6) δ 9.50 (br s, 1H), 8.65 (t, *J* = 5.6 Hz, 1H), 7.89 (d, *J* = 1.2 Hz, 1H), 7.75 (d, *J* = 1.2 Hz, 1H), 7.47 (d, *J* = 2.0 Hz, 1H), 7.20 (dd, *J* =

1.6, 8.4 Hz, 1H), 7.04 (d, *J* = 8.4 Hz, 1H), 4.09 (t, *J* = 6.0 Hz, 2H), 3.43 (q, *J* = 6.0 Hz, 2H), 3.23 (m, 2H), 3.10 (s, 1H), 2.82 (s, 6H), 2.77 (t, *J* = 7.2 Hz, 2H), 2.12 (m, 2H). ^{13}C NMR (100 MHz, DMSO-d_6) δ 159.8, 152.8, 141.1, 133.6, 132.9, 129.7, 129.1, 128.5, 113.8, 110.9, 108.6, 66.0, 54.4, 42.4, 40.6, 33.5, 23.8. HRMS (Q-TOF): *m/z* calc for $C_{18}H_{22}Br_2N_2O_2S$ [M + H]: 488.9847; found 488.9845.

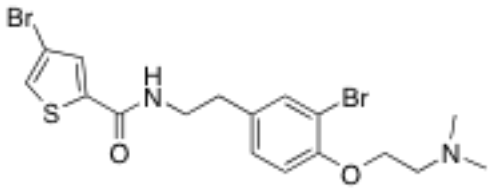

13q

4-bromo-*N*-(3-bromo-4-(2-(dimethylamino)ethoxy)phenethyl)thiophene-2-carboxamide 13q:

^{1}H NMR (400 MHz, DMSO-d_6) δ 9.85 (br s, 1H), 8.66 (t, *J* = 5.2 Hz, 1H), 7.89 (d, *J* = 0.8 Hz, 1H), 7.76 (d, *J* = 0.8 Hz, 1H), 7.50 (d, *J* = 1.6 Hz, 1H), 7.23 (dd, *J* = 1.6, 8.4 Hz, 1H), 7.11 (d, *J* = 8.4 Hz, 1H), 4.37 (t, *J* = 4.8 Hz, 2H), 3.50 (m, 4H), 3.21 (s, 1H), 2.92 (s, 6H), 2.78 (t, *J* = 7.2 Hz, 2H). ^{13}C NMR (100 MHz, DMSO-d_6) δ 159.8, 152.3, 141.1, 134.2, 133.1, 129.7, 129.2, 128.5, 113.9, 110.7, 108.6, 63.9, 55.5, 43.4, 40.6, 33.5. HRMS (Q-TOF): *m/z* calc for $C_{17}H_{20}Br_2N_2O_2S$ [M + H]: 474.9690; found 474.9705.

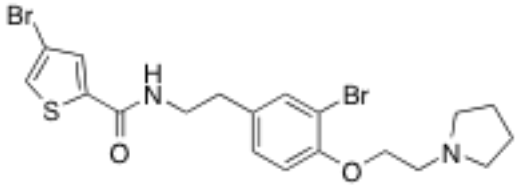

13r

4-bromo-*N*-(3-bromo-4-(2-(pyrrolidin-1-yl)ethoxy)phenethyl)thiophene-2-carboxamide 13r:

^{1}H NMR (400 MHz, DMSO-d_6) δ 10.08 (br s, 1H), 8.66 (t, *J* = 5.6 Hz, 1H), 7.89 (d, *J* = 1.6 Hz, 1H), 7.76 (d, *J* = 1.6 Hz, 1H), 7.51 (d, *J* = 2.0 Hz, 1H), 7.23 (dd, *J* = 2.0, 8.4 Hz, 1H), 7.10 (d, *J* = 8.4 Hz, 1H), 4.35 (t, *J* = 4.8 Hz, 2H), 3.63 (m, 4H), 3.43 (q, *J* = 6.8 Hz, 2H), 3.19 (m, 2H), 2.78 (t, *J* = 7.2 Hz, 2H), 2.04 (m, 2H), 1.87 (m, 2H). ^{13}C NMR (100 MHz, DMSO-d_6) δ 159.7, 152.3, 134.1, 133.2, 129.7, 129.2, 128.5, 113.8, 64.7, 54.4, 52.8, 40.6, 35.7, 33.8, 22.5. HRMS (Q-TOF): *m/z* calc for $C_{19}H_{22}Br_2N_2O_2S$ [M + H]: 500.9847; found 500.9847.

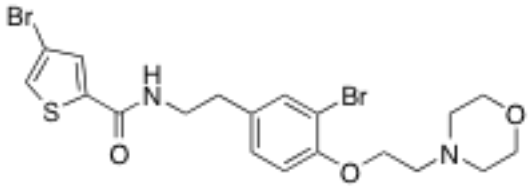

13s

4-bromo-N-(3-bromo-4-(2-morpholinoethoxy)phenethyl)thiophene-2-carboxamide 13s:

^{1}H-NMR (400 MHz, DMSO-d_6) δ 10.32 (br s, 1H), 8.67 (t, J = 5.6 Hz, 1H), 7.89 (d, J = 1.2 Hz, 1H), 7.76 (d, J = 1.2 Hz, 1H), 7.50 (d, J = 2.0 Hz, 1H), 7.23 (dd, J

= 1.6, 8.4 Hz, 1H), 7.10 (d, J = 8.4 Hz, 1H), 4.40 (t, J = 2.8 Hz, 2H), 3.98 (m, 2H), 3.80 (m, 2H), 3.60 (m, 2H), 3.43 (q, J = 6.8 Hz, 2H), 3.34 (m, 2H), 2.78 (t, J = 6.8 Hz, 2H). ^{13}C-NMR (100 MHz, DMSO-d_6) δ 159.8, 152.3, 141.1, 134.2, 133.1, 129.7, 129.2, 128.5, 113.9, 110.7, 108.6, 63.9, 63.4, 55.0, 52.2, 40.6, 33.5. HRMS (Q-TOF): m/z calc for $C_{19}H_{22}Br_2N_2O_3S$ [M + H^+]: 516.9796; found 516.9796.

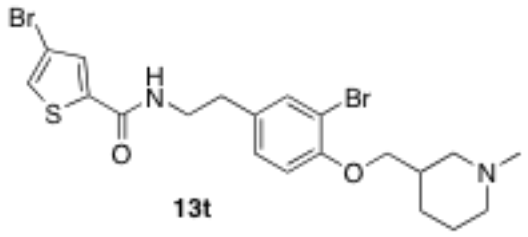

13t

4-bromo-*N*-(3-bromo-4-((1-methylpiperidin-3-yl)methoxy)phenethyl) thiophene-2-carboxamide 13t:

^{1}H NMR (400 MHz, DMSO-d_6) δ 9.62 (br s, 1H), 8.65 (t, *J* = 5.6 Hz, 1H), 7.89 (d, *J* = 1.2 Hz, 1H), 7.57 (d, *J* = 1.2 Hz, 1H), 7.47 (d, *J* = 1.6 Hz, 1H), 7.19 (dd, *J* = 1.6, 8.4 Hz, 1H), 7.03 (d, *J* = 8.4 Hz, 1H), 4.00 (m, 1H), 3.89 (m, 1H), 3.51 (m, 1H), 3.43 (m, 3H), 2.81 (m, 6H), 2.25 (m, 1H), 1.89 (m, 2H), 1.70 (m, 2H), 1.29 (m, 1H). ^{13}C NMR (100 MHz, DMSO-d_6) δ 159.8, 152.7, 141.1, 133.6, 133.0, 129.7, 129.2, 128.5, 113.9, 110.9, 108.6, 70.3, 55.7, 53.7, 43.1, 40.6, 34.3, 33.5, 23.9, 22.1. HRMS (Q-TOF): *m/z* calc for $C_{20}H_{24}Br_2N_2O_2S$ [M + H]: 515.0003; found 515.0017.

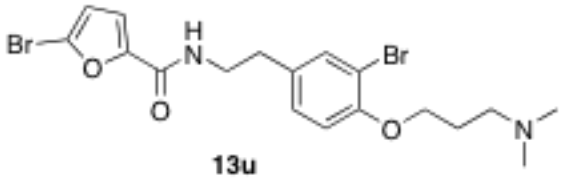

13u

5-bromo-*N*-(3-bromo-4-(3-(dimethylamino)propoxy)phenethyl)furan-2-carboxamide 13u:

^{1}H NMR (400 MHz, DMSO-d_6) δ 9.52 (br s, 1H), 8.48 (t, *J* = 5.6 Hz, 1H), 7.45 (d, *J* = 2.0 Hz, 1H), 7.19 (dd, *J* = 2.0, 8.4 Hz, 1H), 7.10 (d, *J* = 3.6 Hz, 1H), 7.03 (d, *J* = 8.4 Hz, 1H), 6.74 (d, *J* = 3.6 Hz, 1H), 4.09 (t, *J* = 6.0 Hz, 2H), 3.39 (q, *J* = 6.8 Hz, 2H), 3.23 (m, 2H), 2.83 (s, 6H), 2.76 (t, *J* = 7.2 Hz, 2H), 2.10 (m, 2H). ^{13}C NMR (100 MHz, DMSO-d_6) δ 156.6, 152.8, 149.7, 133.6, 132.9, 129.1, 124.2, 115.6, 113.9, 110.9, 66.0, 54.4, 42.4, 33.5, 23.8. HRMS (Q-TOF): *m/z* calc for C-$_{18}H_{22}Br_2N_2O_3$ [M + H]: 473.0075; found 473.0067.

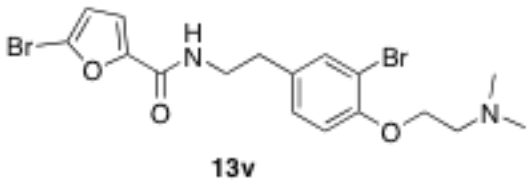

13v

5-bromo-*N*-(3-bromo-4-(2-(dimethylamino)ethoxy)phenethyl)furan-2-carboxamide 13v:

^{1}H NMR (400 MHz, DMSO-d_6) δ 10.08 (br s, 1H), 8.50 (t, *J* = 5.6 Hz, 2H), 7.48 (d, *J* = 1.6 Hz, 1H), 7.21 (dd, *J* = 1.6, 8.4 Hz, 1H), 7.10 (m, 2H), 6.73 (d, *J* = 3.6 Hz, 1H), 4.38 (t, *J* = 4.8 Hz, 2H), 3.55 (m, 2H), 3.40 (q, *J* = 6.8 Hz, 2H), 2.77 (t, *J*

= 6.8 Hz, 2H). ^{13}C NMR (100 MHz, DMSO-d_6) δ 156.6, 152.3, 149.7, 134.2, 133.1, 129.2, 124.2, 115.6, 113.9, 113.8, 110.7, 63.9, 55.5, 43.3, 40.0, 33.6. HRMS (Q-TOF): *m/z* calc for $C_{17}H_{20}Br_2N_2O_3$ [M + H]: 458.9919; found 458.9916.

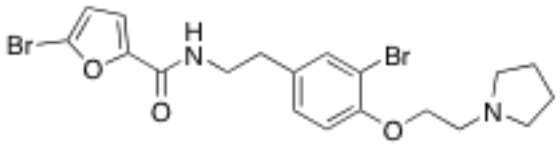

13w

5-bromo-*N*-(3-bromo-4-(2-(pyrrolidin-1-yl)ethoxy)phenethyl)furan-2-carboxamide 13w:

^{1}H NMR (400 MHz, DMSO-d_6) δ 10.2, 8.50 (t, *J* = 5.6 Hz, 1H), 7.48 (d, *J* = 1.2 Hz, 1H), 7.21 (dd, *J* = 1.6, 8.4 Hz, 1H), 7.10 (m, 2H), 6.73 (d, *J* = 3.6 Hz, 1H), 4.35 (t, *J* = 4.8 Hz, 2H), 3.64 (m, 4H), 3.40 (q, *J* = 6.8 Hz, 2H), 3.24 (m, 2H), 2.77 (t, *J* = 7.2 Hz, 2H), 2.04 (m, 2H), 1.89 (m, 2H). ^{13}C NMR(100 MHz, DMSO-d_6) δ 156.6, 152.3, 149.7, 134.1, 133.1, 129.2, 124.2, 115.6, 113.9, 113.8, 110.6, 64.7, 54.4, 52.8, 39.9, 33.6, 22.5. HRMS (Q-TOF): *m/z* calc for $C_{19}H_{22}Br_2N_2O_3$ [M + H]: 485.0075; found 485.0087.

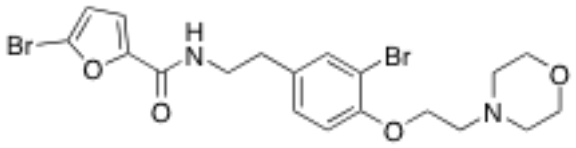

13x

5-bromo-*N*-(3-bromo-4-(2-morpholinoethoxy)phenethyl)furan-2-carboxamide 13x:

^{1}H NMR (400 MHz, DMSO-d_6) δ 10.55 (br s, 1H), 8.50 (t, *J* = 5.6 Hz, 1H), 7.48 (d, *J* = 1.6 Hz, 1H), 7.21 (dd, *J* = 1.6, 8.4 Hz, 1H), 7.10 (m, 2H), 6.73 (d, *J* = 3.6 Hz, 1H), 4.41 (t, *J* = 4.8 Hz, 2H), 3.98 (m, 2H), 3.74 (m, 2H), 3.61 (m, 2H), 3.58 (m, 2H), 3.40 (q, *J* = 6.8 Hz, 2H), 3.34 (m, 2H), 2.77 (t, *J* = 6.8 Hz, 2H). ^{13}C NMR (100 MHz, DMSO-d_6) δ 156.6, 152.3, 149.7, 134.2, 133.1, 129.2, 124.2, 115.6, 113.9, 110.7, 63.9, 63.3, 55.0, 52.2, 39.9, 33.6. HRMS (Q-TOF): *m/z* calc for $C_{19}H_{22}Br_2N_2O_4$ [M + H^+]: 501.0025; found 501.0031.

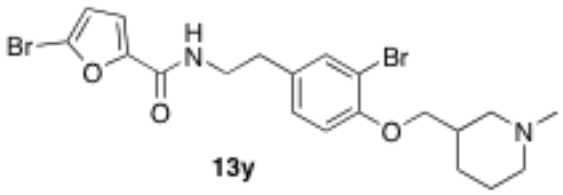

13y

5-bromo-*N*-(3-bromo-4-((1-methylpiperidin-3-yl)methoxy)phenethyl)furan-2-carboxamide 13y:

^{1}H NMR (400 MHz, DMSO-d_6) δ 9.58 (br s, 1H), 8.48 (t, *J* = 5.6 Hz, 1H), 7.45 (d, *J* = 2.0 Hz, 1H), 7.17 (dd, *J* = 1.6, 8.4 Hz, 1H), 7.09 (d, *J* = 3.6 Hz, 1H), 7.03 (d, *J* = 8.4 Hz, 1H), 6.73 (d, *J* = 3.6 Hz, 1H), 3.99 (m, 1H), 3.89 (m, 1H), 3.52 (m, 1H),

3.41 (m, 3H), 2.81 (m, 6H), 2.49 (m, 1H), 1.89 (m, 2H), 1.70 (m, 2H), 1.29 (m, 1H). ^{13}C NMR (100 MHz, DMSO-d_6) δ 156.6, 152.7, 149.7, 133.7, 132.9, 129.1, 124.2, 115.6, 113.9, 113.8, 110.9, 70.3, 55.7, 53.6, 43.2, 34.3, 33.6, 23.9, 22.1. HRMS (Q-TOF): *m/z* calc for $C_{20}H_{24}Br_2N_2O_3$ [M + H]: 499.0232; found 499.0251.

General Synthetic Scheme 2.

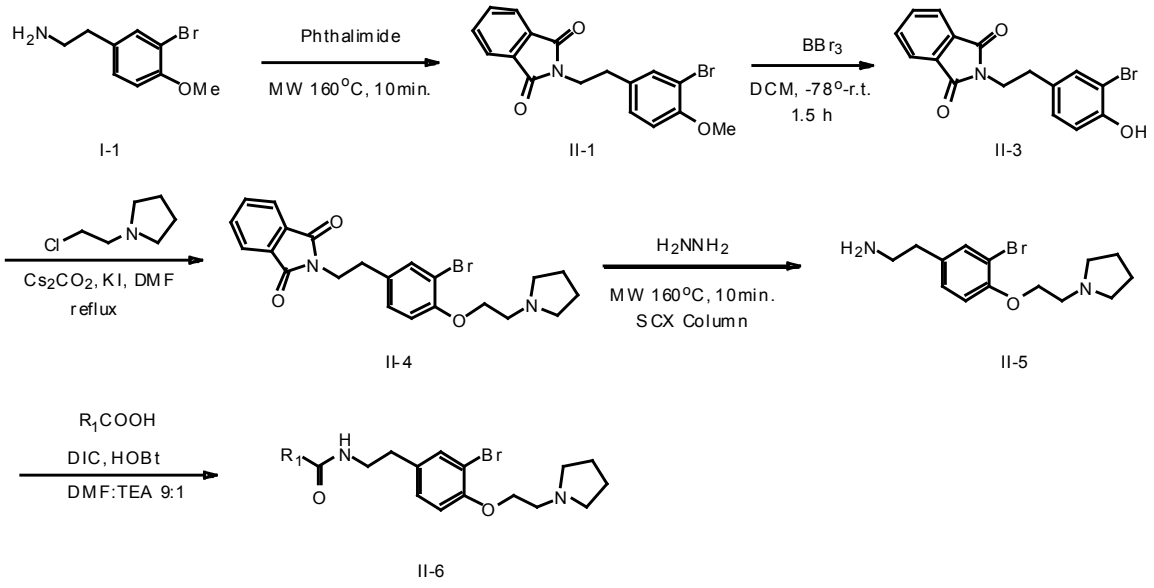

Phthalimide Formation Step:

A 20 mL microwave vial containing **I-1** (1 equivalent), and phthalic anhydride (1 equivalent), was capped and heated to 160 °C for 20 min. The solid was dissolved in hot EtOAc and left to crystallize overnight. The crystals were filtered and washed with ether to obtain **II-1** as a white solid (94% yield).

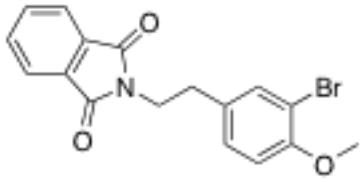

21

2-(3-bromo-4-methoxyphenethyl)isoindoline-1,3-dione 21: ^{1}H NMR (400 MHz, DMSO-d_6) δ 7.83 (m, 4H), 7.41 (d, *J* = 1.6 Hz, 1H), 7.13 (dd, *J* = 8.4, 2.0Hz, 1H), 6.96 (d, *J* = 8.4 Hz, 1H), 3.78 (m, 5H), 2.86 (t, *J* = 7.2 Hz, 2H). LCMS, single peak, 3.43 min, m/e, 360.0 (M+1)

Deprotection Step for Phthalimide Library:

To a stirred solution of protected material **II-1** (1 equivalent) in anhydrous CH_2Cl_2 under argon at -78 ^oC was added BBr_3 (4 equivalents of 1.0 M solution in CH_2Cl_2) over 20 minutes. The solution was stirred at -78 ^oC for 30 minutes and then allowed to warm to 25 ^oC for 1.5 hours. The reaction was slowly quenched with saturated aqueous $NaHCO_3$ until slightly basic by pH paper. This solution was added to a separatory funnel containing water and extracted 3x with CH_2Cl_2. The combined organic layers were washed with saturated aqueous brine solution. The organic layer was dried over $MgSO_4$, and concentrated *in vacuo* to yield the deprotected product **II-3** (100 % yield). This material was used without further purification.

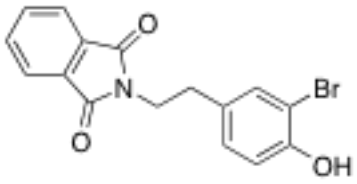

22

2-(3-bromo-4-hydroxyphenethyl)isoindoline-1,3-dione 22:

^{1}H NMR (400 MHz, DMSO-d_6) δ 10.03 (s, 1H), 7.83)m, 4H), 7.29 (d, *J* = 1.6 Hz, 1H), 6.96 (dd, *J* = 8.4, 2.0 Hz, 1H), 6.79 (d, *J* = 8.0 Hz, 1H), 3.75 (t, *J* = 7.2 Hz, 2H), 2.80 (t, *J* = 7.2 Hz, 2H); LCMS, single peak, 2.98 min, m/e, 346.0 (M+1).

Alkylation step for Phthalimide Library:

In a 200 mL round bottom flask containing **II-3** (1 equivalent), alkyl halide (2 equivalents), KI (2 equivalents), and Cs_2CO_3 (2 equivalents) was added anhydrous DMF, 30 mL which was heated to reflux overnight. The reaction was added to a seperatory funnel containing water and extracted 2x with EtOAc. The combined organic layers were washed with saturated aqueous brine solution. The organic layer was dried over $MgSO_4$, and concentrated *in vacuo* to yield **II-4.** This material was used immediately without further purification.

Deprotection step for Phthalimide Library:

A 20 mL microwave vial containing **II-4** (1 equivalent) ethanol, 10 mL, and hydrazine hydrate (10 equivalents), was capped and heated to 120 ^{o}C for 20 min. The solution was immediately added to a SCX cartridge and washed 5x with methanol. The cartidge was then washed 2x with 2M ammonia in methanol and concentrated *in vacuo* to yield **II-5** (60% yield over 2 steps).

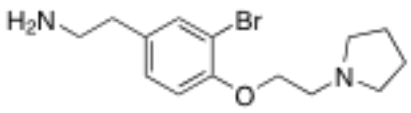

25

2-(3-bromo-4-(2-(pyrrolidin-1-yl)ethoxy)phenyl)ethanamine 25:

^{1}H NMR (400 MHz, DMSO-d_6) δ 7.38 (d, *J* = 2.0 Hz, 1H), 7.12 (dd, *J* = 8.4, 1.6 Hz, 1H), 6.99 (d, *J* = 8.4 Hz, 1H), 4.08 (t, *J* = 5.6 Hz, 2H), 2.78 (t, *J* = 5.6 Hz, 2H), 2.71 (m, 4H), 2.55 (m, 6H), 1.65 (m, 4H); LCMS, single peak, 1.60 min, m/e, 313.1 (M+1).

Coupling Step For Phthalimide Library:

To a stirred solution of acid R_1COOH (1 equivalent), HOBt (2.1 equivalents), and amine **II-5** (1 equivalent) in 9:1 CH_2Cl_2:DIEA at 25 ^oC was added DIC (2 equivalents) and the mixture was stirred overnight. The reaction was filtered, concentrated *in vacuo* and purified via mass directed HPLC to obtain pure **II-6** as the TFA salt (50-95% yield).

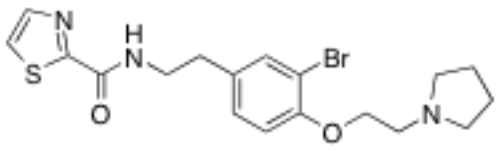

26d

***N*-(3-bromo-4-(2-(pyrrolidin-1-yl)ethoxy)phenethyl)thiazole-5-carboxamide 26d:**

^1H NMR (400 MHz, $CDCl_3$) δ 7.84 (d, *J* = 3.2 Hz, 1H), 7.57 (d, *J* = 3.2 Hz, 1H), 7.44 (d, *J* = 2.0 Hz, 1H), 7.15 (dd, *J* = 8.4, 2.0 Hz, 1H), 6.83 (d, *J* = 8.4 Hz, 1H), 4.41 (m, 2H), 3.95 (m, 2H), 3.67 (q, *J* = 6.8 Hz, 2H), 3.15 (m, 2H), 2.87 (t, *J* = 6.8 Hz, 2H), 2.15 (m, 6H); LCMS, single peak, 2.27 min, m/e, 424.1 (M+1).

General Synthetic Scheme 3.

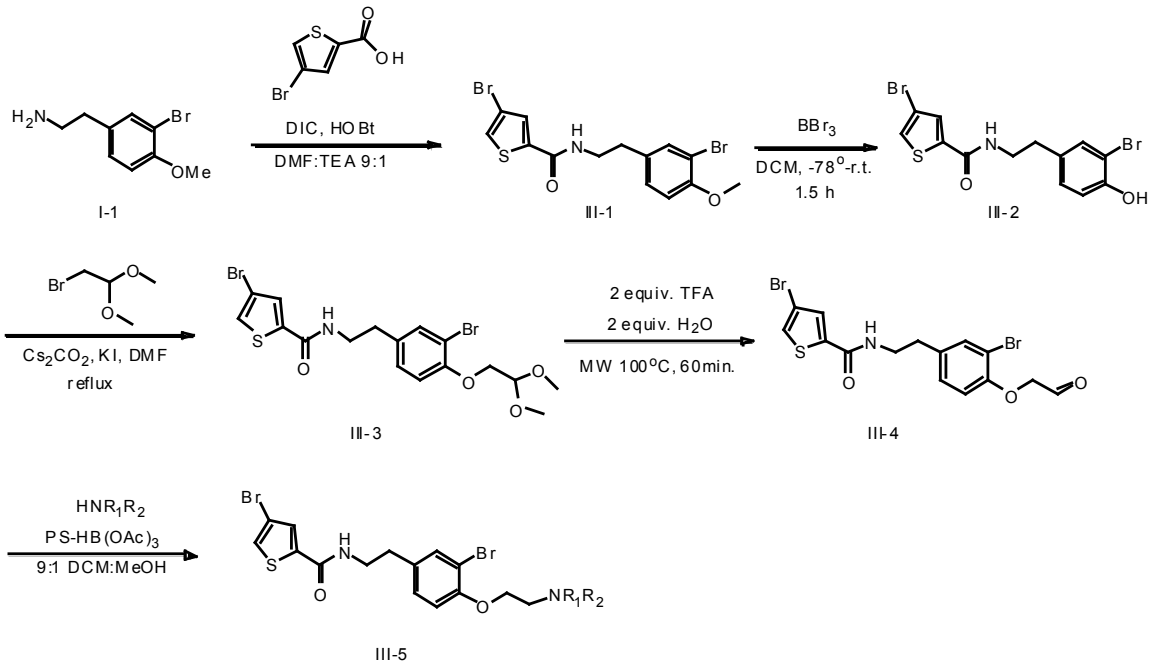

Coupling step:

To a stirred solution of acid R_1COOH (1 equivalent), HOBt (2.1 equivalents), and amine **I-1** (1 equivalent) in 9:1 CH_2Cl_2:DIEA at 25°C was added DIC (2 equivalents) and the mixture was stirred overnight. After quenching with water, the reaction was added to a separatory funnel and extracted 3x with CH_2Cl_2. The organic layers were combined, and washed with saturated aqueous brine solution. The organic layer was dried over $MgSO_4$, and concentrated *in vacuo*. The crude material was then subjected to flash chromatography to give pure **III-1** as a white solid (93 % yield).

Deprotection Step:

To a stirred solution of coupled material **III-1** (1 equivalent) in anhydrous CH_2Cl_2 under argon at -78 ^oC was added BBr_3 (4 equivalents of 1.0 M solution in CH_2Cl_2) over 20 minutes. The solution was stirred at -78 ^oC for 30 minutes and then allowed to warm to 25 ^oC for 1.5 hours. The reaction was slowly quenched with saturated aqueous $NaHCO_3$ until slightly basic by pH paper. This solution was added to a separatory funnel containing water and extracted 3x with CH_2Cl_2. The combined organic layers were washed with saturated aqueous brine solution. The organic layer was dried over $MgSO_4$, and concentrated *in vacuo* to yield the deprotected product **III-2** (92 % yield). This material was used without further purification.

Alkylation step:

In a 20 mL microwave vial containing **III-2** (1 equivalent), alkyl halide (4 equivalents), KI (2 equivalents), and Cs_2CO_3 (2 equivalents) was added anhydrous DMF, 10 mL. This was heated under microwave conditions at 120 ^oC for 60 minutes. The reaction was added to a seperatory funnel containing water and extracted 3x with EtOAc. The combined organic layers were washed with saturated aqueous brine solution. The organic layer was dried with $MgSO_4$ concentrated *in vacuo*. This was filtered through a silica plug, washed 3x with

EtOAc, and concentrated *in vacuo* to yield **III-3** (100 %). This material was used without further purification.

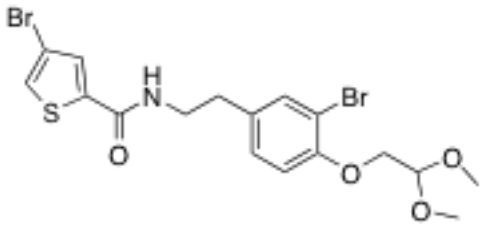

4-bromo-*N*-(3-bromo-4-(2,2-dimethoxyethoxy)phenethyl)thiophene-2-carboxamide 16:

^{1}H NMR (400 MHz, DMSO-d_6) δ 8.64 (t, *J* = 5.2 Hz, 1H), 7.88 (s, 1H), 7.75 (s, 1H), 7.45 (d, *J* = 2.0 Hz, 1H), 7.16 (dd, *J* = 8.4, 1.6 Hz, 1H), 7.06 (d, *J* = 8.4, 1H), 4.68 (t, *J* = 5.2 Hz, 1H), 4.00 (d, *J* = 7.2 Hz, 2H), 3.42 (q, *J* = 6.0 Hz, 2H), 3.37 (s, 6H), 2.76 (t, *J* = 6.8 Hz, 2H).

Aldehyde generation:

A 20 mL microwave vial containing **III-3** (1 equivalent) 1,2 dichloroethane, 10 mL, TFA (2 equivalents), and water (2 equivalents), was capped and heated to 100 ^{o}C for 60 min. This was concentrated *in vacuo* and used without any further purification.

Reductive amination:

To a 20 mL vial containing **III-4** and 9:1 DCM:MeOH, 10 mL, was added PS-triacetoxyborohydride (5 equivalents), and amine (5 equivalents), which was agitated overnight. The reaction was concentrated *in vacuo* and purified via mass directed HPLC to obtain pure **III-6** as the TFA salt (15-70% yield).

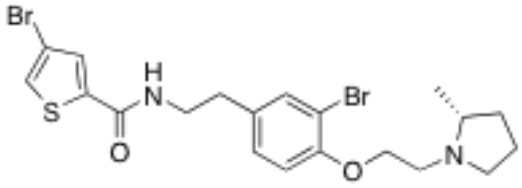

(*R*)-4-bromo-*N*-(3-bromo-4-(2-(2-methylpyrrolidin-1-yl)ethoxy)phenethyl) thiophene-2-carboxamide 18b:

^{1}H NMR (400 MHz, DMSO-d_6) δ 9.86 (br s, 1H), 8.70 (t, *J* = 5.6 Hz, 1H), 7.88 (s, 1H), 7.77 (s, 1H), 7.50 (d, *J* = 2.0 Hz, 1H), 7.23 (dd, *J* = 8.4, 2.0 Hz, 1H), 7.07 (d, *J* = 8.4 Hz, 1H), 4.35 (m, 2H), 3.75 (m, 2H), 3.52 (m, 2H), 3.43 (q, *J* = 6.8 Hz, 2H), 3.33 (m, 1H), 2.78 (t, *J* = 7.2 Hz, 2H), 2.21 (m, 1H), 1.94 (m, 2H), 1.60 (m, 1H), 1.38 (d, *J* = 6.4 Hz, 3H); LCMS, single peak, 2.65 min, m/e, 515.0 (M+1).

H3 Radioligand Binding Assay.

All *in vitro* pharmacology was performed by MDS Pharma services as a fee for service arrangement including the large panel ancillary pharmacology screens (Lead Profile screen) and the H3 assays. The H3 radioligand assay (MDS catalogue #: 239810) employed human recombinant Chinese Hamster Ovary (CHO)-K1 cells and 3 nM [^{3}H] R(-)-α-methylhistamine (RAMH) as the radioligand with 5-point concentration response curves to arrive at K_i (bindng) and/or IC_{50} (inhibition) values following published assay protocols (21, 22). Basic assay methods: Vehicle (1% DMSO), Incubation time/temperature (90 minutes @ 25 ^{o}C), Incubation buffer (50 mM TRis-HCl, pH 7.4, 5 mM $MgCl_2$, 0.04% BSA), ligand ([^{3}H] R(-)-α-methylhistamine), K_d (2.4 nM), B_{max} (4.2 pmole/mg protein), specific binding (95%), quantitation method (radioligand binding), significance criteria (>50% stimulation or inhibition).

References

1. Blunt, J. W.; Copp, B. R.; Hu, W.-P.; Munro, M. H. G.; Northcote, P. T.; Princep, M. R. *Nat. Prod. Rep.,* **2008**, *25*, 35–94.

2. Forenza, S.; Minale, L.; Riccio, R.; Fattorusso, E. *J. Chem. Soc., Chem. Commun.,* **1971**, 1129-1130.

3. Sharma, G.; Magdofffairchild, B. *J. Org. Chem.,* **1977**, 42, 4118-4124.

4. Walker, R. P.; Faulkner, D. J.; Vanengen, D.; Clardy, J. *J. Am. Chem. Soc.,* **1981**, 103, 6772-6773.

5. I.C. Pina, K.N. White, G. Cabrera, E. Rivero, P. Crews, *J. Nat. Prod.,* **2007**, 70, 613-617.

6. (a) Forenza, S.; Minale, L.; Riccio, R.; Fattorusso, E. *J. Chem. Soc. Chem. Commun.* **1971**, 1129-1130; (b) Garcia, E. E.; Benjamin, R. I.; Fryer, R. I. *J. Chem. Soc. Chem. Commun.* **1973**, 78-79; (c) Keiffer, P. A.; Schwartz, R. E.; Koker, M. E.; Hughes, R. G.; Rittschof, D.; Reinhart, K. L. *J. Org. Chem.* **1977**, *42*, 2965-2875; (d) Gautschi, J. T.; Whitman, S.; Holman, T. R.; Crews, P. *J. Nat. Prod.* **2004**, *67*, 1256-1261.

7. E. D. Miller, C. A. Kauffman, P. R. Jensen, W. Fenical, *J. Org. Chem.* **2007**, *72*, 323-330.

8. (a) Tan, D. S.; Foley, M.; Shair, M. D.; Shreiber, S. L. *J. Am. Chem. Soc.* **2000**, *122*, 422-423; (b) Pelish, H. E.; Westwood, N.; Feng, Y.; Kirchhausen, T.; Shair, M. D. *J. Am. Chem. Soc.* **2001**, *123*, 6740-6741; c) Lindsley, C. W.; Bogusky, M. J.; Leister, W. H.; McClain, R. T.; Robinson, R. R.; Barnett, S. F.; Defeo-Jones, D.; Ross, C. W.; Hartman, G. D. *Tetrahedron. Lett.* **2005**, *46*, 2279-2782.

8. For information on MDS Pharma Services, assay details and available molecular targets see: www.**mds**ps.com.

9. Kenny, B. A.; Chalmers, D. H.; Philpott, P. C.; Naylor, A. M. *Br. J. Pharmacol.* **1995**, *115*, 981-986.

10. Uhlen, S.; Porter, A. C.; Neubig, R. R. *J. Pharmacol. Exp. Ther.* **1994**, *271*, 1558-1565.

11. Ruat, M.; Traiffort, E.; Bouthenet, M. L.; Schwartz, J. C.; Hirschfeld, J.; Buschauer, A.; Schunack, W. *Proc. Natl. Acad. Sci. USA* **1990**, *87*, 1658-1662.

12. (a) Yanai, K.; Ryu, J. H.; Sakai, N.; Takahashi, T.; Iwata, R.; Ido, T.; Murakami, K.; Wantanbe, T. *Jpn. J. Pharmacol.* **1994**, *65*, 107-112; (b) Zhu, Y.; Machalovich, D.; Wu, H-L.; Tan, K. B.; Dytko, G. M.; Mannan, I. J.; Boyce, R. J.; Alston, J.; Tierney, L. A.; Li, X.; Herrity, N. C.; Vawter, L.; Sarau, H. M.; Ames, R. S.; Davenport, C. M.; Hieble, J. P.; Wilson, S.; Bergsma,D. J.; Fitzgerald, L. R. *Mol. Pharmacol.* **2001**, *59*, 434-441.

13. a) Piascik, M. T.; Guarino, R. D.; Smith, M. S.; Soltis, E. E.; Saussy, D. L., Jr.; Perez, D. M. *J. Pharmacol. Exp. Ther.* **1995**, *275*, 1583-1588.; b) Chu, C-P.; Kunitake, T.; Kato, K.; Watanabe, S.; Qui, D-L.; Tanoue, A.; Kannan, H. *Neurosci. Lett.* **2004**, *356*, 33-36.

14. Makartis, K.; Johns, C.; Gavras, I.; Altman, J. D.; Handy, D. E.; Bresnahan, M. R.; Gavras, H. *Hypertension* **1999**, *34(3)*, 403-407.

15. Ganellin, C. R. *Analogue-Based Drug Disc.* **2006**, 71-80.

16. Berlin, M.; Boyce, C. W. *Exp. Opin. Ther. Patent* **2007**, *17*, 675-687.

17. (a) For detailed information on the NIH Roadmap and the MLSCN see: http://mli.nih.gov/mlscn/index.php; (b) For details on the Vanderbilt Screening Center for GPCRs Ion Channels and Transporters see: www.vanderbilt.edu/**MLSCN**; (c) Lindsley, C. W.; Weaver, D.; Jones, C.; Marnett, L.; Conn, P. J. *ACS Chem. Bio.* **2007**, *2*, 17-20.

18. Kennedy, J.P.; Williams, L.; Bridges, T.M.; Daniels, R.N.; Weaver, D.; Lindsley, C.W. *J. Comb. Chem.* **2008**, 10, 345-354.

19. Leister, W.H.; Strauss, K.A.; Wisnoski, D.D.; Zhao, Z.; Lindsley, C.W. *J. Comb. Chem*. **2003**, *5*, 322-329.

20. Fadeyi, O.; Lindsley, C.W. *Org. Lett.* **2009**, *11*, 943-946.

21. K. Yanai, J.H. Ryu, N. Sakai, T. Takahashi, R. Iwata, T. Ido, K. Murakami, T. Wantanbe *Jpn. J. Pharmacol.*, **1994**, *65*(2), 107-112.

22. Y. Zhu, D. Machalovich, H-L. Wu, K.B. Tan, G.M. Dytko, I.J. Mannan, R.Y. Boyce, J. Alston, L.A. Tierney, X. Li, N.C. Herrity, L. Vawter, H.M. Sarau, R.S. Ames, C.M. Davenport, J.P. Hieble, S. Wilson, D.J. Bergsma, L.R. Fitzgerald *Mol. Pharmacol.*, **2001**, *59*(3), 434-441.

23. Provisional patent (61/059,975) filed June 9, 2008.

24. All tables and portions of text previously published are used with consent from the publisher.

CHAPTER II

SYNTHESIS AND DESIGN OF SELECTIVE M_4 MUSCARINIC MODULATORS

The five subtypes of the mammalian muscarinic acetylcholine receptor (mAChR1-5 or M_{1-5}) are differentially expressed GPCRs important to a variety of physiological functions, including attention, learning and memory, pain, sleep, movement, gastrointestinal motility, and cardiovascular regulation, among others (4-7). Based on a wide body of data, muscarinic receptors are considered potential therapeutic targets for numerous CNS diseases and disorders such as Alzheimer's disease and Schizophrenia (10-12). However, due to high sequence conservation of the orthosteric binding site across subtypes, discovery of truly subtype-selective compounds has proven historically challenging. Indeed, M_2 and M_3 related side effects (e.g. GI disturbance, salivation, lacrimation, and bradycardia) have contributed to failure in the clinical development of muscarinic agonists despite promising demonstrations of therapeutic efficacy (9,10). Furthermore, deep biological insight into the specific roles of the mAChRs in both basic neurobiology and CNS pathologies has been hindered by the paucity of selective tools.

M_4 activation in particular has been hypothesized to possess therapeutic potential in the treatment of psychosis based on the M_4 localization and M_4 knockout mouse data (24-26). Although M_4 receptors are expressed throughout

the CNS, highest expression is found in the hippocampus, midbrain, and striatal regions where it is believed to play important roles in both cognitive functions and in regulation of dopamine (DA) signaling. The positive symptoms of Schizophrenia are primarily linked to hyperactivity of the mesolimbic DA pathway, **Figure 1**, which is comprised of DA neurons originating in the mid-brain ventral tegmental area (VTA), which project to the nucleus accumbens (NAcc) (27-29).

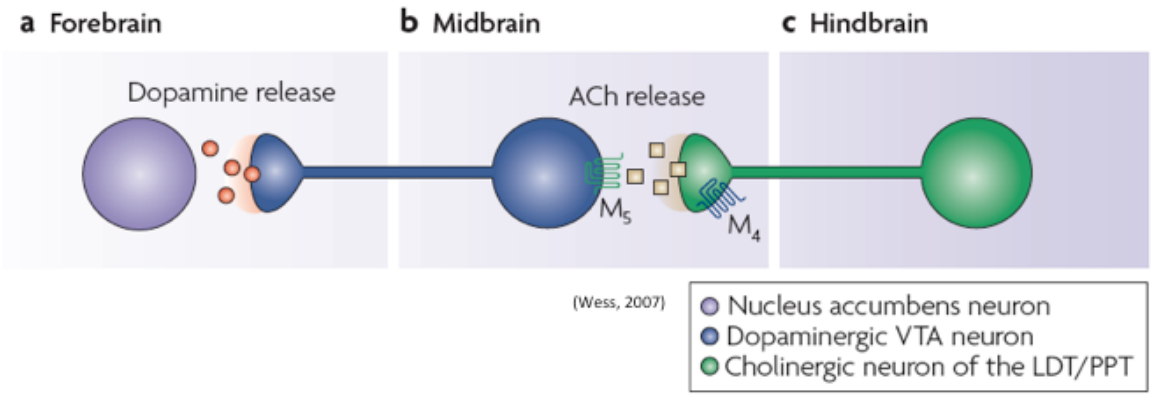

Figure 1. Simplified diagram of mesolimbic dopamine signaling pathway.

Within this pathway, M_4 is believed to exert regulatory control over Ach release from hindbrain cholinergic neurons that innervate the VTA. Thus activation of M_4 autoreceptors in this brain region may result in decreased DA signaling in the forebrain.

Additional support for M_4 as a therapeutic target for Schizophrenia comes from findings with the M_1/M_4 agonist Xanomeline **1**, **Figure 2**, which showed

robust clinical efficacy in reduction of positive, negative, and cognition symptoms (29-31). However, due to lack of true selectivity, M_2/M_3 mediated side effects precluded successful development of Xanomeline. It has remained a longstanding question in the field as to what contribution M_1 and M_4 made to the efficacy of Xanomeline **1**. Therefore, attainment of a truly M_4 selective small molecule would provide deeper insight.

The additional DMPK related challenges inherent to CNS drug discovery have also hampered progress in this area. Despite these hurdles, a number of novel subtype-selective and centrally penetrant muscarinic compounds, including agonists, antagonists, and potentiators, have recently emerged from functional cell-based screening approaches (13-17). The discovery and development of these first selective muscarinic modulators around the structure VU0010010 **2**, and the rational for the design of these compounds was a major undertaking during the early stages of this program. Initial optimization focused on improving the physiochemical properties of lead compound VU0010010 **2**, which possessed an EC_{50} value of 400 nM and elicited a 47-fold leftward shift of an ACh concentration-response curve (CRC) by Ca^{2+} mobilization assay in rat M_4/G_{qi5}- expressing cells, but suffered from solubility issues and lack of brain penetration.

For the chemical optimization of VU0010010 **2**, **Figure 2**, we undertook a diversity-oriented synthesis approach to explode structure-activity relationships (SAR) with a variety of hypothesis-driven structural changes to the lead compound.

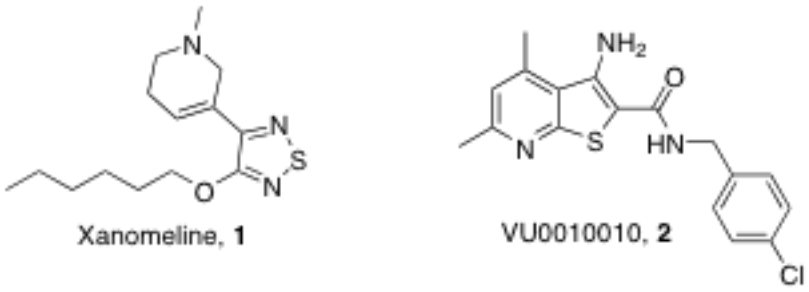

Figure 2. Structure of Xanomeline, **1**, and VU0010010, **2**.

The rationale for this approach for the optimization of VU0010010, **2** is that SAR for allosteric ligands is often "flat" or "shallow", with subtle structural modifications leading to a complete loss of activity, and often only one portion of an allosteric ligand is amenable to change. Therefore, a multidimensional diversity-oriented synthesis library approach provides the best opportunity to quickly identify productive SAR as opposed to a lead optimization strategy based on classical, single compound synthesis (1-2). One explanation for the lack of central activity observed with VU0010010, **2**, could be the result of the poor physiochemical properties alone or in combination with P-glycoprotein (P-gp) efflux. P-gp is an efflux transporter with broad substrate specificity present on the luminal membrane of epithelial cells comprising the blood-brain barrier, which is known to impair the brain penetrability of a number of drugs. The β-aminoamide motif **3** present in VU0010010 represents a potential P-gp liability, which could be removed by cyclization to analogs such as **4**, **Figure 3**, and the

dimethyl functionality can be a potential CYP_{450} site of metabolism, leading to increased clearance.

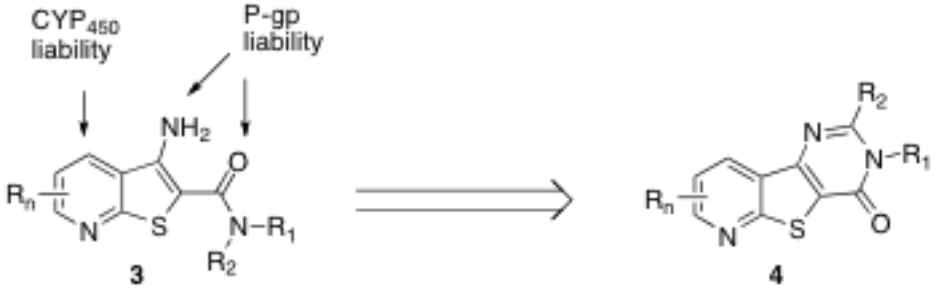

Figure 3. Rational for Library Design arounde VU0010010.

Alternatively, P-gp susceptibility could also be diminished by electronically attenuating the basicity of the amine moieties by the incorporation of distal fluorine atoms. Utilizing solution phase parallel synthesis, **Figure 4**, we synthesized small 12 to 24-member focused libraries around each of the 9 scaffolds, **4** and **7** through **15**, **Figure 4**, which were then purified by mass-directed preparative HPLC to analytical purity (>98%).

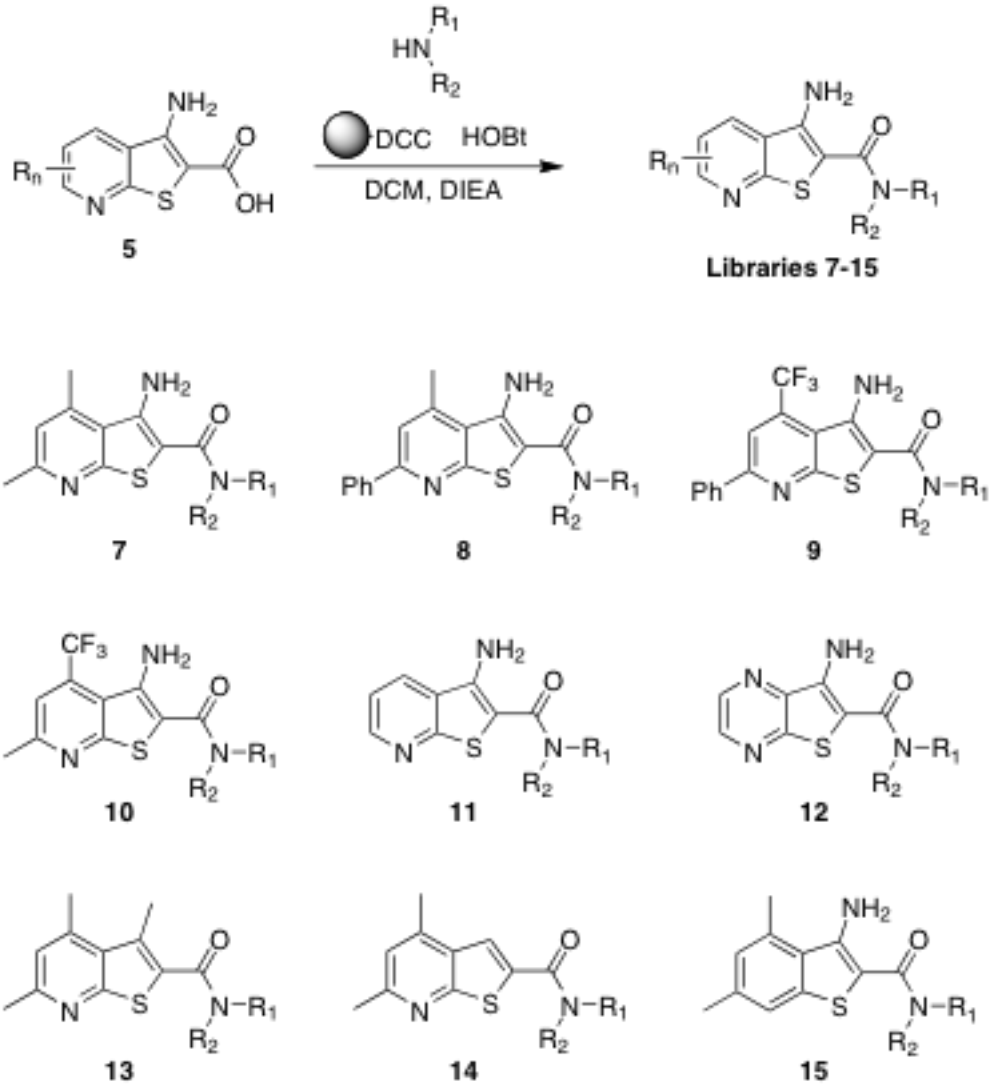

Figure 4. Synthesis and chemical optimization of lead compound VU0010010, **1**.

This collection of VU0010010 analogs incorporated CF_3 moieties, scaffolds **9** and **10**, to electronically attenuate potential P-gp susceptibility, deletion of the amino moiety, scaffold **14**, or replacement of the β-amino moiety with an isosteric methyl group, scaffold **13**. Other scaffolds explored the deletion

of substituents on the pyridine nucleus, scaffold **11**, incorporation of an additional nitrogen atom to afford a pyrimidine nucleus, scaffold **12**, or removal of the pyridine nitrogen atom in VU0010010, scaffold **15**. Finally, scaffold **7** focused on maintaining the core structure of VU0010010 but explored alternative amides selected to improve physiochemical properties and lower the log P value.

As observed with positive allosteric modulators of class C GPCRs, SAR around VU0010010 was relatively flat, possibly due to a shallow binding pocket (1-2). An EC_{20} triage screen, employing a functional fluorescence-based Ca^{2+} assay in CHO cells stably coexpressing the rat M_4 mAChR and the chimeric G protein, G_{qi5}, quickly eliminated all VU0010010 analogs with the exception of those in library **7**, built around the original lead thienopyridine scaffold. Within library **7**, all aliphatic and nonbenzyl amides were inactive, and only benzyl and heteroaryl methyl congeners of VU0010010, compounds **7a** through **7p**, retained M_4 PAM activity, **Table 1**. Analogs were synthesized utilizing resin bound peptide coupling techniques, and purified via mass directed HPLC. To identify compounds that potentiated agonist activation of M_4, the response to an EC_{20} concentration of ACh was determined in the absence and presence of test compound. The potency of each compound was determined by preincubating cells with vehicle or increasing concentrations of test compound followed by the addition of an EC_{20} concentration of ACh to yield concentration response curves (CRCs). Subtle substitution changes on the arene ring lost activity 5 to 10-fold in terms of M_4 EC_{50} and/or -fold shift of the ACh CRC, **Table 1**. Compound **7d**, in which the 4-Cl moiety of VU0010010 is moved to the 3-position, results in a loss

in potency of over 9-fold (EC_{50} = 3.7 μM). The unsubstituted phenyl congener **7a** retains M_4 PAM activity (EC_{50} = 630 nM), but the -fold shift diminishes to 8.6-fold versus the 47-fold shift observed for VU0010010 (3). In general, functionalized benzyl amides, as well as pyridyl methyl congeners, compounds **7f** and **7g**, were well tolerated, providing selective M_4 PAMs with EC_{50} values ranging from 380 nM to 3.7 μM and with -fold shifts of the ACh dose-response curve from 8.6 to 70-fold.

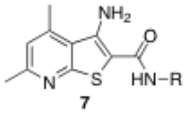

7

Compound	R	Rat M_4 EC_{50} μM	Rat M_4 Ach -Fold Shift	Compound	R	Rat M_4 EC_{50} μM	Rat M_4 Ach -Fold Shift
7a		0.63	8.6	**7i**	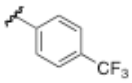	1.80	N.D.
7b		0.83	11.8	**7j**	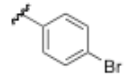	2.96	N.D.
7c		1.83	N.D.	**7k**	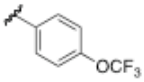	3.04	N.D.
7d	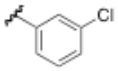	3.70	N.D.	**7l**	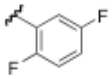	0.88	N.D.
7e	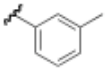	2.63	N.D.	**7m**	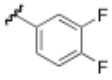	1.12	N.D.
7f		2.04	N.D.	**7n**	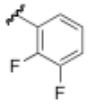	0.72	13.7
7g		2.88	N.D.	**7o**	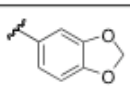	0.40	29.7
7h	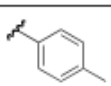	1.44	N.D.	**7p**	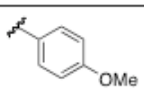	0.38	70.1

Table 1. Structures, activities, and ACh CRC -fold shifts of M_4 PAM analogs **7**.

Although, these compounds increase the potency of ACh at M_4, they lack intrinsic agonist activity on their own. Initial optimization focused on improving the physio-chemical properties of lead compound VU0010010 **1**, which possesses a 400 nM EC_{50} and caused a 47-fold leftward shift of an ACh concentration response curve (CRC) by Ca^{2+} mobilization in rat M_4/G_{qi5}-expressing cells, but suffered from solubility issues and lack of brain penetration. Analogs, VU0152099 **7o** and VU0152100 **7p**, which had similar potency and comparable efficacy to the parent compound VU0010010 **1** but were centrally penetrant and displayed *in vivo* activity in a rodent behavioral model predictive of antipsychotic efficacy. These compounds were also devoid of ancillary pharmacological activity across a large number of off-target GPCRs, ion channels, and enzymes. Despite the utility of **7o** and **7p** for *in vitro* and *in vivo* pharmacological studies, we sought to further explore the SAR of this series with a more exhaustive optimization campaign by employing an iterative analog library approach. The rationale for this effort stemmed in part from the rodent DMPK profiles of these 'first generation' analogs **7o** and **7p**, **Figure 5**, which were adequate but not ideal.

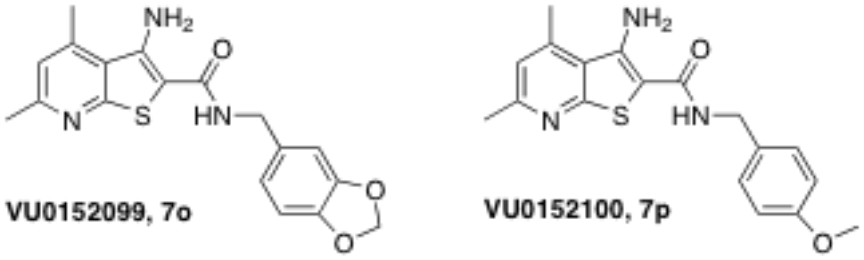

Figure 5. First-Generation Library Leads from Optimization of VU0010010.

Having tentatively designated the *p*-methoxybenzamide of **7p** as favored based on its *in vitro* activity at M_4, we first held this side chain constant during derivatization of the pyridine core at the 6-position. This was also chosen in part to address metabolic hydroxylation liability at the 5-position. Synthesis of initial 20-member alkylamine library, as shown in **Scheme 1**, began with condensation between 3-aminocrotonitrile **16** and 2-cyanothioacetamide **17** to furnish the aminopyridyl core **18** (19). This was cyclized with α-chloro-*p*-methoxybenzamide **19** to give the diaminothienopyridine scaffold with the *p*-methoxybenzamide **20**. To produce the 20-member amine library, **20** was reacted with various alkyl chlorides to generate **21a-p**. The ether library was synthesized in a similar fashion **Scheme 2**. Ethylacetoacetate **22** was reacted with 2-cyanothioacetamide **17** to provide the core pyridone **23**, (19) which was then cyclized with **19** and finally alkylated to obtain analogs **25a-s**.

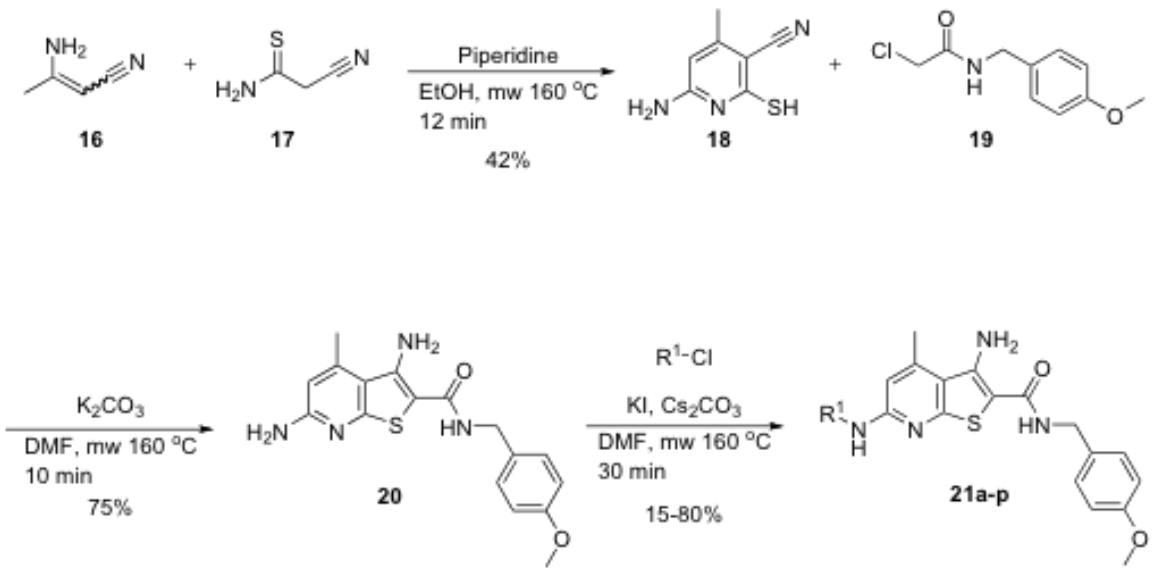

Scheme 1. Synthesis of amine analog libraries **21a-p**.

These 'second generation' libraries were first screened in a single-point Ca^{2+} mobilization assay using a fixed 10 μM compound concentration added to rM_4/G_{qi5}-cells prior to addition of a submaximal concentration (~EC_{20}) of ACh. This allowed efficient triage of analogs for further characterization. In general, alkylamine library **21a-p** showed weak efficacy with elevation of the ACh response ranging from none (inactive) to modest (<50% ACh max). However, ether library **25a-s** contained a number of robust potentiators (>60% to 90% ACh Max). EC_{50} values for compounds selected from both libraries based on their potentiation efficacy and structural characteristics were then obtained from full CRC assays, **Table 2**.

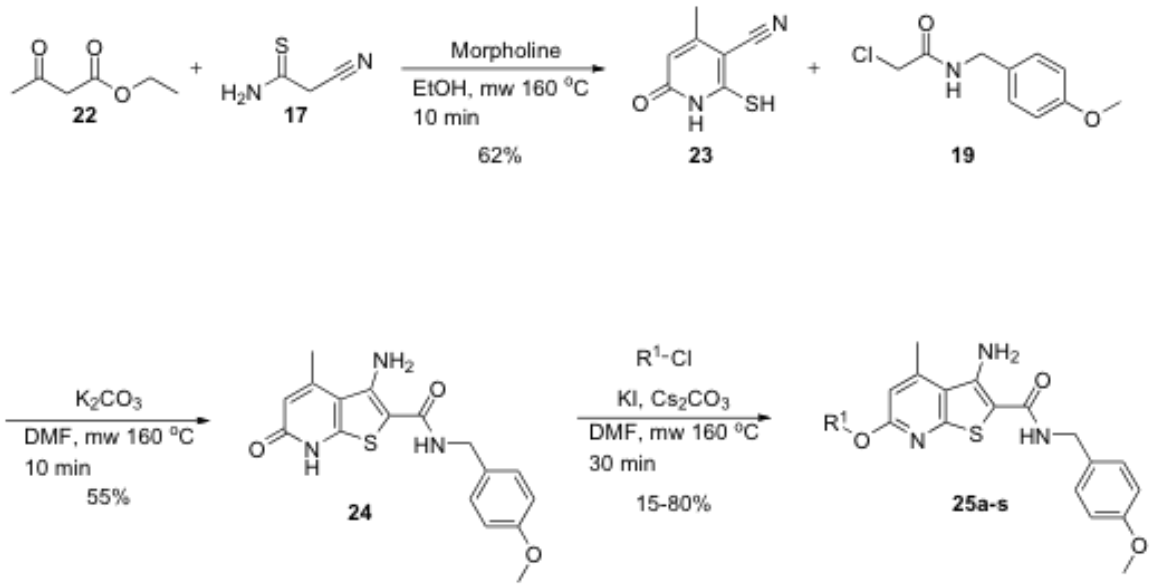

Scheme 2. Synthesis of ether analog libraries **25a-s**.

More than half of these compounds possessed EC_{50} values over 10 μM with potentiation effects emerging only at the 10 μM and 30 μM concentrations. Among alkylamines **21a-s**, only the ethyl morpholine congener **21c** had an EC_{50} just below 10 μM, reflecting relatively weak activity of this library. In contrast, compounds chosen from the ether library **25a-s** possessed better potencies. Particularly, the picolyl analogs **25k**, **25l**, and **25m** each exhibited an EC_{50} of approximately 2 μM. A full concentration response curve for **25k** in the presence of fixed ACh EC_{20} is presented in **Figure 6**. **25k** elicited a robust potentiation of M_4 activation, elevating the submaximal ACh response to over 130% of the maximum response induced by a high concentration of ACh alone. Looking ahead to *in vivo* vehicle formulations, the structure of **25k** was particularly advantageous, as the presence of a basic amine would allow for an HCl salt to

confer greater aqueous vehicle solubility. Based on these potency data, the six compounds having EC_{50} values below 10 μM were examined for their ability to leftshift a full ACh CRC when applied at a fixed 30 μM concentration in a similar functional Ca^{2+} assay with rM_4/G_{qi5}-cells (i.e. foldshift assay). In the case of other allosteric potentiators of GPCRs, compound potency often fails to correlate tightly with foldshift. For example, a compound with high potency but low efficacy can exhibit next to no foldshift, and conversely a compound with low potency but high efficacy can exhibit a substantial foldshift. Hence, evaluation of foldshift for novel potentiators having upper single-digit micromolar potencies can sometimes uncover SAR that would have otherwise been missed.

As shown in **Table 2**, neither morpholino compound **21c** nor ethyl compound **21p** caused a leftward shift in the ACh CRC thus demonstrating the compromised activity found with alkylamine modification at the 6-position of the scaffold. The same lack of effect was seen with the tertiary amine analog **25a** from the ether library. However, the ether linked morpholino **25c** and pyrrolidine **25d** analogs demonstrated strong respective 37x and 25x foldshift effects. Interestingly, movement of the nitrogen from the 2-position or 3-position of the picolyl ethers **25m** and **25l** to the 4-position of **25k**, **Table 2**, progressively increased the foldshift from 5x to 9x and ultimately 50x, respectively.

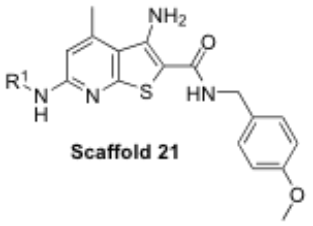

Scaffold 21

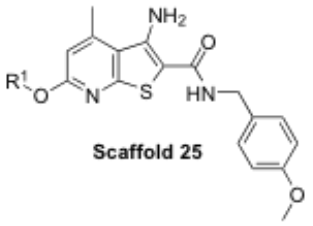

Scaffold 25

Compound	R^1	EC_{50} (μM)	Foldshift
21a		>10	-
21b	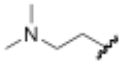	>10	-
21c	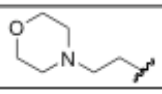	9.1	1x
21e	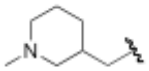	>10	-
21l	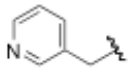	>10	-
21n		>10	-
21o		>10	-
21p		>10	1x

Compound	R^1	EC_{50} (μM)	Foldshift
25a	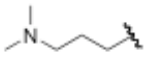	>10	1x
25b	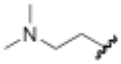	>10	-
25c	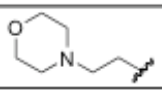	6.5	37x
25e	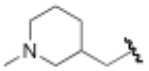	>10	-
25d	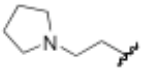	8.2	25x
25k	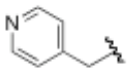	2.0	50x
25l	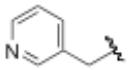	2.2	9x
25m	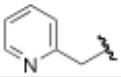	1.8	5x

Table 2. Structures, activities, and ACh CRC -fold shifts of M_4 PAM analog libraries **21** and **25**.

Taken together, these data suggested ether-linked modifications to the 6-position of the scaffold were more tolerated than alkylamine-linked changes. However, despite retention of robust potentiation properties in terms of foldshift for **25c**, **25d**, and especially **25k**, the potency of these analogs was moderately diminished relative to parent compound VU0152100, **7p**. Furthermore, the SAR for these two libraries underlines the aforementioned importance of considering

both foldshift and potency when evaluating allosteric potentiators. Although each of the three picolyl ether analogs had ~2 μM EC_{50} values, their potentiation effects on the ACh CRC revealed dramatic differences in efficacy.

For the next library iteration, we postulated that with the picolyl or ethyl morpholine ether moieties on the left-hand side of the molecule, the *p*-methoxybenzyl on the right-hand side might no longer be the favored amide side chain. We considered that a different side chain could allow retention of strong potentiator activity and at the same time return the sub-micromolar potency of the parent structure. To this end, we opted to re-scan with approximately 18 side chain groups while holding constant each of the three picolyl ether modifications, the morpholino ether, and the dimethylpropylamine ether. The morpholino and 4-picolyl were clear choices based on their degree of foldshift, but the 2-picolyl and 3-picolyl were also included to be comprehensive. Likewise, the dimethylpropylamine ether was used to provide for the possibility that a different amide side chain may rescue the activity of **25a** (i.e. a matrix-like approach to broaden SAR).

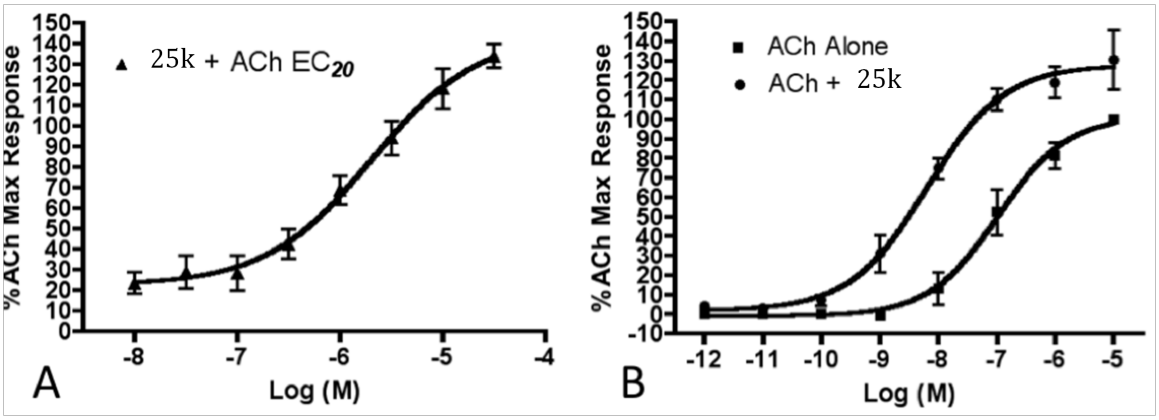

Figure 6. Potentiation effects of **25k** at rM_4 by functional Ca^{2+} mobilization assay. (A, left) Concentration response curve for **25k** in the presence of a fixed submaximal concentration of ACh (~EC_{20}). (B, right) Full concentration response curve for ACh in the presence and absence of a fixed 30 μM concentration of **25k**. All data represent the mean values of at least three experiments with similar results.

These third generation libraries began with the cyclization between pyridone **23** and ethyl chloroacetate **26** to produce thienopyridone ethyl ester **27**. To obtain the five alkyl ethers **28a-e**, **27** was reacted with the five selected side chains from our previously mentioned second generation library. These five scaffolds were saponified and immediately coupled with 18 amines to produce five alkyl ether libraries with different amide side chains **29a-p, 30a-r, 31a-o, 32a-p, 33a-o**, **Scheme 3**.

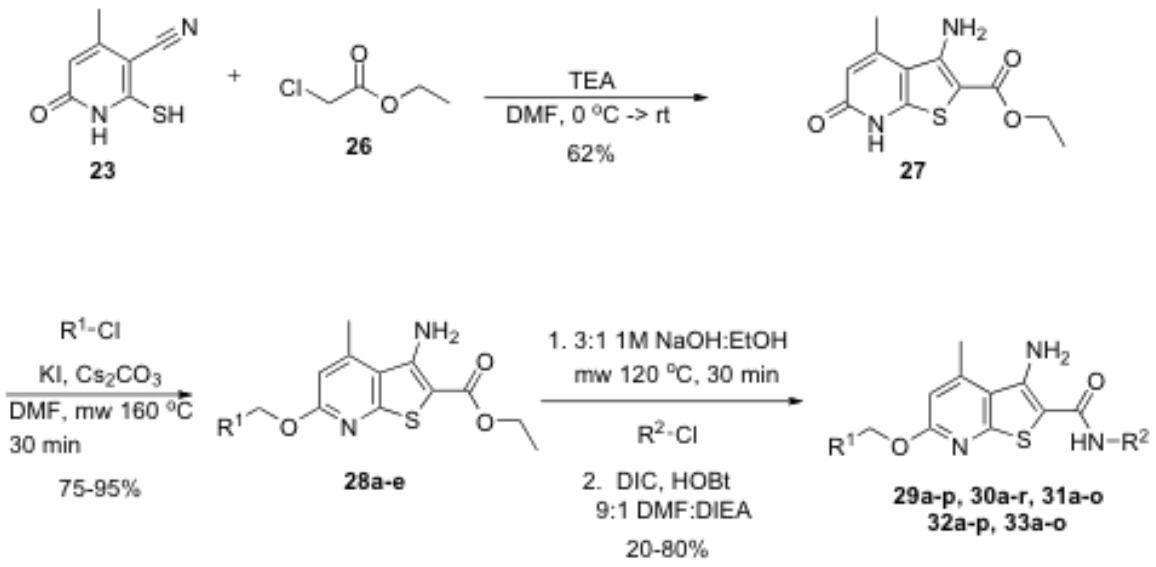

Scheme 3. Synthesis of analog libraries **29-33**, utilizing the 5 best alkyl ether functional groups.

As before, these libraries were screened first in a single-point 10 μM potentiation assay that tested their ability to enhance the response of a submaximal (~EC_{20}) concentration of ACh in rM_4/G_{qi5}-cells, **Figure 7**. Potentiation ranged from absent to pronounced within each of these libraries, revealing generally consistent SAR across all of the five ether-linked modifications held constant on the left-hand side of the structure. From this, eleven compounds were selected for CRCs and foldshift assays based on degree of potentiation. The associated SAR data for the chosen compounds from libraries **29-33** obtained from these assays are shown in **Table 3**.

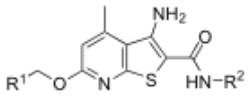

Scaffolds 29-33

	R^1	R^2	EC_{50} (μM)	Foldshift		R^1	R^2	EC_{50} (μM)	Foldshift
29o	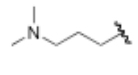	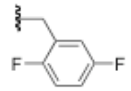	2.75	14x	**30h**	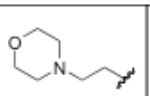		8.73	62x
30a	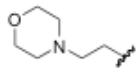		7.42	40x	**31n**	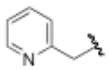	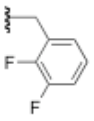	5.40	28x
30b	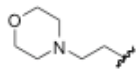		6.25	67x	**31o**	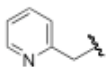	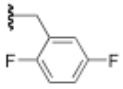	>10	41x
30c	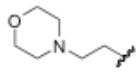		5.81	51x	**33n**	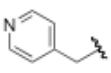	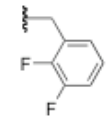	2.44	44x
30g	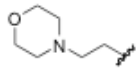		7.15	36x	**33o**	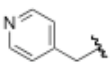	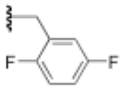	3.78	64x

Table 3. SAR for select analogs from libraries **29-33** chosen based on an initial single-point potentiation screen at rM_4.

All compounds evaluated possessed an EC_{50} below 10 μM, except for **31n**, the di-flurobenzyl substituted 2-picolyl compound. As found and discussed previously with regard to earlier libraries, foldshift did not track tightly with potency, as shown for example with **30h**. This *t*-butyl substituted morpholine analog had near 9 μM potency but caused a robust 62x foldshift of the ACh CRC. The dimethylpropyl analogs **29o** displayed approximately 3 μM potency yet had only moderate ACh foldshift effects. Interestingly, this dimethylpropylamine

motiety at R^1 conferred poor potency (> 10 μM) in its parent compound **21b** possessing the *p*-methoxybenzyl group at R^2, but the amide scan producing library **29a-p** discovered side chains that rescued activity for this left-hand side modification.

In general, di-fluorinated benzylic substitutions at R^2 were favored, providing analogs with 2-5 μM range potencies and broad foldshift values. The 4-picolyl moieties of R^1 with the 2,3-difluoro and 2,5-difluoro substitutions at R^2 of **33n** and **33o** proved most desired when a balance of both potency and

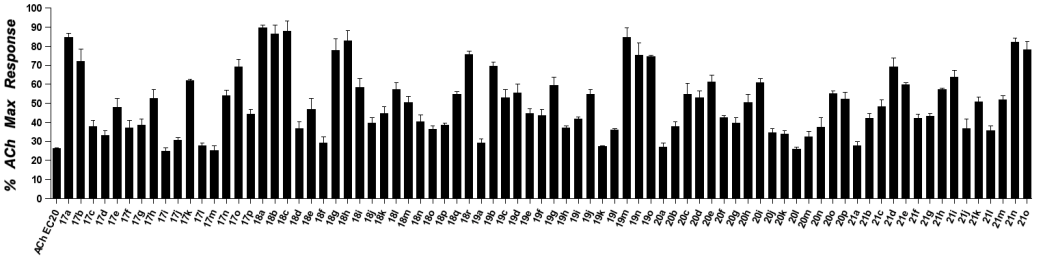

potentiation efficacy, consistent with previous SAR.

Figure 7. Single-point potentiator screen of libraries **29-33** in rM_4-cells. Test compound (fixed 10 μM) is added prior to addition of a submaximal (~EC_{20}) concentration of Ach. Intracellular Ca^{2+} mobilization is used as a functional readout for M_4 activation. All data shown here represent the mean values from at least three experiments with similar results.

The morpholines at R^1 of library **30a-r** with bare alkyl and mono-oxygenated side chains at R^2 possessed strong foldshift effects despite moderately weaker potency compared with **31n** and **33n**. The best lead compounds for this library are summarized in **Figure 8**.

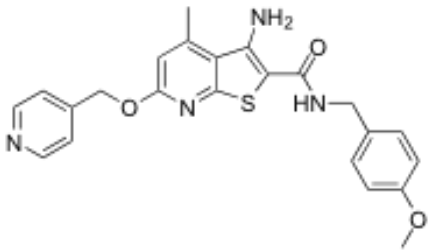

25k, EC_{50} = 2.0μM Foldshift = 50x

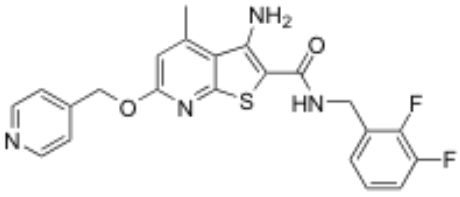

33n, EC_{50} = 2.4μM Foldshift = 44x

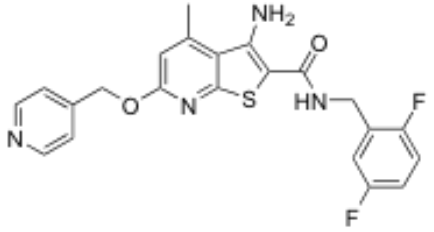

33o, EC_{50} = 3.8μM Foldshift = 64x

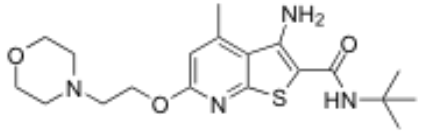

30h, EC_{50} = 8.7μM Foldshift = 62x

Figure 8. Summary of second generation leads.

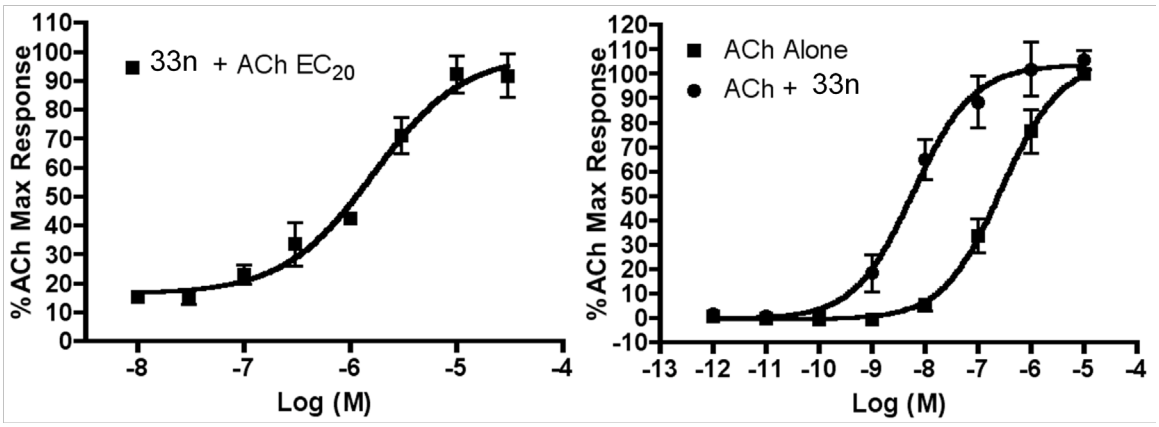

Figure 9. The CRC for elevation of an ACh ~EC_{20} and foldshift on a full ACh CRC for analogue **33n**. Interestingly, this 2,3-difluorobenzyl substituted analogue did not elevate the maximal response of ACh at the top of the CRC, which contrasts with 4-methoxybenzyl analogue **25k.**

Despite generation of a multidimensional library of analogues varying both sides of the lead scaffold, the approximately 400 nM potency (rat M_4) of the first generation compounds **7o** and **7p** could not be improved upon despite retention of strong potentiation activity in terms of ACh CRC fold-shift (e.g. >50x). Indeed, compounds **25k**, **30b**, and **33o** each caused substantial leftward shift of ACh CRCs when applied at 30 μM, but were approximately an order of magnitude less potent than the first generation compounds at rat M_4 receptor. These SAR suggest the presence of a possible ~2 μM potency floor for this chemotype with 6-position ether or amine modifications, as variation of the amide side chain failed to provide congers with EC_{50} values below this level. In parallel, we evaluated the microsomal stability of **25k**, **33n**, **33o**, and **30h** in both rat and

human microsomes. Replacement of the metabolically labile 6-methyl group with the ether linkage did indeed improve metabolic stability for all four analogues **25k**, **33n**, **33o**, and **30h** (>90% parent remaining after 90 min) as compared to **7o** and **7p** (<10% parent remaining after 90 min). Moreover, incorporation of the basic amine moieties in **25k**, **33n**, **33o**, and **30h** also improved solubility providing either homogeneous solutions or uniform microsuspensions, as the HCl salts at 10 mg mL^{-1}, across a panel of pharmaceutically acceptable vehicles (β-cyclodextrin, PEG400/H_2O, etc.) relative to **7o** and **7p**, which were only soluble in 10% Tween80. In fact, **33n** afforded a homogeneous solution at 15 mg/mL^{-1} in pH 3 saline.

Despite micromolar potency at rat M_4, we evaluated **25k**, **33n**, and **33o** in our standard reversal of amphetamine-induced hyperlocomotion *in vivo* model, since a long-standing question in the PAM field has centered on whether EC_{50} or fold-shift is more relevant to provide in vivo efficacy (21). Both **7o** and **7p** (EC_{50} values ~400 nM, fold-shifts of 30x and 70x, respectively) were efficacious in this model. Interestingly, both **25k** and **33o** produced modest decreases in amphetamine-induced hyperlocomotion while **33n** had no effect over the time course tested, **Figure 10**.

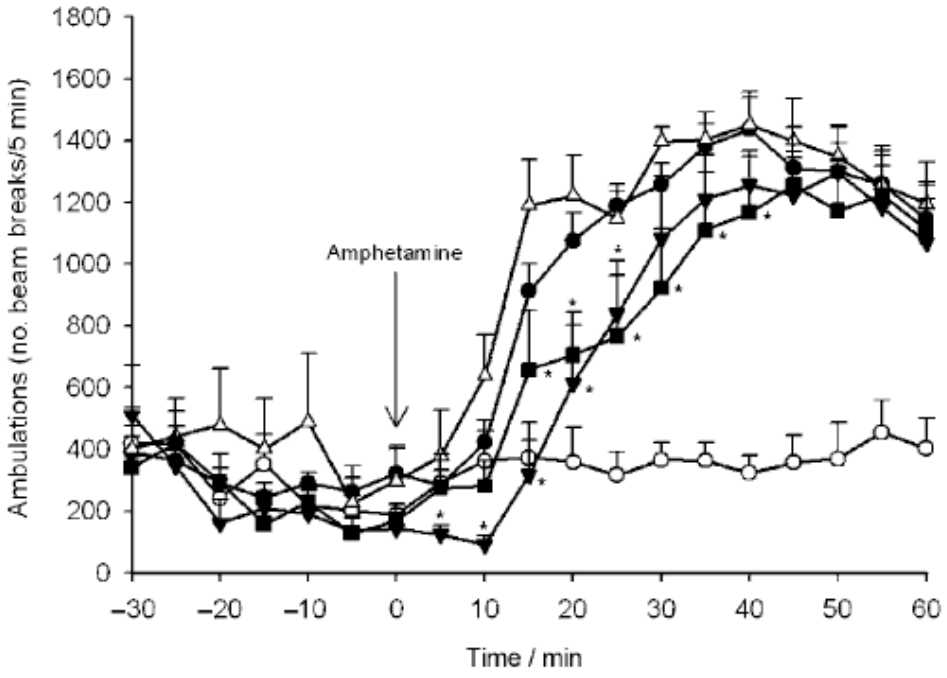

Figure 10. Modest reversal by **25k** and **33o** of amphetamine-induced hyperlocomotor activity in rats. Rats were pretreated for 30 min with vehicle (10% Tween80 i.p., n=9; light circle and dark circle) or a 56.6 $mgkg^{-1}$ dose of either **25k**, **33n**, or **33o** i.p. (n=4), then given an injection of 1 mg/kg^{-1} s.c. amphetamine (indicated at t=0 min) except vehicle control, which was dosed with H_2O instead and locomotor activity was measured for an additional 60 min. The error bars represent the mean value plus or minus SEM. * denotes $P<0.05$ versus vehicle plus amphetamine control group (dark circle).

These findings suggest that the diminished potency of these new compounds may have translated to reduced in vivo efficacy relative to **7o** and **7p**. Primarily, our efforts were aimed at exploring SAR at rat M_4 and optimizing this series for beneficial DMPK and vehicle formulation properties for in vivo rodent behavioral studies. While stability and physiochemical properties were improved, potency at rat M_4 was diminished to a point where in vivo efficacy was reduced and, in the case of **33n**, in vivo efficacy was lost. However, rat and human mAChRs do diverge and species differences have been noted for other mAChR PAMs. Therefore, we opted to evaluate representative compounds **25k**, **33n**, **33o**, and **30h** in analogous functional cellbased Ca^{2+} assays using cells expressing the human M_4 receptor (and promiscuous G_{q15} for Ca^{2+} mobilization readout). To this end, these four compounds were submitted to Millipore Corp. (St. Charles, USA) and assayed by their GPCR Profiler Service, which provided potency and ACh CRC fold-shift values with the human M_4 receptor. Remarkably, each compound possessed EC_{50} values approximately in the 100–200 nM range at human M_4 **Figure 11a**, more than an order of magnitude greater potency than at the rat M_4 receptor. Each compound also elicited large leftward shifts of the control ACh CRC in human M_4 cells **Figure 11b** similar to their respective fold-shifts at rat M_4. In contrast, the prototypical M4 PAMs **7o** and **7p** and about 20 other first generation analogues, displayed near equivalent EC_{50} values at rat and human M_4, suggesting the basic residues in these newer analogue contact divergent residues in human M_4.

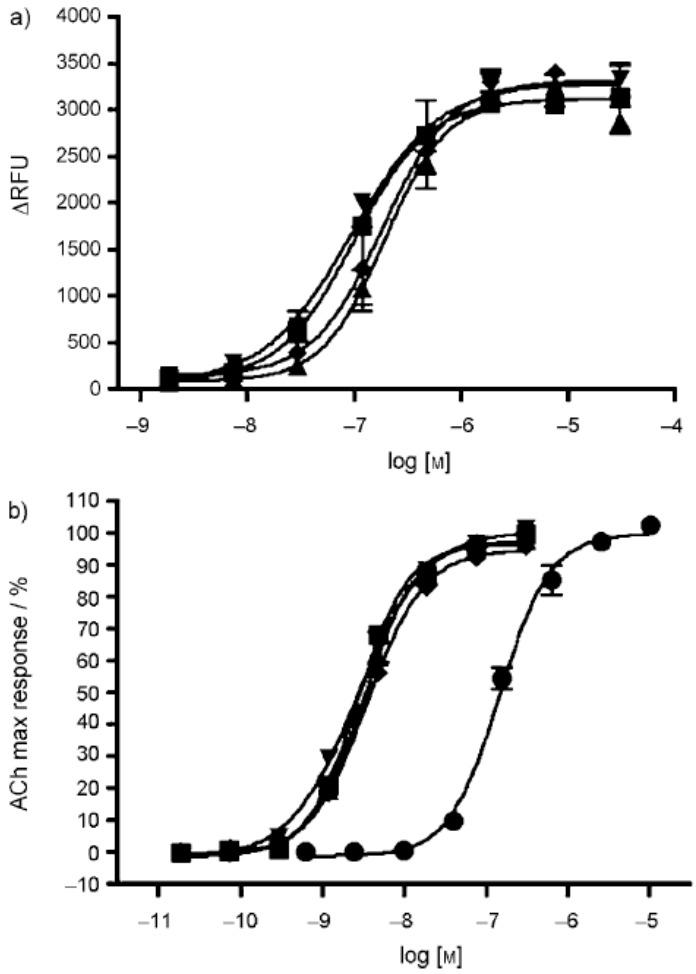

Figure 11. Potentiation effects of **25k**, **30h**, **33n**, and **33o** in human M_4/G_{q15} expressing cells by functional Ca^{2+} mobilization assay.

While receptor expression levels in the two cell lines is not known, ACh EC_{50} values in the two cell lines are equivalent (rat M_4 ACh, EC_{50}=154 nM; human M_4 ACh, EC_{50}=100 nM), and all first generation analogues were also equipotent. These human M_4 data exemplify the differences that may exist between species in terms of compound potency, efficacy, and other pharmacological parameters, despite relatively high structural similarity between

rat and human mAChRs. In addition, **25k**, **33n**, **33o**, and **30h** and related second generation analogues remained highly M_4 selective at both human and rat mAChR cell lines **Figure 12**. Whereas a 30 μM concentration of **25k**, **33n**, **33o**, and **30h** afforded large leftward shifts (44–63x) of the ACh CRCs of M_4, these same concentrations of compound had no effect on the ACh CRCs of M_1, M_2, M_3 or M_5 (data shown is for rat mAChRs).

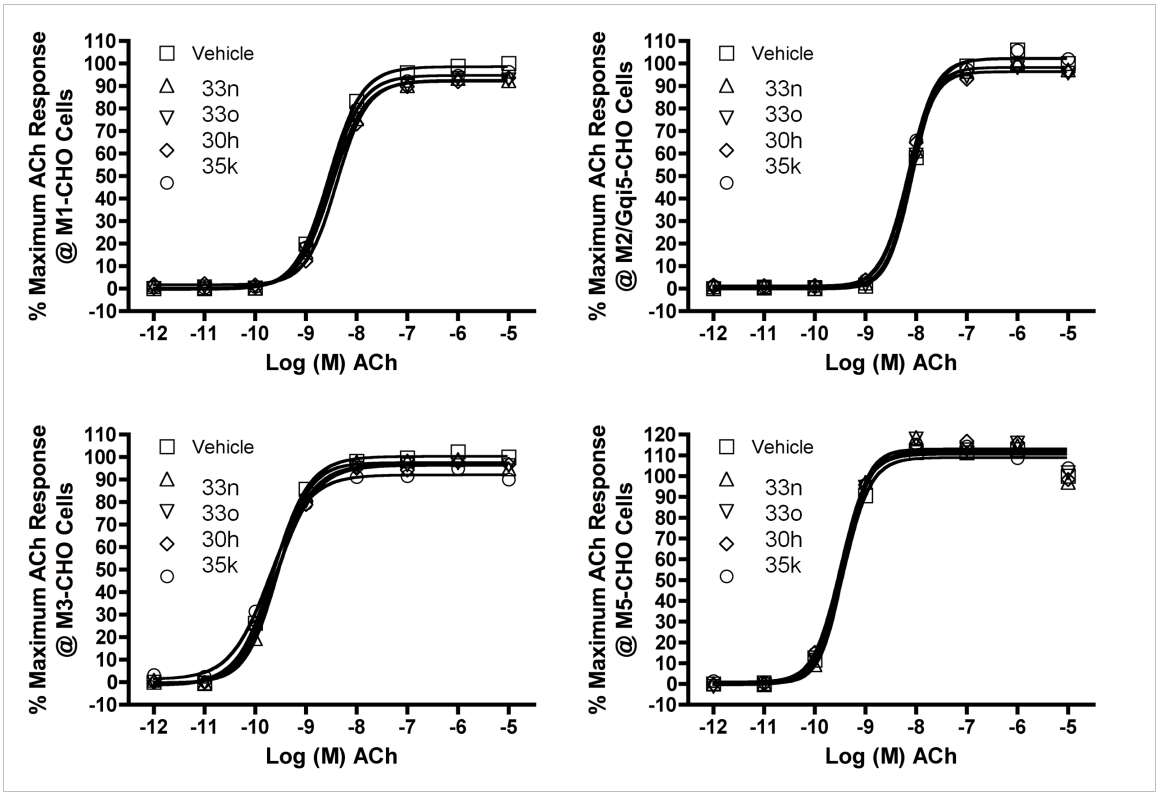

Figure 12. Full concentration response curves for ACh in the absence and presence of a fixed 30 μM concentration of potentiators **25k**, **30h**, **33n**, and **33o** on M_1, M_2, M_3, and M_5 cells.

Finally, while M_1 PAMs and allosteric agonists have the potential to effect both the positive and cognitive symptom clusters of schizophrenia, M_4 PAMs should only treat the positive symptoms (12-16). Upon recognition that compounds **25k**, **33n**, **33o**, and **30h** possess the basic features of the refined H_3 pharmacophore model, **Figure 13**, we evaluated these compounds for their ability to function as H_3 antagonists and provide procognitive attributes (22, 23).

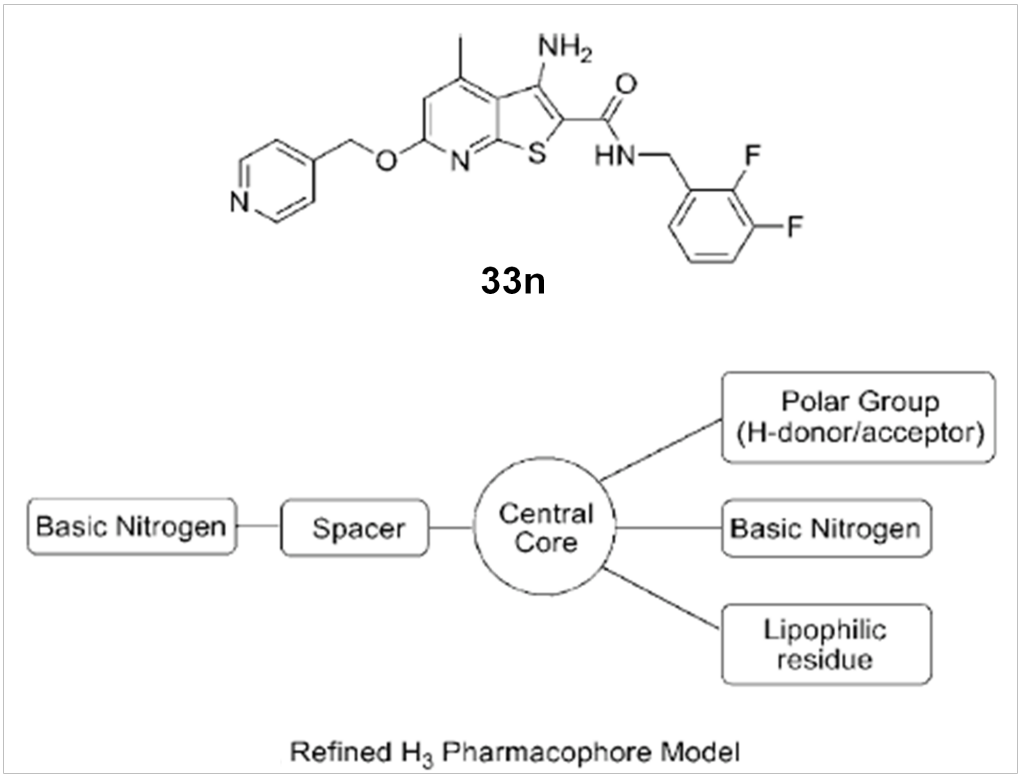

Figure 13. Refined H_3 pharmacophore model and alignment with M_4 PAM **33n**.

Compounds **25k**, **33o** and **30h** were found to inhibit human H_3 with IC_{50} values of ~10 μM, while **33n** afforded an IC_{50} value of 6.3 μM. While weak, this

result suggests that it is possible to "dial in" H_3 antagonist activity into this new series of M_4 PAMs, and future efforts will focus on optimizing compounds with comparable M_4 PAM and H_3 antagonist activity for the treatment of the positive and cognitive symptom clusters of schizophrenia. In summary, a lead optimization campaign around VU0010010, **1**, furnished M4 PAMs **7o** and **7p**, elaborating on these compounds provided novel analogues with improved metabolic stability and physiochemical properties, but diminished efficacy at rat M_4 (EC_{50} values ~2 μM) while retaining comparable foldshift (14–67x) of the ACh CRC. Moreover, though weak at rat M_4, several analogues displayed modest *in vivo* efficacy in reversing amphetamine-induced hyperlocomotion, a classic preclinical antipsychotic model. Surprisingly, we noted significant species differences within this new series of M_4 PAMs, where analogues such as **33n** displayed an order of magnitude greater potency at human M_4 (EC_{50}=95 nM) than at the rat M_4 receptor (EC_{50}=2.4 μM) with comparable fold-shifts (human, 60x; rat, 44x) and high M_4 mAChR subtype selectivity. To further expand the therapeutic relevance of these new M_4 PAMs for the treatment of schizophrenia beyond the positive symptom cluster, we evaluated analogues against the H_3 receptor as they align well with the refined H_3 pharmacophore model. M_4 PAM **33n** was found to provide modest inhibition of H_3 with an IC_{50} value of 6.3 μM, suggesting that it might be possible to develop analogues with dual M_4 PAM and H_3 antagonist activity to effectively treat both the positive and cognitive symptom clusters of schizophrenia.

M_4 Experimental Section-

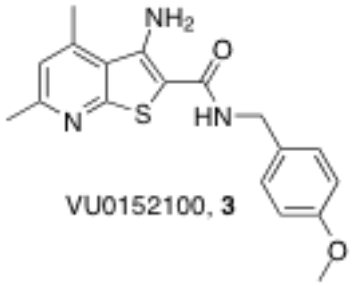

VU0152100, **3**

Synthesis of 3-amino-*N*-(4-methoxybenzyl)-4,6-dimethylthieno[2,3-*b*]pyridine-2-carboxamide, VU0152100, 3:

The following components were added to a stirred solution of 3-amino-4,6-dimethylthioenol[2,3-*b*]-pyridine-2-carboxylic acid (2.50 g, 11.26 mmol; ChemBridge Corporation) in CH_2Cl_2 (90 mL) at 25°C under room atmosphere: *N,N*-diisopropylethylamine (10 mL, 56.66 mmol); 1-hydroxybenzotriazole hydrate (1.52 g, 11.26 mmol, 1.0 equivalents); piperonylamine (1.87 g, 12.38 mmol, 1.1 equivalents); and *N*-(3-dimethylaminopropyl)-*N*'-ethyl-carbodiimide hydrochloride (4.32 g, 22.52 mmol, 2 equivalents). After 48 h, macroporous triethylammonium methylpolystyrene carbonate (3.66 g, 11.26 mmol, 3.077 mmol/g, 1.0 equivalents) was added to the solution, which was then stirred for 3 h at 25 °C under room atmosphere. The solution was vacuum-filtered next, and the filtrate was separated with citric acid (1.0 M in water) and CH_2Cl_2. The organics were dried over $MgSO_4$ and concentrated in vacuo to produce a dark yellow solid. The solid was purified by column chromatography (silica gel, fixed 1:2 EtOAc/hexanes) to afford 2.0 g (5.63 mmol, 50%) of the title compound **3** as a

yellow solid. Analytical LC/MS (J-Sphere80-S4, 3.0 X 50 mm, 4.0 min gradient, 5%[CH_3CN]: 95%[0.1% trifluoroacetic acid/H2O] to 100%[CH3CN]): 2.740 min, 99% (214 nm and ELSD), M + 1 peak *m/e* 356.10; ^{1}H NMR (400 MHz, DMSO-d6) δ = 8.38 (s, 1H), 7.18 (s, 1H), 6.88 (s, 1H), 6.84 (d, *J* = 8.0 Hz, 1H), 6.78 (d, *J* = 8.0 Hz, 1H), 5.98 (br s, 2H), 5.97 (s, 2H), 4.30 (d, *J* = 5.2 Hz, 2H), 2.77 (s, 3H), 2.57 (s, 3H); ^{13}CNMR (100 MHz, DMSO-d6) δ = 179.9, 164.8, 161.7, 158.0, 153.4, 147.4, 133.8, 122.4, 121.9, 120.5, 108.0, 107.9, 100.8, 92.8, 42.1, 22.4, 20.0; high-resolution mass spectroscopy (Q-ToF): *m/z* calc for $C_{18}H_{17}N_3O_3S$ [M + H]: 356.0991; found, 356.1069.

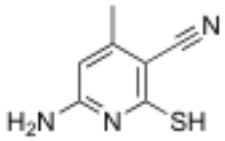

18

6-amino-2-mercapto-4-methylnicotinonitrile 18:

To five 20 mL microwave vials containing 2-cyanothioacetamide (0.01 mol) each was added 3-aminocrotonitrile (0.01 mol) and then EtOH (10 mL). Once dissolved pyridine (0.05 mol) was added and the vial was capped. The reaction mixtures were heated to 160 ^{o}C for 12 min. consecutively. The crude reaction mixtures were combined and concentrated to a reddish oil. To this was added MeOH (150 mL) and heated to reflux, upon cooling an orange solid crashed out which was filtered and washed with ether to afford 3.47g of pure **(6)** (42%). ^{1}H NMR (400MHz, DMSO-d_6): δ = 7.20 (br s, 2H), 5.90 (s, 1H), 2.2 (s, 3H). ^{13}C

(100MHz, DMSO-d_6): d= 175.3, 155.1, 153.5, 118.0, 100.2, 98.9, 20.8. HRMS calcd for $C_7H_7N_3S$ [M + H] 166.0435; found 166.0439.

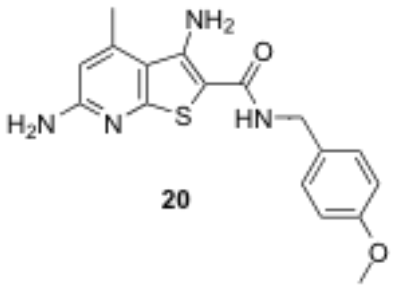

20

3,6-diamino-*N*-(4-methoxybenzyl)-4-methylthieno[2,3-*b*]pyridine-2-carboxamide 20:

To a 20 mL microwave vial containing **18** (3.0 mmol) was added K_2CO_3 (6 mmol), and DMF (10 mL). To this solution was added solid **19** then capped, and heated to 160 ^oC for 10 min. Once complete the reaction was partitioned between H_2O (100 mL) and DCM (100 mL), separated, and the aqueous layer extracted 2x with DCM (100 mL). The organic layer was dried with solid $MgSO_4$, filtered, and concentrated to a light brown solid. This solid was crystallized in EtOAc and Hexanes and filtered to obtain 0.8g of pure **20** as a light yellow solid (75%). ^1H NMR (400MHz, DMSO-d_6): δ = 8.41 (s, 1H), 7.13 (d, *J* = 8.8Hz, 2H), 6.98 (br s, 2H), 6.83 (d, *J* = 8.4 Hz, 2H), 6.12 (s, 1H), 3.89 (s, 2H), 3.72 (s, 3H), 2.22 (s, 3H). ^{13}C (100MHz, DMSO-d_6): δ = 167.4, 160.8, 160.1, 158.1, 151.0, 131.1, 128.3, 116.7, 113.7, 103.9, 55.0, 41.9, 32.8, 19.6. HRMS calcd for $C_{17}H_{18}N_4O_2S$ [M + H] 343.1222; found 343.1229.

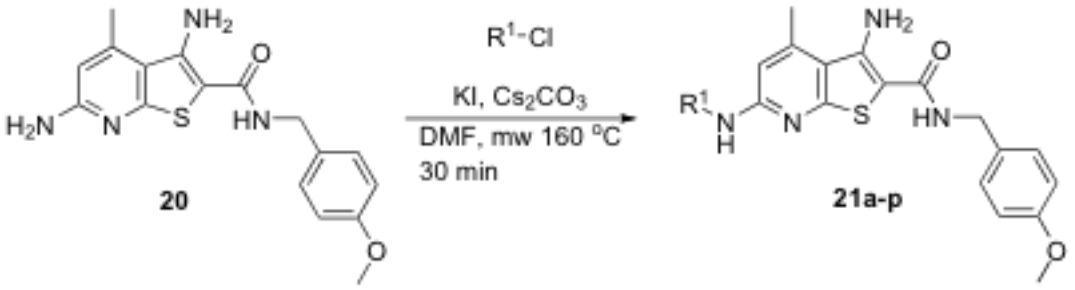

Alkylamine Library (21a-p) General Procedure:

To a 5 mL microwave vial containing **20** (0.073 mmol), was added Cs_2CO_3 (0.21 mmol), KI (0.073 mmol), R^1-Cl (0.080 mmol), and DMF (3 mL). The reaction was stirred 5 min. to eliminate CO_2, capped, and heated to 160 ^oC for 30 min. Once complete the reaction was partitioned between H_2O (5 mL), and DCM (5 mL), separated via a 12 mL IST phase separator, concentrated and purified by mass directed HPLC to furnish **21a-p** (15-80%).

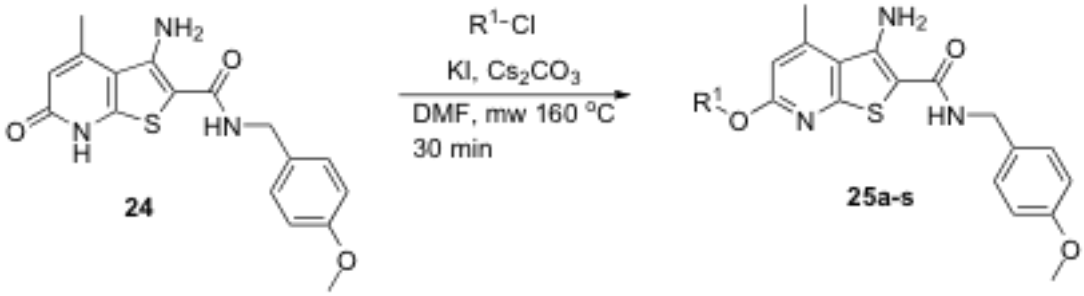

Alkylether Library (25a-s) General Procedure:

To a 5 mL microwave vial containing **24** (0.146 mmol), was added Cs_2CO_3 (0.438 mmol), KI (0.291 mmol), R^1-Cl (0.219 mmol), and DMF (3 mL). The

reaction was stirred 5 min. to eliminate CO_2, capped, and heated to 160 ^oC for 30 min. Once complete the reaction was partitioned between H_2O (5 mL), and DCM (5 mL), separated via a 12 mL IST phase separator, concentrated and purified by mass directed HPLC to furnish **25a-s** (15-80%).

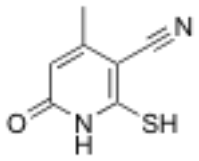

23

2-mercapto-4-methyl-6-oxo-1,6-dihydropyridine-3-carbonitrile 23:

^1H NMR (400MHz, DMSO-d_6): δ = 10.40 (br s, 1H), 8.67 (br s, 1H), 5.38 (s, 1H), 1.99 (s, 3H). ^{13}C (100MHz, DMSO-d_6): δ = 176.3, 162.4, 151.0, 120.7, 106.8, 92.7, 20.5. HRMS calcd for $C_7H_6N_2OS$ [M + H] 167.0277; found 167.0279.

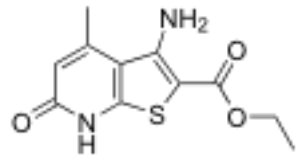

27

ethyl 3-amino-4-methyl-6-oxo-6,7-dihydrothieno[2,3-*b*]pyridine-2-carboxylate 27:

^1H NMR (400MHz, DMSO-d_6); δ = 6.42 (s, 1H), 4.12 (m, 4H), 2.34 (s, 3H), 1.18 (t, J = 7.2 Hz, 3H). ^{13}C (100MHz, DMSO-d_6): δ = 168.3, 164.8, 160.0, 154.5,

115.5, 106.8, 97.8, 59.9, 19.7, 13.9. HRMS calcd for $C_{11}H_{13}N_2O_3S$ [M + H] 253.0647, found 253.0644.

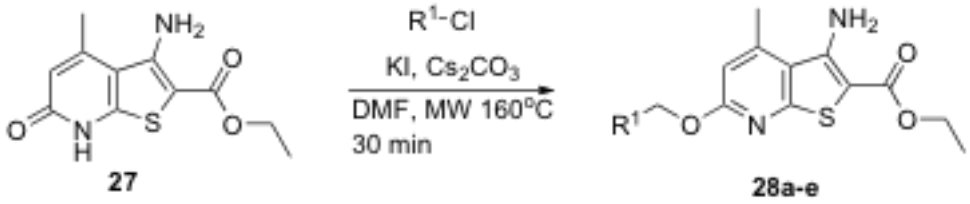

Alkyl Pyridone Ethyl Ester (28a-e) General Procedure:

To a 20 mL microwave vial containing **27** (0.04 mol), was added Cs_2CO_3 (0.012 mol), KI (0.008 mol), R^1-Cl (0.0044 mmol), and DMF (10 mL). The reaction was stirred 5 min. to eliminate CO_2, capped, and heated to 160 ^oC for 30 min. Once complete the reaction was partitioned between H_2O (50 mL), and DCM (50 mL), separated, and the aqueous extracted 1x with DCM (50 mL). The organic layer was dried with $MgSO_4$, filtered and concentrated. The resulting material was added to a 10g 60CC SCX cartridge and washed with 3 column volumes of MeOH. The product was then eluted with 2 column volumes of 2M NH_3 in MeOH to provide pure **28a-e** (75-95%).

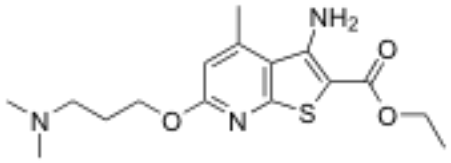

28a

ethyl 3-amino-6-(3-(dimethylamino)propoxy)-4-methylthieno[2,3-*b*]pyridine-2-carboxylate 28a:

^{1}H NMR (400MHz, DMSO-d_6); δ = 6.72 (s, 2H), 6.57 (s, 1H), 4.25 (m, 4H), 2.66 (s, 3H), 2.37 (t, *J* = 7.2 Hz, 2H), 2.16 (s, 6H), 1.84 (m, 2H), 1.27 (t, *J* = 6.8 Hz, 3H). ^{13}C (100MHz, DMSO-d_6): δ = 164.7, 163.8, 159.3, 150.3, 147.6, 119.1, 109.5, 64.5, 59.7, 55.5, 44.9, 26.3, 19.8, 14.4. HRMS calcd for $C_{16}H_{24}N_3O_3S$ [M + H] 338.1538, found 338.1527.

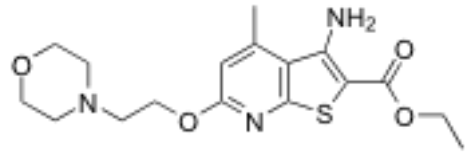

28b

ethyl 3-amino-4-methyl-6-(2-morpholinoethoxy)thieno[2,3-*b*]pyridine-2-carboxylate 28b:

^{1}H NMR (400MHz, DMSO-d_6); δ = 6.76 (s, 2H), 6.65 (s, 1H), 4.57 (br s, 2H), 4.24 (q, *J* = 14.4, 7.2 Hz, 2H), 3.72 (br s, 4H), 3.20 (br s, 6H), 2.70 (s, 3H), 1.27 (t, *J* = 6.8 Hz, 3H). ^{13}C (100MHz, DMSO-d_6): δ = 164.7, 163.1, 159.0, 150.3, 148.1, 119.6, 118.7, 115.7, 109.6, 64.3, 59.8, 55.5, 52.3, 19.9, 14.4. HRMS calcd for $C_{17}H_{24}N_3O_4S$ [M + H] 366.1488, found 366.1476.

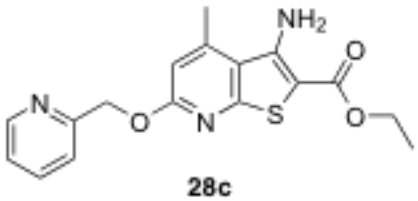

28c

ethyl 3-amino-4-methyl-6-(pyridin-2-ylmethoxy)thieno[2,3-*b*]pyridine-2-carboxylate 28c:

^{1}H NMR (400MHz, DMSO-d_6); δ = 8.55 (d, *J* = 4.4 Hz, 1H), 7.80, (t, *J* = 8.0 Hz, 1H), 7.46 (d, *J* = 8.0 Hz, 1H), 7.33 (t, *J* = 6 Hz, 1H), 6.74 (s, 2H), 6.73 (s, 1H), 5.45 (s, 2H), 4.23 (q, *J* = 14.0, 7.2 Hz, 2H), 2.70 (s, 3H), 1.26 (t, *J* = 7.2 Hz, 3H). ^{13}C (100MHz, DMSO-d_6): δ = 164.7, 163.3, 159.0, 156.3, 150.2, 149.1, 148.1, 136.8, 122.9, 121.7, 119.6, 109.6, 68.1, 59.8, 19.9, 14.4. HRMS calcd for $C_{17}H_{18}N_3O_3S$ [M + H] 344.1069, found 344.1057.

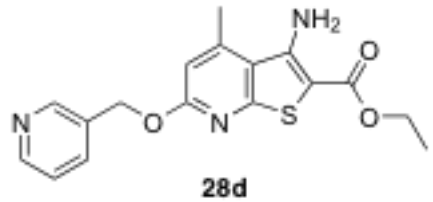

28d

ethyl 3-amino-4-methyl-6-(pyridin-3-ylmethoxy)thieno[2,3-*b*]pyridine-2-carboxylate 28d:

^{1}H NMR (400MHz, DMSO-d_6); δ = 8.70 (s, 1H), 8.54 (d, *J* = 4.8 Hz, 1H), 7.89 (d, *J* = 8.0 Hz, 1H), 7.42 (t, *J* = 4.8 Hz, 1H), 6.75 (s, 2H), 6.97 (s, 1H), 5.42 (s, 2H),

4.24 (q, *J* = 14.4, 7.2 Hz, 2H), 2.69 (s, 3H), 1.28 (t, *J* = 6.8 Hz, 3H). ^{13}C (100MHz, DMSO-d_6): δ = 164.7, 163.3, 159.0, 150.3, 149.4, 149.1, 148.1, 136.1, 132.3, 123.5, 119.6, 109.6, 65.3, 59.8, 19.9, 14.4. HRMS calcd for $C_{17}H_{18}N_3O_3S$ [M + H] 344.1069, found 344.1064.

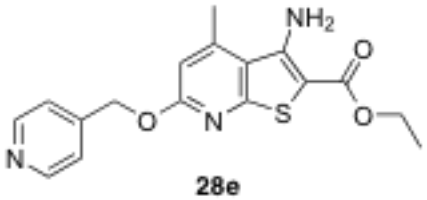

28e

ethyl 3-amino-4-methyl-6-(pyridin-4-ylmethoxy)thieno[2,3-*b*]pyridine-2-carboxylate 28e:

^1H NMR (400MHz, DMSO-d_6); δ = 8.56 (d, *J* = 6.0 Hz, 2H), 7.45 (d, *J* = 6.0 Hz, 2H), 6.77 (s, 1H), 6.75 (s, 2H), 5.45 (s, 2H), 4.24 (q, *J* = 14.0, 6.8 Hz, 2H), 2.71 (s, 3H), 1.27 (t, *J* = 7.2 Hz, 3H). ^{13}C (100MHz, DMSO-d_6): δ = 164.6, 163.1, 159.0, 150.2, 149.6, 148.3, 145.9, 122.0, 109.6, 65.7, 59.8, 19.9, 14.4. HRMS calcd for $C_{17}H_{18}N_3O_3S$ [M + H] 344.1069, found 344.1057.

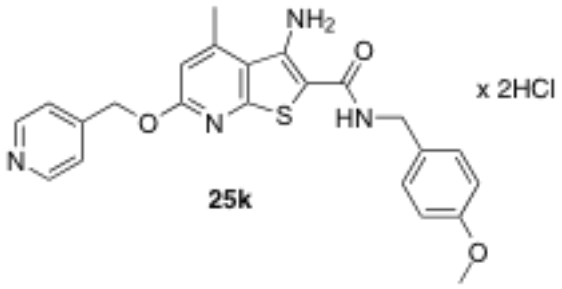

25k

3-amino-*N*-(4-methoxybenzyl)-4-methyl-6-(pyridin-4-ylmethoxy)thieno[2,3-*b*]pyridine-2-carboxamide dihydrochloride 25k: ^{1}H NMR (400MHz, DMSO-d_6): δ = 8.90 (d, *J* = 6.4 Hz, 2H), 8.14 (t, *J* = 5.6 Hz, 1H), 8.05 (d, *J* = 6.4 Hz, 2H), 7.22 (d, *J* = 8.8 Hz, 2H), 6.87 (d, *J* = 8.8 Hz, 2H), 6.84 (s, 1H), 5.73 (s, 2H), 4.32 (d, *J* = 5.6 Hz, 2H), 3.72 (s, 3H), 2.74 (s, 3H).). ^{13}C (100MHz, DMSO-d_6): δ = 165.0, 162.0, 158.1, 156.9, 148.1, 147.9, 142.2, 132.0, 129.3, 128.5, 124.1, 121.0, 115.1, 113.6, 109.4, 65.3, 55.0, 41.6, 19.9. HRMS calcd for $C_{23}H_{23}N_4O_3S$ [M + H] 435.1491, found 435.1490.

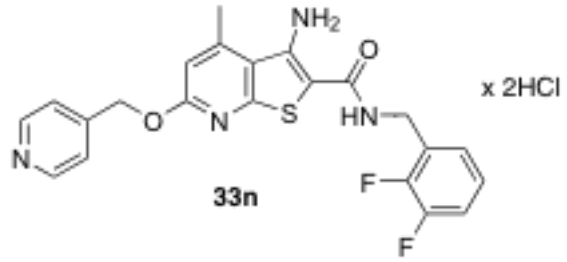

33n

3-amino-*N*-(2,3-difluorobenzyl)-4-methyl-6-(pyridin-4-ylmethoxy)thieno[2,3-*b*]pyridine-2-carboxamide dihydrochloride 33n: ^{1}H NMR (400MHz, DMSO-d_6): δ = 8.92 (d, *J* = 6.8 Hz, 2H), 8.30 (t, *J* = 5.6 Hz, 1H), 8.09 (d, *J* = 6.4 Hz, 2H), 7.32 (m, 1H), 7.16 (m, 2H), 6.85 (s, 1H), 5.75 (s, 2H), 4.46 (d, *J* = 5.6 Hz, 2H),

2.74 (s, 3H). ^{13}C (100MHz, DMSO-d_6): δ = 165.2, 162.1, 157.8, 157.0, 150.8, 148.8, 148.3, 148.1, 146.4, 146.2, 141.4, 129.3 (d, *J* = 11.0 hz), 124.5, 124.3, 120.9, 115.6 (d, *J* = 17.0 Hz), 109.5, 65.3, 35.7, 19.9. HRMS calcd for $C_{22}H_{19}N_4O_2F_2S$ [M + H] 441.1197, found 441.1196.

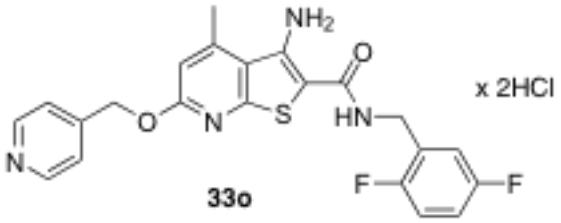

33o

3-amino-*N*-(2,5-difluorobenzyl)-4-methyl-6-(pyridin-4-ylmethoxy)thieno[2,3-*b*]pyridine-2-carboxamide dihydrochloride 33o: ^{1}H NMR (400MHz, DMSO-d_6): δ = 8.57 (d, *J* = 6.0 Hz, 2H), 8.19 (t, *J* = 5.6 Hz, 1H), 7.44 (d, *J* = 6.0 Hz, 2H), 7.24 (m, 1H), 7.10 (m, 2H), 6.77 (br s, 2H), 6.77 (s, 1H), 5.46 (s, 2H), 4.43 (d, *J* = 5.6 Hz, 2H), 2.72 (s, 3H).). ^{13}C (100MHz, DMSO-d_6): δ = 165.3, 162.7, 159.3, 157.2, 156.9, 154.7, 149.6, 148.4, 147.9, 146.0, 128.8 (dd, *J* = 7.0, 17.0 Hz), 121.9, 120.6, 116.6 (dd, *J* = 8.0, 24.0 Hz), 115.2 (dd, *J* = 5.0, 25.0 Hz), 114.9 (dd, *J* = 8.0, 24.0 Hz), 109.6, 65.7, 35.9, 19.9. HRMS calcd for $C_{22}H_{19}N_4O_2F_2S$ [M + H] 441.1197, found 441.1194.

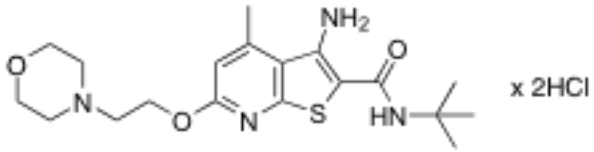

30h

3-amino-*N-tert*-butyl-4-methyl-6-(2-morpholinoethoxy)thieno[2,3-*b*]pyridine-2-carboxamide dihydrochloride 30h: ^{1}H NMR (400MHz, DMSO-d_6): δ = 6.65 (s, 1H), 6.62 (s, 1H), 6.31 (br s, 3H), 4.71 (t, *J* = 4.8 Hz, 2H), 3.87 (m, 4H), 3.50 (m, 4H), 3.17 (m, 2H), 2.70 (s, 3H), 1.36 (s, 9H). ^{13}C (100MHz, DMSO-d_6): δ = 165.3, 162.2, 162.1, 156.6, 147.6, 147.1, 120.9, 109.5, 62.0, 60.5, 54.7, 51.6, 51.2, 28.8, 19.9. HRMS calcd for $C_{19}H_{29}N_4O_3S$ [M + H] 393.1960, found 393.1958.

Cell Culture:

All recombinant CHO cell lines used were previously described (13, 15). CHO cells stably expressing rat M_1, human M_3, or human M_5 were plated at a seeding density of 50,000 cells/100mL/well. CHO cells stably co-expressing human M_2/G_{qi5} and rat M_4/G_{qi5} were plated at a seeding density of 60,000 cells/100mL/well. For calcium mobilization assays, cells were incubated in antibiotic-free medium overnight at 37 °C/5% CO_2 and assayed the following day.

Calcium Mobilization Assay:

All calcium mobilization assays were performed similar to those previously described (13,15). Cells were loaded with calcium indicator dye (Fluo-4 AM, 2μM) for 60 min at 37 °C. Dye was removed and replaced with the appropriate volume of assay buffer, pH 7.4 (1X HBSS (Hanks' Balanced Salt Solution), supplemented with 20 mM HEPES and 2.5 mM probenecid). All compounds were serially diluted in assay buffer for a final 2X stock in 0.6% DMSO. This stock was then added to the assay plate for a final DMSO concentration of 0.3%. Acetylcholine (~EC_{20} concentration or full dose-response curve) was prepared at a 10X stock solution in assay buffer prior to addition to assay plates. Calcium mobilization was measured at 25 °C using a FLEXstation II (Molecular Devices, Sunnyvale, CA). Cells were preincubated with test compound (or vehicle) for 1.5 min prior to the addition of the agonist, acetylcholine. Cells were then stimulated for 50 sec with a submaximal concentration (EC_{20}) or a full dose-response curve of acetylcholine. The signal amplitude was first normalized to baseline and then as a percentage of the maximal response to acetylcholine; plotted data and pharmacological parameters were obtained using GraphPad Prism (v4.0c) software. Indicated data values represent means from at least three experiments with similar results.

References

1. Lindsley, C.W.; Wisnoski, D.D.; Leister, W.H.; O'Brien, J.A.; Lemaire, W.; Williams, D.L. Jr.; Burno, M.; Sur, C.; Kinney, G.G.; Pettibone, D.J. et al. *J. Med. Chem.,* **2004**, 47**,** 5825–5828.

2. Zhao, Z.; Wisnoski, D.D.; O'Brien, J.A.; Lemaire, W.; Williams, D.L. Jr.; Jacobson, M.A.; Wittman, M.; Ha, S.N.; Schaffhauser, H.; Sur, C. et al. *Bioorg. Med. Chem. Lett.* **2007**, 1, 1386–1391.

3. Shirey, J.K.; Xiang, Z.; Orton, D.; Brady, A.E.; Johnson, K.A.; Williams, R.; Ayala, J.E.; Rodriguez, A.L.; Wess, J.; Weaver, D. et al. *Nat. Chem. Biol.,* **2008**, 4, 42–50.

4. Bonner, T. I.; Buckley, N. J.; Young, A. C.; Brann, M. R. *Science,* **1987**, 237:4814, 527-532.

5. Bonner, T. I. ; Young, A. C.; Brann, M. R.; Buckley, N. J. *Neuron*, **1988**, 1:5, 403-410.

6. Caulfield, M. P.; Pharmacol, Ther.,**1993**, 58(3), 319-379.

7. Bymaster, F. P.; McKinzie, D. L.; Felder, C. C.; Wess, J. *Neurochem. Res.,* **2003**, 28(3-4), 437-442.

8. Wess, J.; Duttaroy, A.; Zhang, W.; Gomeza, J.; Cui, Y.; Miyakawa, T.; Bymaster, F. P.; McKinzie, L.; Felder, C. C.; Lamping, K. G.; Faraci, F. M.; Deng, C.; Yamada, M. *Receptors Channels,* **2003**, 9(4), 279-290.

9. Clader, J. W.; Wang, Y.; *Curr. Pharm. Des*. **2005**, 11(26), 3353-3361.

10. Langmead, C. J.; Watson, J.; Reavill, C. *Pharmacol. Ther.* **2008**, 117(2), 232-243.

11. Wess, J.; Eglen, R. M.; Gautam, D.; *Nat. Rev. Drug Discov.,* **2007**, 6(9), 721-733.

12. Felder, C. C.; Bymaster, F. P.; Ward, J.; DeLapp, N.; *J. Med. Chem.* **2000**, 43(23), 4333-4353.

13. Brady, A. E.; Jones, C. K.; Bridges, T. M.; Kennedy, J. P.; Thompson, A. D.; Heiman, J. U.; Breininger, M. L.; Gentry, P. R.; Yin, H.; Jadhav, S. B.; Shirey, J. K.; Conn, P. J.; Lindsley, C. W.; *J. Pharmacol. Exp. Ther.* **2008**, 327(3), 941-953.

14. Jones, C. K.; Brady, A. E.; Davis, A. A.; Xiang, Z.; Bubser, M.; Tantawy, M. N.; Kane, A. S.; Bridges, T. M.; Kennedy, J. P.; Bradley, S. R.; Peterson, T. E.; Ansari, M. S.; Baldwin, R. M.; Kessler, R. M.; Deutch, A. Y.; Lah, J. J.; Levey, A. I.; Lindsley, C. W.; Conn, P. J.; *J. Neurosci.* **2008**, 28(41), 10422-10433.

15. Shirey, J. K.; Xiang, Z.; Orton, D.; Brady, A. E.; Johnson, K. A.; Williams, R.; Ayala, J. E.; Rodriguez, A. L.; Wess, J.; Weaver, D.; Niswender, C. M.; Conn, P. J.; *Nat. Chem. Biol.* **2008**, 4(1), 42-50.

16. Langmead, C. J.; Austin, N. E.; Branch, C. L.; Brown, J. T.; Buchanan, K. A.; Davies, C. H.; Forbes, I. T.; Fry, V. A.; Hagan, J. J.; Herdon, H. J.; Jones, G. A.; Jeggo, R.; Kew, J. N.; Mazzali, A.; Melarange, R.; Patel, N.; Pardoe, J.;

Randall, A. D.; Roberts, C.; Roopun, A.; Starr, K. R.; Teriakidis, A.; Wood, M. D.; Whittington, M.; Wu, Z.; Watson, J.; *J. Pharmacol.* **2008**, 154(5), 1104-1115.

17. Spalding, T. A.; Trotter, C.; Skjaerbaek, N.; Messier, T. L.; Currier, E. A.; Burstein, E. S.; Li, D.; Hacksell, U.; Brann, M. R.; *Mol. Pharmacol.* **2002**, 61(6), 1297-1302.

18. Bridges, T. M.; Lindsley, C. W.; *ACS Chem. Biol.* **2008**, 3(9), 530-541.

19. F. A. H. Abu-Shanab, A.; Gaber, H.; Mousa, Sayed A. S. *Journal of Sulfur Chemistry,* **2006**, 27(4), 293-305.

20. Litvinov, V. P. S.; Yu. A.; Promonenkov, V. K.; Rodinovskaya, L. A.; Shestopalov, A. M.; Mortikov, V. Yu. *Seriya Khimicheskaya,* **1984**, 8, 1869-1870.

21. Conn, P. J.; Christopolous, A.; Lindsley, C. W. *Nat. Rev. Drug Discovery,* **2009**, 8, 41–54.

22. Celanire, S.; Wijtmans, M.; Talaga, P.; Leurs, R.; de Esch, J. P. *Drug Discovery Today*, **2005**, 10, 1613–1627.

23. Esbenshade, T. A.; Brownman, K. E.; Bitner, R. S.; Strakhova, M.; Cowart, M. D.; Brioni, J. D. *J. Pharmacol.,* **2008**, 154, 1166–1181.

24. Yasuta, R.P.; Ciesla, W.; Flores, L.R.; Wall, S.J.; et al. *Mol. Pharmacol.* **1993**, 43, 149-157.

25. Wirtshafter, D.; Osbron, C.V. *J. Chem. Neuroanat.* **2004**, 28, 107-116.

26. Tzavara, E.T.; Bymaster, F.P.; Davis, R.J.; et al. *FASEB J.* **2004**, 18, 1410-1412.

27. Wess, J.; Eglen, R. M.; Guatam, D. *Nat. Rev. Drug Disc.* **2007**, 6, 721-733.

28. Bridges, T. M.; LeBois, E. P.; Hopkins, C. R.; Wood, M. R.; Jones, C. K.; Conn, P. J.; Lindsley, C. W. *Drug News Perspect.* **2010**, 23, 229-240.

29. Vilaro, M.T.; Palacios, J.M.; Mengod, G. *Neurosci. Lett.* **1990**, 114, 154-159.

30 Bodick, N.C.; Offen, W.W.; Levey, A.I.; Cutler, N.R.; Gauthier, S.G.; Satlin, A.; Shannon, H.E.; Tollefson, G.D.; Rasmussen, K.; Bymaster, F.P. et al. *Arch. Neurol.* **1997**, 54, 465-473.

31. Shekhar, A.; Potter, W.Z.; Lightfoot, J.; Lienemann, J.; Dube´, S.; Mallinckrodt, C.; Bymaster, F.P.; McKinzie, D.L.; Felder, C.C. *Am. J. Psychiatry.* **2008**, 165, 1033-1039.

32. All tables and portions of text previously published are used with consent from the publisher.

Chapter III

EXPLORATION OF THE SYNTHESIS OF PIPERAZIMYCIN A

Fenical and co-workers recently reported on the isolation of piperazimycin A **1** from the fermentation broth of a *Streptomyces* sp., cultivated from marine sediments near the island of Guam (1). A cyclic hexadepsipeptide, **1** is composed of rare amino acids such as hydroxyacetic acid (HAA), α-methylserine, a novel (*S*)-2-amino-8-methyl-4,6-nonadecadienoic acid (AMNA), two γ-hydroxypiperazic acids (*S,S*)-γOHPip1 and (*R,R*)-γOHPip2 and one γ-chloropiperazic acid (*R,S*)-γClPip, **Figure 1** (1).

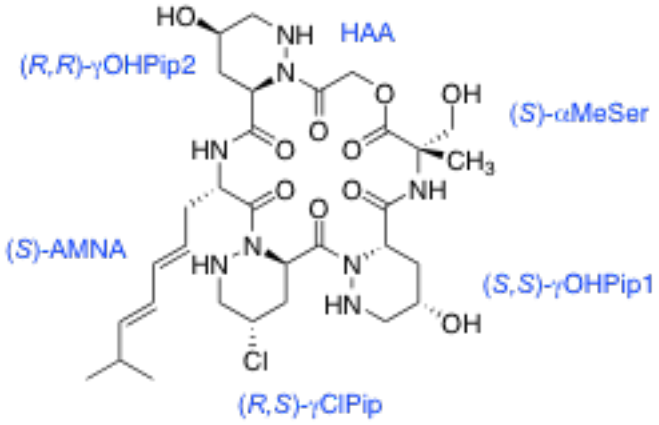

Piperazimycin A, **1**

Figure 1. Structure of Piperazimycin A, **1**.

Piperazimycin A, **1,** proved to be a potent cancer cell cytotoxin which exhibited in vitro cytotoxicity toward multiple tumor cell lines with a mean GI_{50} of 100 nM (1). Based on its novel molecular architecture, the diversity of non-proteogenic amino acid building blocks and its potent cytotoxicity, we embarked on a total synthesis campaign aimed at delivering piperazimycin A, **1** in sufficient quantities to elucidate the molecular target(s) responsible for the biological activity.

The retrosythesis of Piperazimycin A, **1** was planned according to the individual unnatural amino acids present in the parent structure, **Figure 2**.

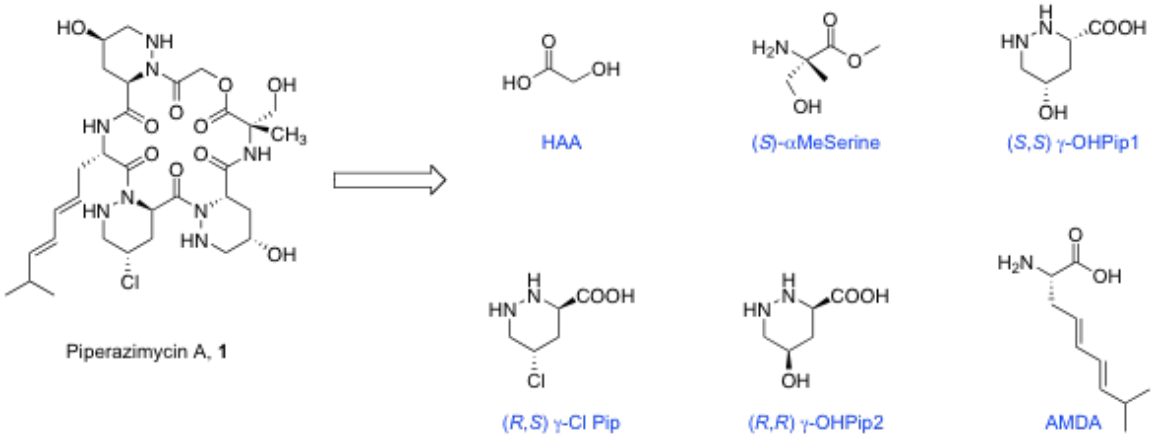

Figure 2. Structures of the individual components of Piperazimycin A, **1**.

The envisioned synthetic plan would be to make all of the individual components of Piperazimycin A, **1**, and join these individual components utilizing traditional peptide coupling methodology.

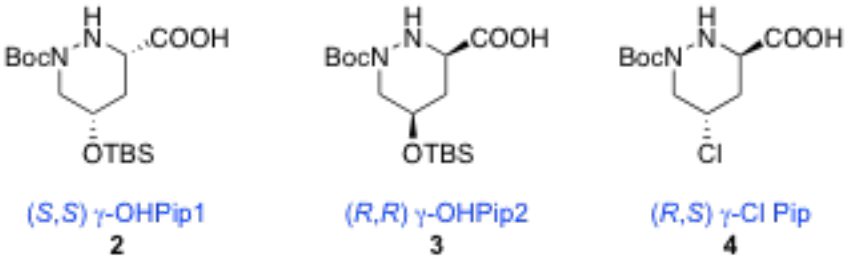

Figure 3. γ-functionalized piperazic acid target molecules **2**-**4**.

In order to complete a total synthesis of **1**, we first had to synthesize the requisite γ-functionalized piperazic acids **2**-**4**, **Figure 3**. Upon examination of the literature, we were surprised that there are very few synthetic routes to these unnatural amino acids, especially with mono-*N*-protection (2-8). A single report by Hamada and co-workers demonstrated that the mono-*N*-Boc analogues **2** and **3** could be accessed, which we desired for the sequence of peptide couplings en route to **1** (2). In accord with a report from Hale and co-workers (7), we anticipated that deprotection of the TBS group of **3** and exposure to PPh_3 and MeCN-CCl_4 would install the chlorine with inversion providing the corresponding γ-ClPip **4**; however, this step had never been performed on a mono-*N*-protected piperazic acid (3,7).

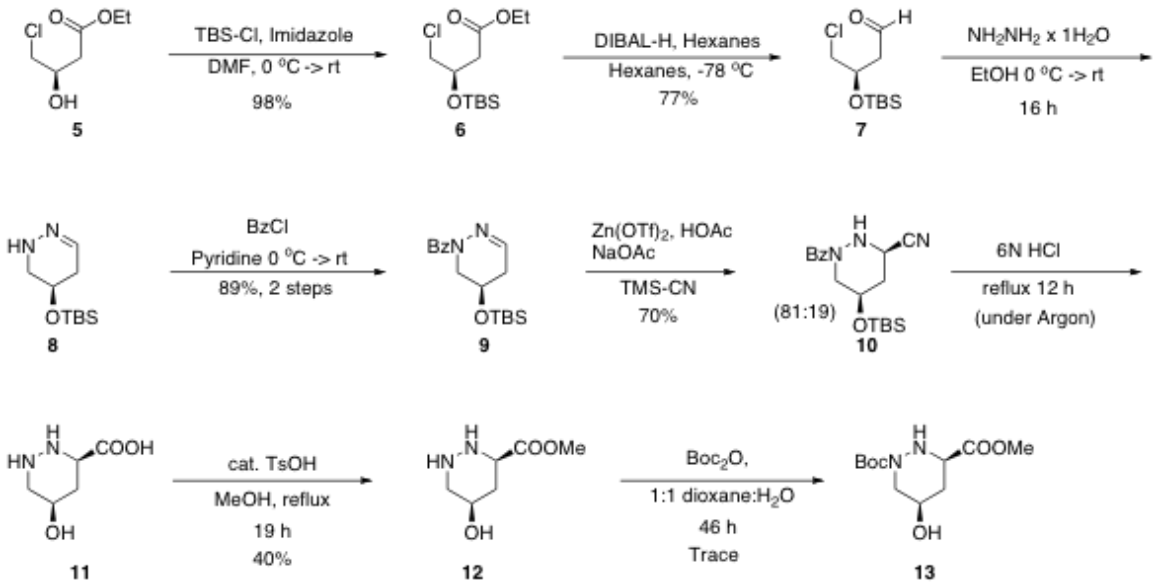

Scheme 1. Piperazic acid synthesis utilizing the Hamada methodology.

Hamada's protocol begins with (*R*)-4-chloro-3-hydroxybutanoic acid ethyl ester **5** which is O-TBS protected to give protected alcohol **6**, in 98% yield. **6** is then reduced with DIBAL-H in hexanes to deliver aldehyde **7** in 77% yield **Scheme 1** (2). Exposure of **7** to hydrazine hydrate in EtOH for 16 hours afforded the cyclic hydrazone **7**, which was then mono-*N*-benzylated to provide **8** in 89% yield over 2 steps. A Lewis acid-promoted Strecker reaction with stoichiometric $Zn(OTf)_2$ results in an 81:19 ratio of diastereomers in favor of the cis adduct **10**, which can be easily separated by column chromatography. Deprotection and hydrolysis with 6 N HCl at reflux for 12 hours under argon led to **12** which is then esterified **13** with catalytic TsOH in refluxing methanol for 19 hours. Finally, **13** is selectively mono-Boc protected at the *N*1 position by treatment with Boc_2O in 1:1 dioxane:water for 46 hours to deliver **14**, two steps away from (*R,R*)-γOHPip2 **4**

(2). Moreover, the analogous precursor to (*S,S*)-γOHPip1 **3** could also be accessed *via* this route by starting the sequence with (*S)*-4-chloro-3-hydroxybutanoic acid ethyl ester in place of **5**. While this was an attractive route, we felt there was room to optimize throughout this synthesis, as many steps required long reaction times (12-46 hours) (2).

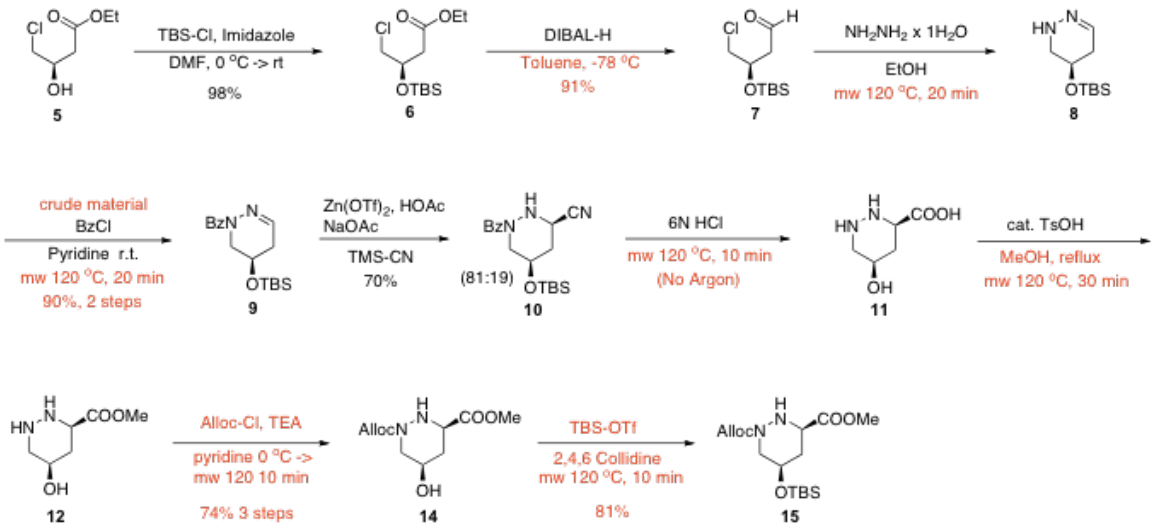

Scheme 2. Optimized Hamada route to piperazic acids.

Our modified Hamada protocol employed microwave-assisted organic synthesis (MAOS) to dramatically reduce reaction times for four key steps (9, 10). As shown in **Scheme 2**, the changes to the original protocol are highlighted in red. In our hands, (*R*)-4-chloro-3-hydroxybutanoic acid ethyl ester **5** is silylated and reduced with DIBAL-H in *toluene*, in place of hexanes, to deliver aldehyde **7** in an improved yield of 91% for the reduction. An MAOS

condensation of **7** with hydrazine provides the cyclic hydrazone **8** in only 20 minutes (versus 16 h), which is then mono-*N*-benzylated under microwave irradition (120 ^{o}C, 20 min) to provide **9** in 90% yield over 2 steps. The key Strecker reaction was performed as prescibed and delivered an 81:19 ratio in favor of desired compound **10**, which was separated by flash column chromatography from its diasteriomer to afford a 57% yield of the *cis* diastereomer **10**. Although attempts were made to reduce the reaction time for the asymmetric Strecker reaction, any microwave irradiation only led to decomposition. Deprotection and saponification with 6 N HCl in the microwave (120 ^{o}C, 10 min) delivers **11**, which is then subjected to another MAOS reaction (120 ^{o}C, 30 min) with cat. TsOH in MeOH to provide ester **12** in 75% yield for the two steps. At this point, the modified reaction protocol reduced total reaction time for the synthesis dramatically and provided improvements in the overall yield on a multi-gram scale. Specifically, the reaction times for the synthesis of **8**, **9**, **11** and **12** were reduced from 49 hours to only 80 minutes (a ~40-fold reduction) by virtue of microwave irradiation.

However, we were unable to access the mono-*N*-Boc derivative **13** in reasonable yield. While we could prepare **13** on an ~25 mg scale in yields ranging from 5-25%, the reaction failed on a larger, synthetically useful scale en route to the total synthesis of piperazimycin A, **1**. Revisiting Hamada's paper indicated that they only prepared **13** on a <30 mg scale, and did not perform the reaction on larger scale (2). We explored alternative protocols (MAOS and conventional) and alternative reagents for formation of the *t*-butyl carbamate, but

all attempts provided very little conversion to **13**. Danishefsky and co-workers previously demonstrated that the analogous Teoc derivative of **13** could be prepared on a large scale, however we decided to attempt this route using an alloc protecting group (4-6).

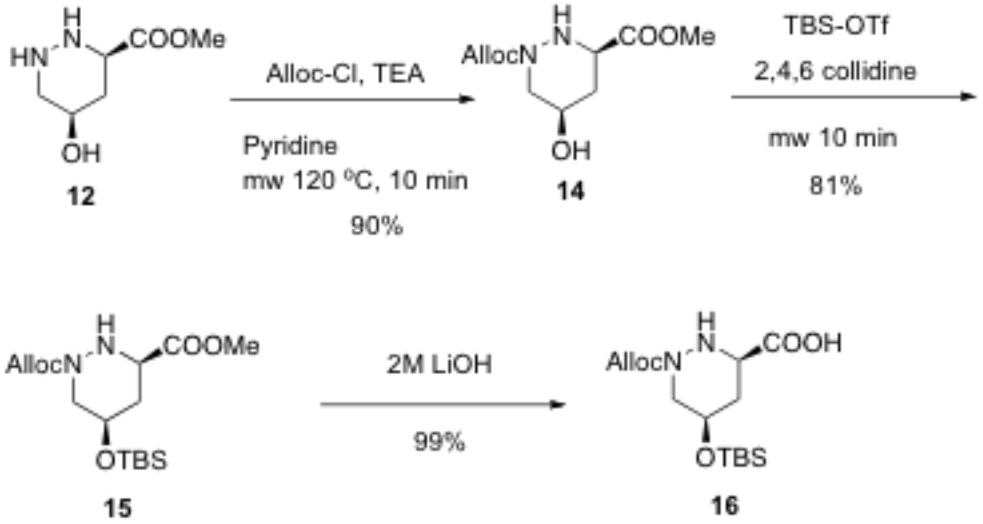

Scheme 3. Synthesis of Alloc protected piperazic acids.

After many unsuccessful attempts, we developed a high-yielding route to an Alloc-protected congener of **13** as our modified MAOS-route to **12** worked well on multi-gram scale. As shown in **Scheme 3**, addition of Alloc-Cl to **12** at 0 ^{o}C in pyridine, then exposing to microwave irradiation for 10 minutes at 120^{o}C provides the previously undescribed *N*-Alloc congener (*R,R*)-**14** in 74% yield. Another MAOS mediated silylation provided **15** in 81% yield, followed by a saponification step to deliver the key *N*-Alloc-(*R,R*)-γ-OTBSPip2 **16** in quantitative yield which

was used in further couplings without purification. Following **Scheme 2**, but substituting the (*R*)-4-chloro-3-hydroxybutanoic acid ethyl ester **5** with the corresponding (*S*)-enantiomer **17** provides **18** in equivalent yield and diastereomeric ratio as **9**, **Scheme 4**. Deprotection and hydrolysis with 6 N HCl in the microwave (120 ^{o}C, 10 min) delivers **19**, which is then subjected to another MAOS reaction (120 ^{o}C, 30 min) with cat. TsOH in MeOH to provide ester **20**. Finally, **20** is selectively mono-Alloc protected at the *N*1 position by treatment with Alloc-Cl in pyridine at 0 ^{o}C and then irradiated in the microwave for 10 minutes at 120 ^{o}C provides the previously undescribed *N*-Alloc congener (*S,S*)-**21** in 75% yield for the three steps. Another MAOS mediated silylation provided **22** in 83% yield, followed by a saponification step to deliver the key *N*-Alloc-(*S,S*)-γ-OTBSPip1 **23** in quantitative yield.

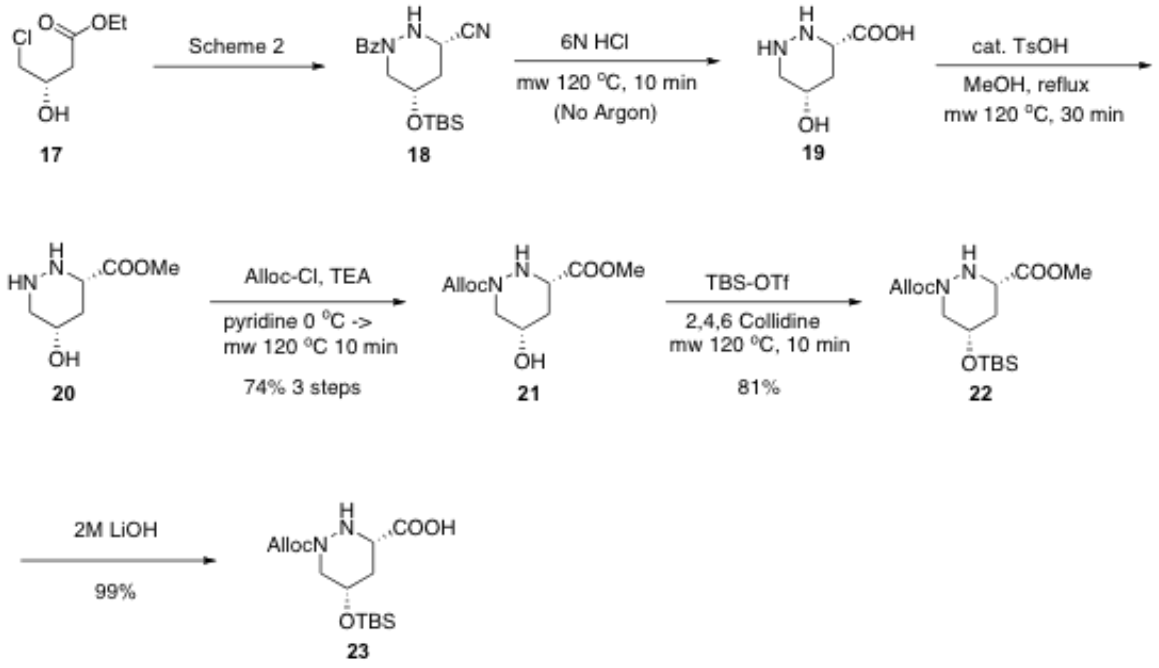

Scheme 4. Synthesis of (*S,S*)-γ-OTBSPip1 **22**.

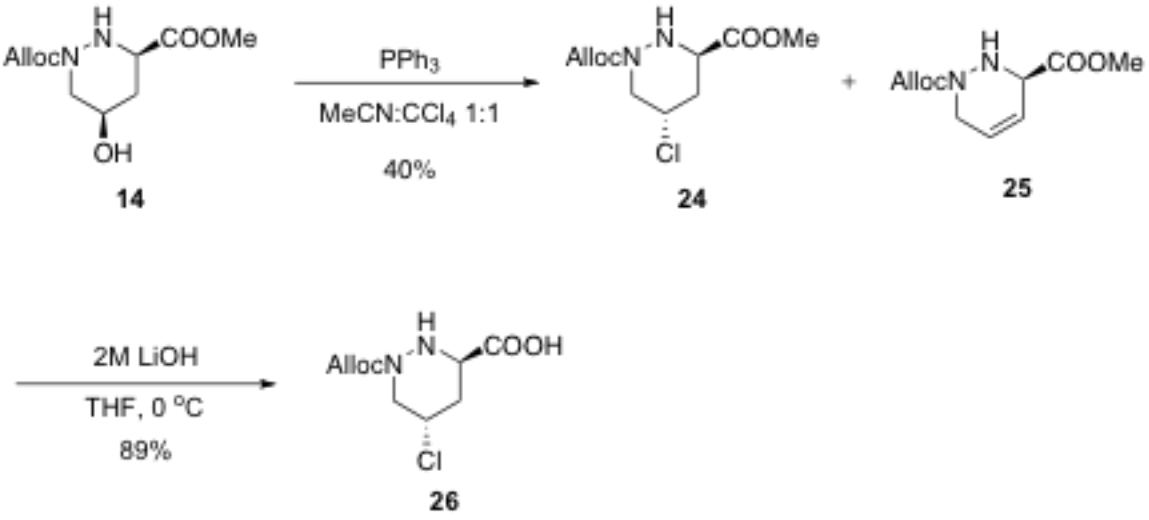

Scheme 5. Synthesis of (*R,S*)-γ-Cl Pip **26**.

With two of the three requisite piperazic acids in hand, effort now focused on preparing the remaining *N*-Alloc analogue of target molecule (*R,S*)-γ-ClPip **26**. As shown in **Scheme 5**, the application of the Hale protocol (7), using PPh_3, MeCN:CCl_4 1:1, employing (*R,R*)-**14** provided (*R*,*S*)-**24** in 40% isolated yield along with a 20% yield of the elimination product **25**. We were pleased to see that the first application of the Hale protocol (7) with a mono-*N*-protected substrate provided an equivalent yield to the di-*N*-protected piperazic acids without greater propensity for elimination to form **25**. With **24** in hand, mild saponification conditions delivered previously unknown *N*-Alloc-(*R,S*)-γ-ClPip **26** in 89% yield.

At this point in the synthesis of the piperazic acids of piperazamycin A we have modified Hamada's original approach and developed an accelerated, high yielding protocol, taking advantage of the power of MAOS, for the synthesis of γ-functionalized piperazic acids. We have also demonstrated that selective mono-Boc protection at the *N*1 position of piperazic acids is a poor reaction that proceeds only on small scale. Importantly, we have developed a scalable MAOS protocol for selective Alloc protection at the *N*1 position of functionalized γ-piperazic acids. Following this new synthetic route, we have prepared *N*-Alloc-(*S,S*)-γ-OTBSPip1 **23**, *N*-Alloc-(*R,R*)-γ-OTBSPip2 **16**, and *N*-Alloc-(*R,S*)-γ-ClPip **26.**

During the course or our work towards piperazimycin A it was found that the alloc protected versions of the piperazic acids were incompatible with the

AMNA diene. To remedy this problem we decided to prepare Teoc derivatives of the piperazic acids **22**, **15**, and **25**, shown in **Scheme 6**. Overall yields for the 8 step synthesis of **27** and **28** averaged 65%, and **29** was obtained in 9 steps and 22% overall yield.

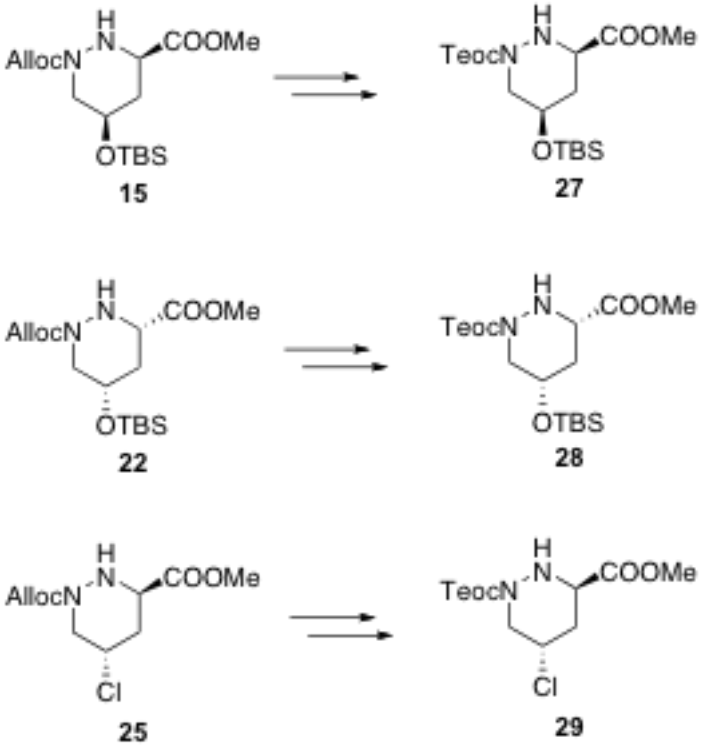

Scheme 6. Synthesis of *N*-Teoc-protected, γ-substiuted piperazic acids **27-29**.

For the purpose of a model coupling reaction, we also required a *bis*-Boc congener **35** to explore amide coupling conditions en route to a total synthesis of **1**. To this end, we followed a variation of Danishevsky's published route, **Scheme 7** (4-6). Starting with commercial (*R*)-lactone **30**, opening with

methoxide, followed by conversion of the primary hydroxyl to the bromide affords **31** in 45% yield for the two steps. TBS protection of the secondary hydroxyl, followed by enolate formation and trapping with di-*tert*-butyl azodicarboxylate (DBAD) provides **32**, in 56% yield for the two steps. Deprotonation with NaH and cyclization delivers a 1:1 diastereomeric mixture of piperazic esters **33**. Careful column chromatography delivers (*R,S*)-γ□TBSPip**34** in 40% yield. Removal of the TBS group, application of the Hale protocol (7) to install the γ-chloro functionality and hydrolysis provided the target **35** in 45% yield for the three steps. Overall, the 8-step sequence proceeded in 4.6% yield on multi-gram scales.

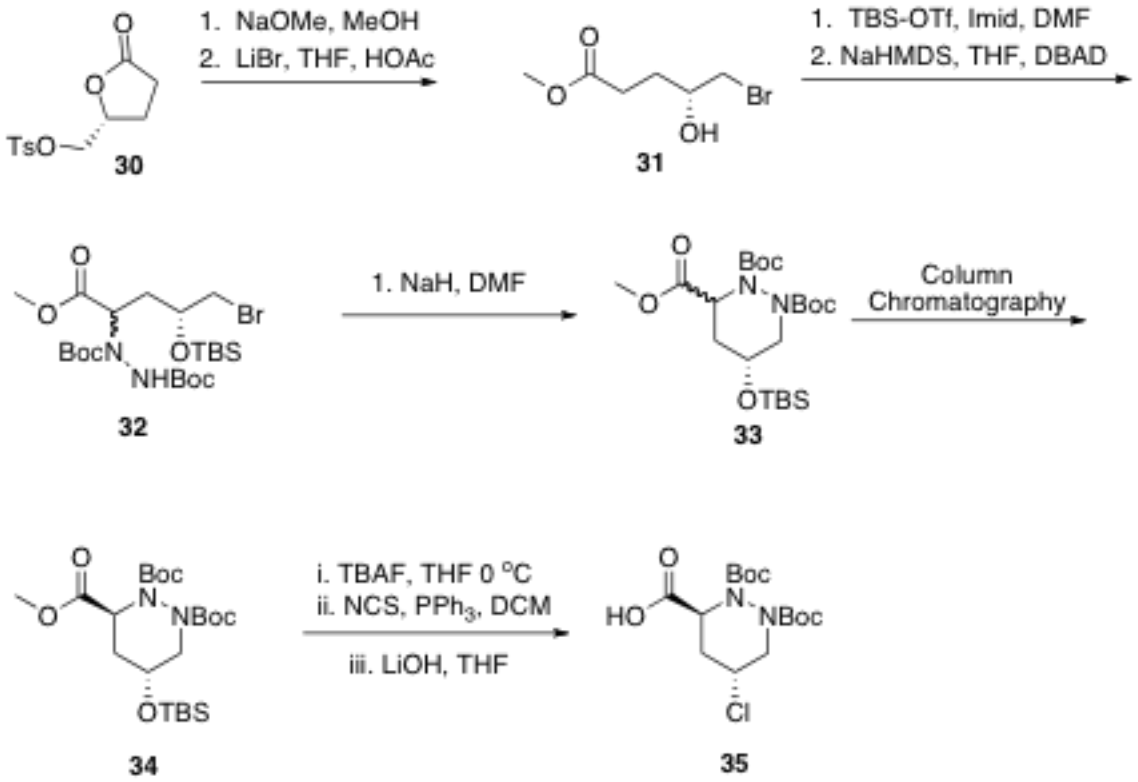

Scheme 7. Synthesis of Bis-Boc-(*R*,*S*)-γ-Cl Piperazic Acid.

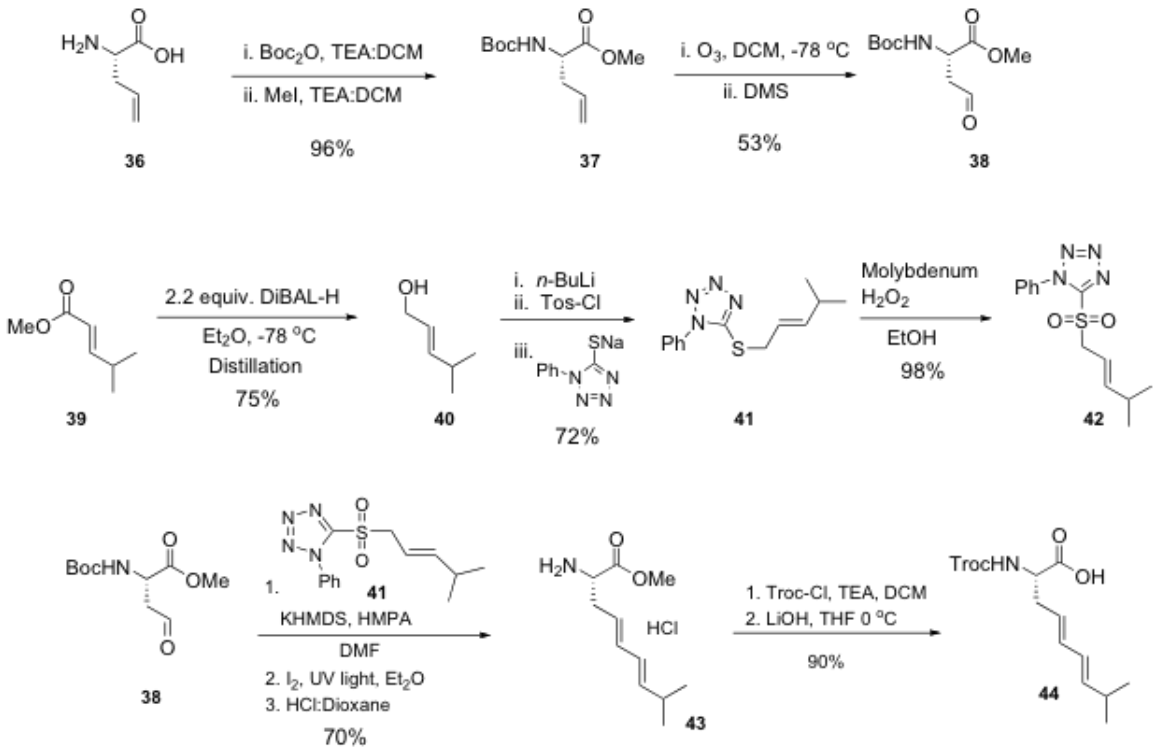

Scheme 8. Synthesis of AMNA, **40**.

With all of the requisite γ-substituted piperazic acids **27**-**29** and **35** in hand, attention now focused on preparing the unnatural AMNA, **40**, **Scheme 8**. Beginning with a commercial (*S*)-allyl glycine derivative **36**, Boc protection and esterification affords **37** in 96% yield. Ozonolysis delivers aldehyde **38** in 53% yield, and delivers one component for the envisioned Julia-Kocienski olefination (11-13) to provide the (*E,E*)-stereochemistry in AMNA. The second component was derived from commercially available (*E*)-methyl-4-methylpent-2-enoate **39**.

Reduction with DIBALH provides, after distillation, allylic alcohol **40** in 75% yield. Deprotonation with *n*-BuLi, conversion to the tosylate and displacement of the allylic tosylate with the thiotetrazole and oxidation affords **41** in 53% yield for the four steps. The Julia-Kocienski olefination proceeds by deprotonation of **41** with KHMDS in DMF/HMPA to provide an 80:20 mixture of E:Z isomers (11-13). Exposure to iodine and UV light isomerizes the diene to >95:5 E:Z. Deprotection of the Boc group with HCl delivers the bench stable AMNA congener, **43** in 70% yield for the three steps. **43** was also protected with the Troc group and the ester hydrolyzed to afford congener **44**.

For the final component of piperazimycin A we prepared the protected forms of (*S*)-α-MeSerine amino acid **45** for subsequent coupling, **Scheme 9**. Commercial (*S*)-2-amino-3-hydroxy-2-methylpropanoic acid **45** was Boc protected, followed by protection of the primary hydroxyl as a TBDPS ether to deliver **46** in 98% for the two steps. **46** was then further elaborated with the HAA moiety to provide **47** to complete the northeastern fragment of piperazimycin A **1**.

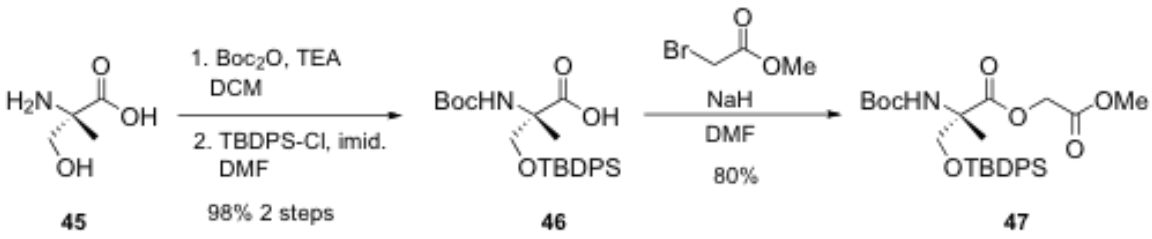

Scheme 9. Synthesis of protected α-MeSer **46**, and α-MeSer-HAA **47**.

With all of the non-proteogenic amino acid components prepared, effort focused on construction of key dipeptides en route to a total synthesis of **1**. As described by Ma, (14) the peptide couplings were not trivial and each had to be optimized independently surveying dozens of coupling reagents, additives, solvents and alternative protecting groups on the various amino acid congeners. In the recently reported total synthesis of **1** by Ma, (14) they state that they were unable to affect the never before described γ-substituted piperazic acid-piperazic acid coupling between suitable congeners of **35** and **28**. Thus in their work, they

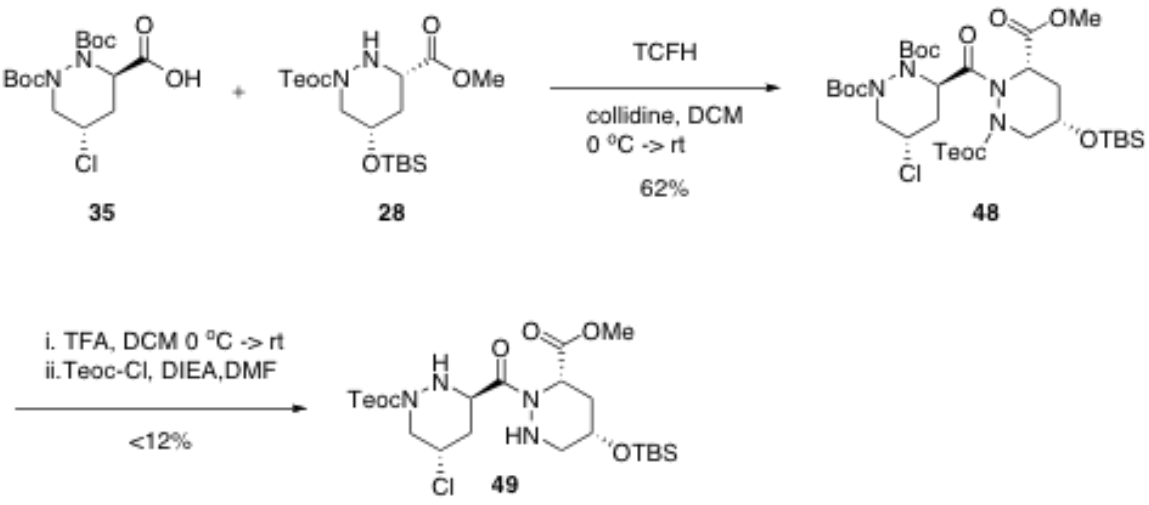

Scheme 10. Formation of piperazic-piperazic bond utilizing TCFH.

followed the Danishefsky approach, (4-6) coupling acyclic amino acids and then cyclizing to form the piperazic acids as shown in **Scheme 7**. In our hands, we also were unable to couple analogs of **28** and **29**; however, protecting groups

proved to be the key for this difficult transformation. The bis-Boc γ-ClPip **35** was successfully coupled to **28** in 62% yield employing freshly made tetramethylchloroformamidinium hexafluorophosphate (TCFH), to form the acid chloride *in situ*, and provide **48**, and the first example of a γ-substituted piperazic acid-piperazic acid coupling. The Boc groups were then removed with TFA and subsequent Teoc protection provided **49**, however this was in low yield (<12% for the two steps). This provided the southern C5-C14 piperazic acid-piperazic acid fragment.

To construct the eastern half of **1**, the Boc group of **47** was chemoselectively removed with HCl(g) in EtOAc to deliver **50**, (15) which was then coupled to **23**, under standard HATU coupling conditions to deliver **51** in 26% yield for the two steps **Scheme 11**.

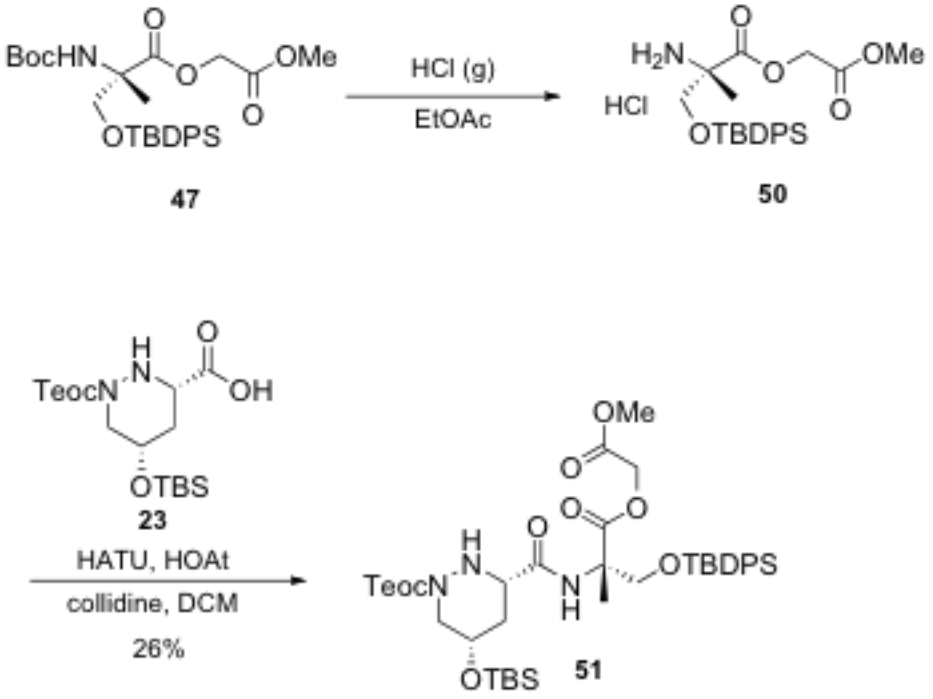

Scheme 11. Synthesis of eastern half of piperazimycin A.

In parallel, the Troc-protected AMNA **44** (14) was coupled to **29** under TCFH conditions (all others failed entirely) to deliver this dipeptide **52** in 49% yield. Hydrolysis generated **53** in quantitative yield, **Scheme 12**.

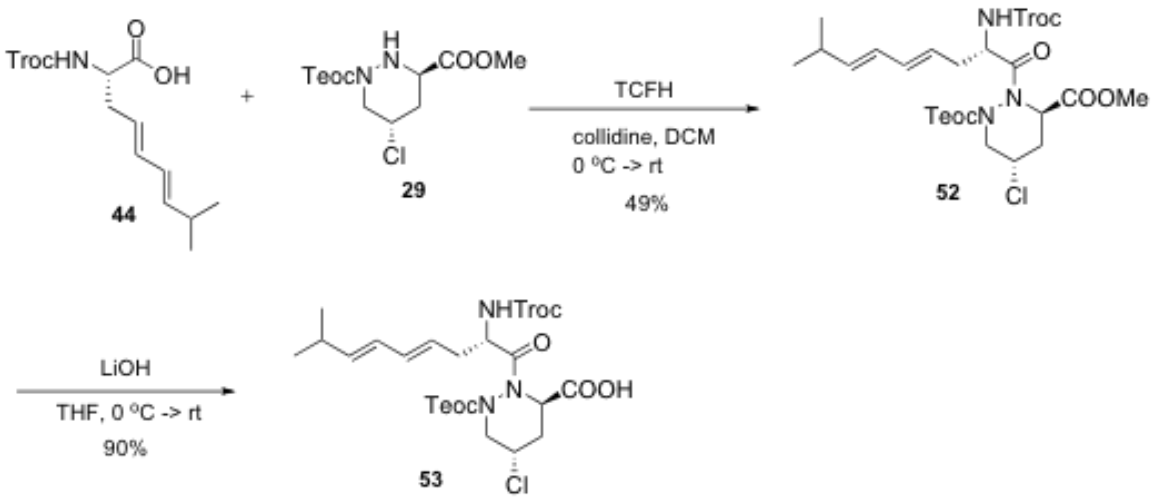

Scheme 12. Synthesis of AMNA, γ-Chloro Piperazic acid dipeptide.

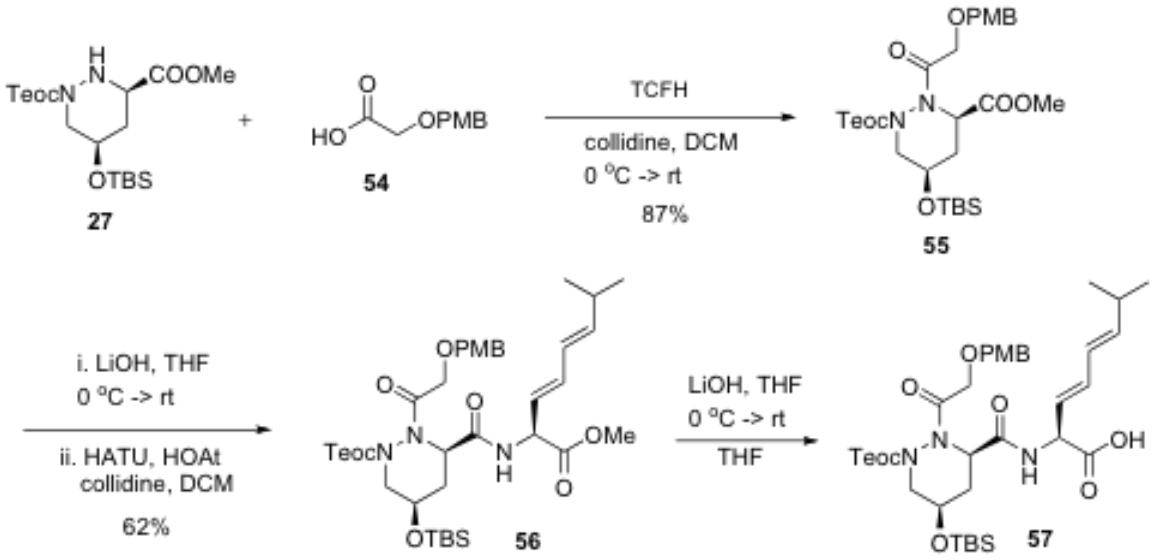

Scheme 13. Synthesis of northwestern fragment of piperazimycin A.

The northwestern portion of **1** was also prepared, **Scheme 13**. γ-OHPip **27** was coupled to a PMB protected HAA congener **54** to provide **55** in 87% yield. Hydrolysis, subsequent HATU-mediated coupling with AMNA congener **56** and a

second hydrolysis led to dipeptide **57** in 60% yield for the three steps. However, our most optimal coupling conditions developed in **Scheme 10** utilizing freshly prepared TCFH proved ineffective to achieve the γ-substituted piperazic-piperazic bond between **57** and **29**, **35** and **51**.

During the course of this work we have synthesized all five of the non-proteogenic amino acids found in piperazimycin A **1**, and synthesized four advanced dipeptides (two with the HAA motif attached). Importantly, we achieved the first successful γ-substituted piperazic acid-piperazic acid coupling, mediated by TCFH, to synthesize the southern (*R,S*)-γClPip-(*S,S*)-γOHPip dipeptide **49**. It is unfortunate that our peptide coupling approach ultimately failed to produce piperazimycin A, however a new efficient MAOS route was developed to produce γ-substituted piperazic acids, and a new peptide coupling route was developed utilizing TCFH as a coupling reagent for piperazic acids.

By combining our peptide approach toward the synthesis of piperazimycin A and the acyclic approach of Ma (14) it may be possible to synthesize piperazimycin A in the future, **Scheme 14**.

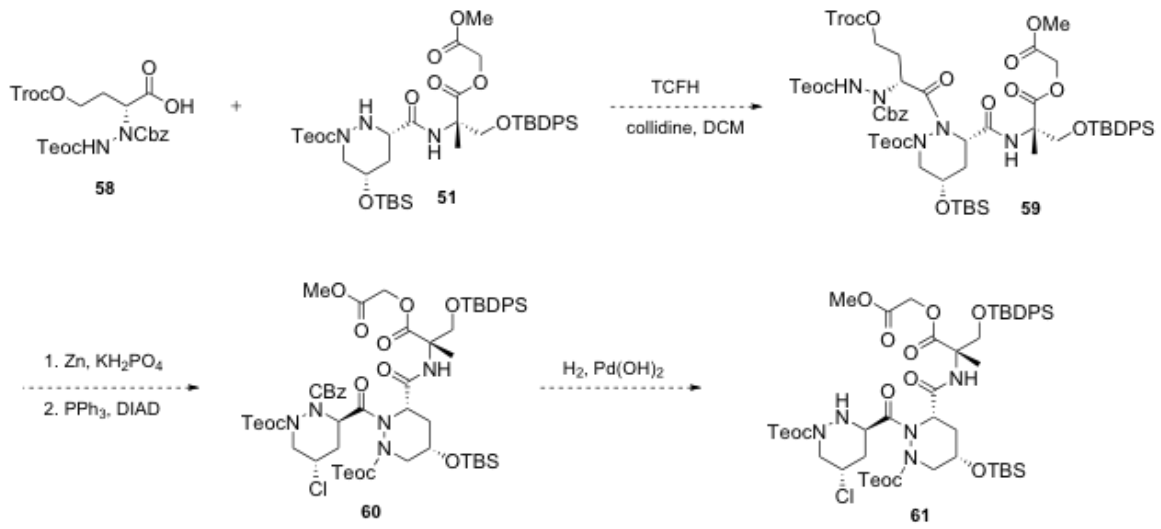

Scheme 14. Proposed alternative route towards the synthesis of piperazimycin A, **1**.

By utilizing advanced intermediate **58**, synthesized by Ma, TCFH mediated coupling with **51** should produce coupled material **59**. With **59** in hand a zinc mediated deprotection of the Troc protecting group will furnish the alcohol which can then be cyclized under Mitsunobu conditions to give **60**, (14). After the cyclization, removal of the CBz protecting group with Pearlman's catalyst, $Pd(OH)_2$, should give the mono-teoc protected bis-piperazic coupled compound **61**.

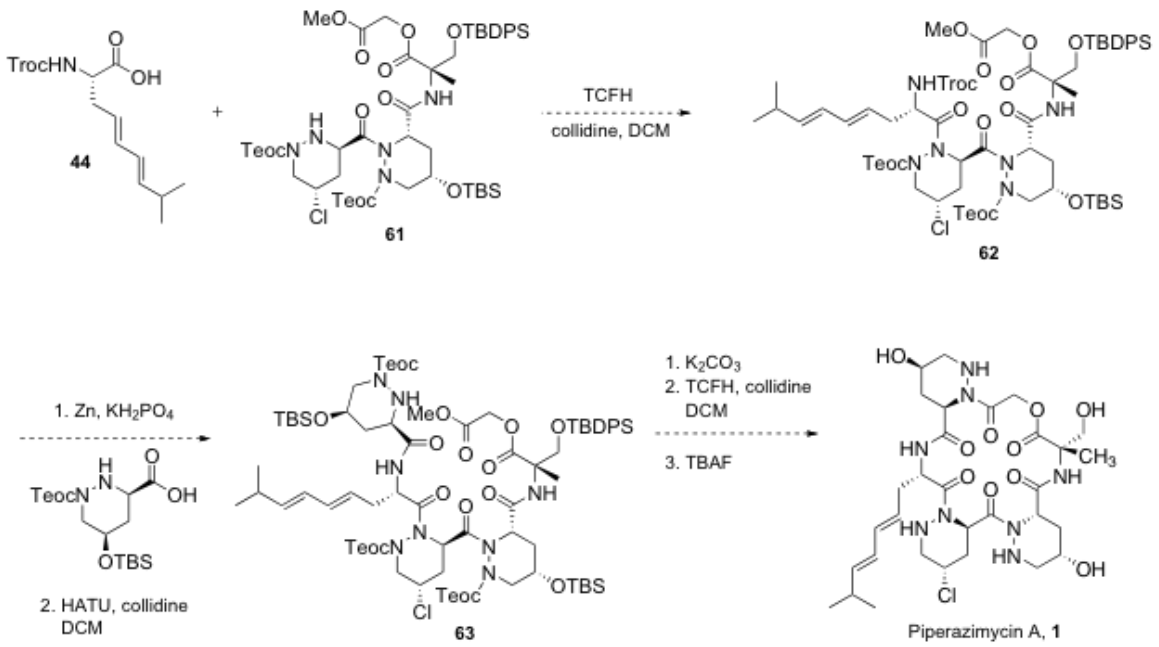

Scheme 15. Proposed completion of piperazimycin A, **1**.

Once **61** is completed coupling with **44** utilizing our TCFH methodology should provide coupled material **62**. Troc deprotection with zinc and coupling of (*R*,*R*) piperazic acid with HATU could provide **63**. After successful synthesis of **63**, saponification with K_2CO_3, cyclization with TCFH, and global deprotection with TBAF could be a potential new route to provide the natural product piperazimycin A.

Another potential reagent that could be useful toward an alternative synthesis of piperazimycin A was recently reported by Ley for the total synthesis of Chloptosin (16). To form the piperazic-piperazic bond, Ley utilized the Ghosez' coupling reagent, 1-chloro-*N,N*-2-trimethyl-1-propenylamine, **Figure 4**. (17).

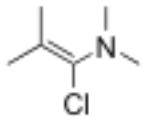

Ghosez' Reagent, **64**

Figure 4. Structure of Ghosez' Reagent.

The Ghosez' reagent is very similar to TCFH, and may be able to produce the γ-substituted piperazic-piperazic bond formation on the fragments of Piperazimycin A, **1**, where TCFH failed. With these two alternate route it may be possible to complete the total synthesis of Piperazimycin A in the future utilizing a peptide-based approach.

Piperazimycin Experimental-

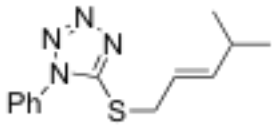

41

(*E*)-5-(4-methylpent-2-enylthio)-1-phenyl-1*H*-tetrazole 41:

To a 500 mL flask containing alcohol **40** (2.45 g, 0.024 mol), under argon, was added anhydrous THF (200 mL), and cooled to -78 ^{o}C. n-BuLi (16.8 mL, 0.027 mol) was added over a 5 min period and allowed to stir at -78 ^{o}C for 15 min. Solid *p*-toluene sulfonyl chloride (5.49 g, 0.029 mmol) was added under positive argon pressure all at once, and the reaction was stirred for 3 h at -78 ^{o}C. To the reaction was added solid sodium thiotetrazole (7.21 g, 0.056 mol) all at once at -78 ^{o}C, and the reaction was allowed to warm to room temperature overnight. Once complete the reaction was added to a separatory funnel containing 250 mL H_2O, and 250 mL EtOAc, the layers were separated and the product extracted 2x with 250 mL EtOAc. The organic layers were washed with 500 mL brine solution, dried with $MgSO_4$, filtered, and concentrated. The crude material was purified by column chromatography with a 1:3 EtOAc:Hexanes to obtain thioether **41** (4.5 g, 72 % yield). ^{1}H NMR (400 MHz, $CDCl_3$) ™ 7.55 (m, 5H), 5.77 (dd, *J* = 6.4, 15.2 Hz, 1H), 5.55 (m, 1H), 3.99 (s, 2H), 2.27 (m, 1H), 0.96 (s, 3H), 0.95 (s, 3H). ^{13}C NMR (100 MHz, $CDCl_3$) ™ 144.3, 130.3, 130.0, 124.1, 120.1, 36.1, 31.1, 22.2. HRMS (Q-TOF): *m/z* calc for $C_{13}H_{16}N_4S$ [M + H]: 261.1174; found 261.1174.

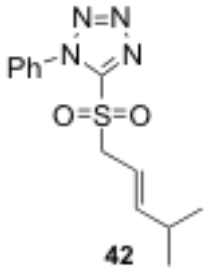

42

(*E*)-5-(4-methylpent-2-enylsulfonyl)-1-phenyl-1*H*-tetrazole 42:

To a 250 mL flask containing **41** (5.15 g, 0.20 mol), was added EtOH (60 mL), and H_2O_2 (67 mL, 0.594 mol). To this was added ammonium heptamolybdate tetrahydrate (4.89 g, 0.004 mol) and the reaction stirred overnight. Once complete the reaction was diluted with H_2O (100 mL), cooled to 0 ^oC, and slowly quenched with sodium thiosulfate until bubbling ceased and the reaction turned blue. The reaction was added to a separatory funnel and extracted 3x 200 mL EtOAc. The organic layer was dried with $MgSO_4$, filtered, and concentrated. The crude material was purified by column chromatography using 1:3 EtOAc:Hexanes to obtain pure **42** (5.70 g, 98 % yield). ^1H NMR (400 MHz, $CDCl_3$) ™ 7.62 (m, 5H), 5.92 (dd, *J* = 6.8, 15.6 Hz, 1H), 5.44 (m, 1H), 4.37 (d, *J* = 7.6 Hz, 2H), 2.33 (m, 1H), 0.98 (s, 3H), 0.96 (s, 3H). ^{13}C NMR (100 MHz, $CDCl_3$) ™ 151.8, 131.4, 129.6, 125.1, 110.0, 59.8, 31.3, 21.5. HRMS (Q-TOF): *m/z* calc for $C_{13}H_{16}N_4O_2S$ [M + H]: 293.1072; found 293.1080.

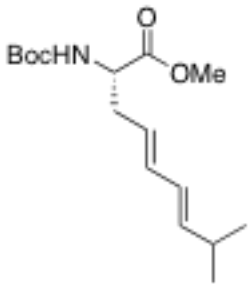

(*S*,4*E*,6*E*)-methyl 2-(*tert*-butoxycarbonylamino)-8-methylnona-4,6-dienoate

scheme 8:

A 250 mL shlenck flask with solid KHMDS (2.46 g, 0.0123 mol) was vacuum purged 3x with argon, anhydrous DMF was then added (80 mL), and cooled to -78 ^{o}C. A solution of **42** (3.08 g, 0.0105 mol) in anhydrous DMF (20 mL) was added over 10 min. and the reaction stirred at -78 ^{o}C for 5 min. A solution of aldehyde **38** (2.03 g, 0.0088 mol) in anhydrous DMF (20 mL) was added over 10min. and the reaction was stirred and allowed to warm to room temperature overnight. Once complete the reaction was quenched with H_2O (250 mL) and added to a separatory funnel with EtOAc (400 mL). The layers were separated and the water layer extracted 2x 250 mL EtOAc. The organic layer was then washed with 500 mL saturated brine solution, dried with $MgSO_4$, filtered, and concentrated. The crude material was purified by column chromatography using 1:3 EtOAc:Hexanes to obtain pure **8** (1.83 g, 70 % yield). To obtain mainly the trans diene, the pure material was dissolved in Et_2O (100 mL), and a catalytic amount of I_2 (50 mg) was added, this was then refluxed utilizing UV light overnight to furnish the desired material in quantitative yield. ^{1}H NMR (400 MHz, $CDCl_3$) ™ 6.21 (m, 2H), 5.70 (m, 2H), 4.37 (m, 1H), 3.72 (s, 3H), 2.71 (m, 1H),

2.50 (m, 1H), 2.33 (m, 1H), 1.42 (s, 9H), 1.04 (s, 3H), 1.01 (s, 3H). ^{13}C NMR (100 MHz, $CDCl_3$) ™ = 172.3, 154.4, 143.3, 137.2, 129.7, 129.4, 79.4, 54.6, 49.9, 36.0, 32.2, 28.1, 21.7. HRMS (Q-TOF): *m/z* calc for $C_{16}H_{28}NO_4$ [M + H]: 299.2052; found 299.2048.

Representative experimental for the synthesis of (*3R,5S*)-1-(allooxycarbonyl)-5-chloropiperazine-3-carboxylic acid (*N*-Alloc-(*R,S*)-γ-ClPip) 25:

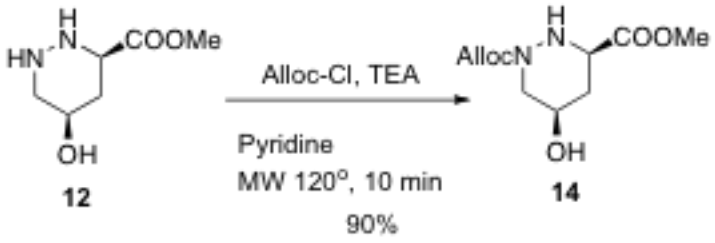

Weighed **12** (116 mg, 0.724 mmol) into a 5 mL microwave vial and dissolved in 4 ml pyridine, and cooled to 0 °C. Slowly added allyl chloroformate (154 □L, 1.45 mmol) via pipette. The MW vial was then capped and heated to 120 °C for 10 min. The reaction was added to an addition funnel with 100 ml sat. $NaHCO_3$ and 100 ml EtOAc, the layers were separated and extracted with an additional 100 ml EtOAc. The organic layers were washed with 100 ml brine, dried over $MgSO_4$ and concentrated. The crude material was purified via silica chromatography with EtOAc:Hexanes 1:3 to 1:2 gradient. The fractions were concentrated to a light brown oil to afford pure **14** (130 mg, 74%). ^{1}H-NMR (400 MHz, $CDCl_3$) δ 5.94 (m, 1H), 5.33 (d, *J* = 17.2 Hz, 1H), 5.25 (d, *J* = 10.4 Hz, 1H), 4.65 (d, *J* = 6.0

Hz, 2H), 4.07 (m, 1H), 3.87 (m, 1H), 3.78 (s, 3H), 3.15 (m, 1H), 2.36 (m, 1H), 1.76 (m, 1H). ^{13}C-NMR (100 MHz, $CDCl_3$) δ = 171.4, 155.4, 132.7, 118.4, 77.5, 67.1, 64.7, 57.1, 52.8, 51.4. LC/MS = 1.404.

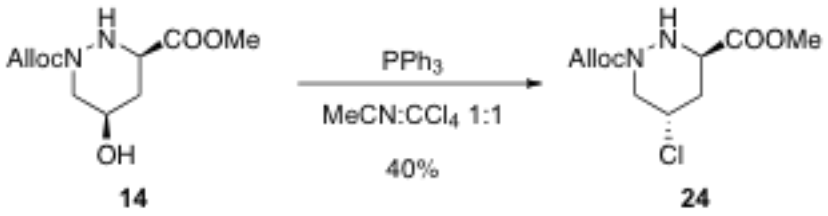

14 **24**

Weighed **14** (50 mg, 0.205 mmol) into a 25 mL r.b. flask, dissolved in 5 mL 1:1 ACN:CCl_4, and cooled to 0 ^{o}C. Triphenylphosphine (81 mg, 0.307 mmol) was then added all at once. The reaction was allowed to reach r.t. and stirred overnight. Once complete the reaction was concentrated *in situ* and purified via column chromatography with EtOAc:Hexanes 1:1. The fractions were concentrated to a clear oil to afford pure **24** (54 mg, 40%). ^{1}H-NMR (400 MHz, $CDCl_3$) δ 5.91 (m, 1H), 5.31 (d, *J* = 17.2 Hz, 1H), 5.21 (d, *J* = 10.4 Hz, 1H), 4.65 (d, *J* = 7.6 Hz, 2H), 4.33 (m, 1H), 4.02 (m, 2H), 3.73 (s, 3H), 3.69 (m, 1H), 2.21 (m, 2H). ^{13}C-NMR (100 MHz, $CDCl_3$) δ = 171.0, 155.7, 132.6, 118.2, 71.8, 67.0, 53.8, 52.6, 50.9, 35.8. LC/MS = 2.431.

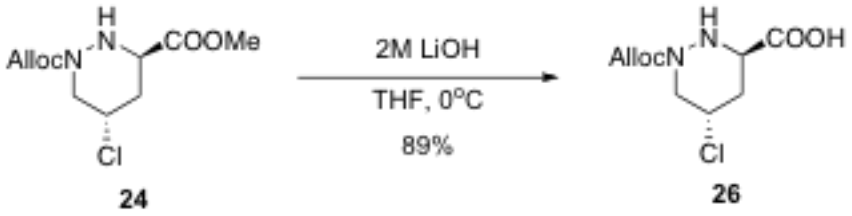

24 **26**

Weighed **24** (65 mg, 0.247 mmol) into a 5 mL r.b. flask, dissolved in THF, and cooled to 0 °C. Slowly added 140 □L of 2M LiOH viapipette and stirred for 20 min. The reaction was acidified to pH 3 with 2M HCl, and extracted 2x with 25 ml EtOAc. The organic layers were washed with 50 ml brine, dried over $MgSO_4$ and concentrated to a light yellow oil which needed no purification (55 mg, 90%). ^{1}H-NMR (400 MHz, $CDCl_3$) δ 5.92 (m, 1H), 5.32 (d, *J* = 17.2 Hz, 1H), 5.25 (d, *J* = 10.4 Hz, 1H), 4.65 (m, 2H), 4.20 (m, 1H), 4.02 (m, 1H), 3.90 (m, 1H), 3.75 (m, 1H), 2.49 (m, 1H), 2.20 (m, 1H) . ^{13}C-NMR (100 MHz, $CDCl_3$) δ = 173.0, 155.5, 132.6, 118.9, 77.5, 72.1, 67.6, 52.1, 51.2, 35.3. LC/MS = 2.106.

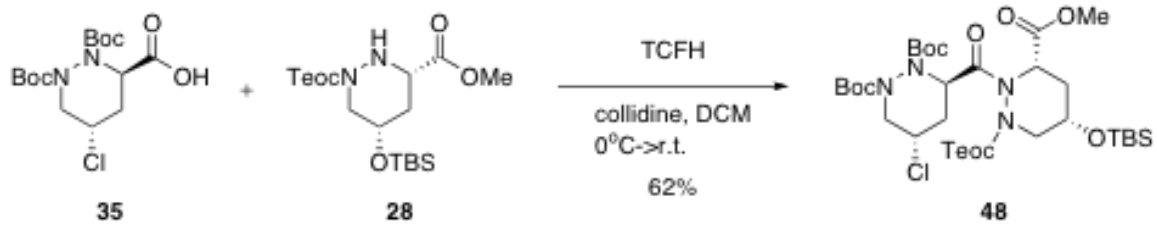

35 **28** **48**

A flame-dried 50ml flask outfitted with a stirbar was charged with acid **35** (160 mg, 0.439 mmol), and amine **28** (184 mg, 0.439 mmol) was vacuum purged 3x with argon. DCM (10 mL) followed by collidine (175 □L, 1.32 mmol) was added and the reaction stirred until homogeneous. Freshly made TCFH (246 mg, 0.878 mmol) was added all at once and the reaction stirred overnight. Once

determined complete by LC/MS and TLC the reaction was quenched with H_2O and $NaHCO_3$ and extracted with DCM 3x. The organic layer was dried with $MgSO_4$, filtered and concentrated to afford the crude material which was purified by silica gel chromatography (EtOAc:Hex 1:3) to afford pure **48** in 62% yield (207mg, 0.272mmol). ^{1}H NMR (400 MHz, $CDCl_3$) δ5.15 (m, 1H), 5.10m, 1H), 4.27 (m, 1H), 4.10 (m, 2H), 4.00 (m, 1H), 3.67 (s, 3H), 2.92 (m, 1H), 2.50 (m, 1H), 2.22 (m, 1H), 1.78 (m, 2H), 1.60 (m, 2H), 1.59 (s, 3H), 1.44 (s, 3H), 1.42 (s, 18H), 1.30 (m, 2H), 1.06 (m, 1H), 0.90 (s, 9H), 0.05 (s, 9H). ^{13}C NMR (100 MHz, $CDCl_3$) δ = 170.4, 155.8, 153.2, 81.8, 64.9, 63.5, 51.9, 49.6, 48.8, 34.5, 31.7, 30.3, 29.7, 28.3, 26.9, 25.7, 25.3, 22.6, 20.7, 18.3, 14.1, -1.6, -5.1. HRMS (Q-ToF): *m/z* calc for $C_{33}H_{61}N_4O_{10}NaSi_2Cl$ [M + Na] 787.3528, found 787.3512.

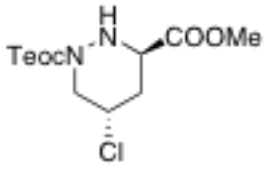

29

(3*R*,5*S*)-3-methyl 1-(2-(trimethylsilyl)ethyl) 5-chloropiperazine-1,3-dicarboxylate 29:

Weighed teoc-protected **14** (1.23 g, 0.004 mol) into a 250 mL r.b. flask, dissolved in 50 mL 1:1 ACN:CCl_4, and cooled to 0 °C. Triphenylphosphine (2.12 g, 0.0.0081 mol) was then added all at once. The reaction was allowed to reach room temperature and stirred overnight. Once complete the reaction was concentrated *in situ* and purified via column chromatography with

EtOAc:Hexanes 1:1. The fractions were concentrated to a clear oil to afford pure **29** (0.52 g, 40%). ^{1}H NMR (400 MHz, $CDCl_3$) δ=4.42 (m, 1H), 4.28 (m, 2H), 3.88 (m, 1H), 3.81 (s, 3H), 3.63 (m, 1H), 3.08 (m, 1H), 2.62 (m, 1H), 1.92 (m, 1H), 1.07 (m, 2H), 0.06 (s, 9H). HRMS (Q-ToF): *m/z* calc for $C_{12}H_{24}N_2O_4ClSi$ [M + H], 323.1194; found 323.1192.

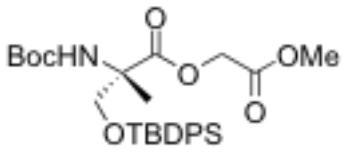

47

(*S*)-2-methoxy-2-oxoethyl 2,2,6,10,10-pentamethyl-8-oxo-3,3-diphenyl-4,9-dioxa-7-aza-3-silaundecane-6-carboxylate 47:

To a 250 mL round bottom flask containing **46** (345 mg, 0.754 mmol) and methyl glycolate (60 mg, 0.90 mmol) was added a solution of 9:1 DCM:collidine (30 mL). Diisopropylcarbodiimide (190 mg, 1.51 mmol) was added all at once and the reaction stirred overnight. Once complete the reaction was quenched with 2M citric acid (50 mL) and extracted with 3 x 30 mL DCM. The organic layer was dried with $MgSO_4$, filtered, and concentrated. The crude material was purified via column chromatography using 1:1 EtOAc:Hexanes to obtain pure **47** (380 mg, 95 % yield). ^{1}H NMR (400 MHz, DMSO-d_6) δ=7.62 (m, 4H), 7.44 (m, 6H), 7.34 (br s, 1H), 4.63 (s, 2H), 3.76 (m, 2H), 3.64 (s, 3H), 1.46 (s, 3H), 1.38 (s, 9H), 1.00 (s, 9H). ^{13}C NMR (100 MHz, $CDCl_3$) δ = 172.4, 167.7, 154.5, 135.5, 133.0, 129.7,

127.7, 79.5, 66.2, 61.1, 52.1, 28.3, 26.7, 20.0, 19.2. HRMS (Q-ToF): *m/z* calc for $C_{28}H_{39}NO_7Si$ [M + H], found.

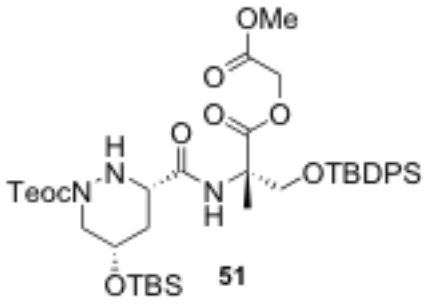

51

(3*S*,5*S*)-2-(trimethylsilyl)ethyl 5-(*tert*-butyldimethylsilyloxy)-3-((*S*)-7,11,11-trimethyl-3,6-dioxo-10,10-diphenyl-2,5,9-trioxa-10-siladodecan-7-ylcarbamoyl)piperazine-1-carboxylate 51:

To a 25 mL round bottom flask was added amine **50** (100 mg, 0.215 mmol), acid **23** (87 mg, 0.215 mmol), HOAt (59 mg, 0.430 mmol), and vacuum purged 3x with argon. The solid material was dissolved in a solution of 9:1 DCM:collidine (3 mL), and cooled to 0 ^{o}C. Solid HATU (164 mg, 0.43 mmol) was added all at once and the reaction allowed to warm to room temperature overnight. Once complete the reaction was concentrated *in situ* then dissolved in EtOAc (50 mL) and 1N HCl (50 mL). The organic layer was extracted with 2 x 50 mL EtOAc, the combined organic layers were washed with saturated sodium bicarbonate (50 mL) and then saturated brine (50 mL). The organic layer was dried with $MgSO_4$, filtered and concentrated. The crude material was purified via column chromatography using 2:3 EtOAc:Hexanes to afford **51** (60 mg, 34 % yield). ^{1}H

NMR (400 MHz, $CDCl_3$) δ=7.60 (m, 4H), 7.41 (m, 6H), 4.20 (m, 2H), 4.11 (m, 1H), 4.04 (m, 1H), 3.88 (m, 1H), 3.71 (s, 3H), 3.68 (m, 1H), 3.39 (m, 1H), 2.75 (m, 1H), 2.27 (m, 1H), 1.62 (m, 1H), 1.53 (s, 3H), 1.04 (s, 9H), 0.08 (s, 3H), 0.06 (s, 3H), 0.03 (s, 9H). HRMS (Q-ToF): *m/z* calc for $C_{40}H_{66}N_3O_9Si_3$ [M + H] 816.4107; found 816.4101.

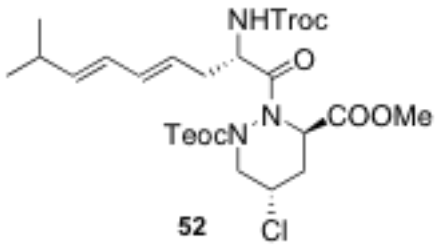

52

(3*R*,5*S*)-3-methyl 1-(2-(trimethylsilyl)ethyl) 5-chloro-2-((*S*,4*E*,6*E*)-8-methyl-2-((2,2,2-trichloroethoxy)carbonylamino)nona-4,6-dienoyl)piperazine-1,3-dicarboxylate 52:

A 50 mL shlenck flask with amine **29** (130 mg, 0.403 mmol), and acid **44** (144 mg, 0.403 mmol) was purged 3x with argon. The solid material was dissolved in a solution of 9:1 DCM:collidine (5 mL), and cooled to 0 ^oC. Solid tetramethylchloroformamidinium hexafluorophosphate (452 mg, 1.61 mmol) was added all at once and the reaction stirred overnight. Once complete the reaction was quenched with H_2O (20 mL) and DCM (20 mL). The reaction was added to a separatory funnel and the organic layer separated. The water layer was extracted with 2 x 20 mL DCM, the combined organic layers were dried with

$MgSO_4$, filtered, and concentrated. The crude material was purified via column chromatography with 1:3 EtOAc:Hexanes to afford **52** (130 mg, 49 % yield).

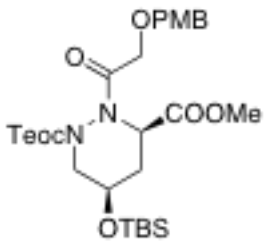

55

(3*R*,5*R*)-3-methyl 1-(2-(trimethylsilyl)ethyl) 5-(*tert*-butyldimethylsilyloxy)-2-(2-(4-methoxybenzyloxy)acetyl)piperazine-1,3-dicarboxylate 55:

Weighed amine **27** (250 mg, 0.597 mmol) into 100 mL shlenck flask and and vacuum purged 3x with argon. Dissolved in anhydrous DCM (20 mL) then added collidine (217 mg, 1.79 mmol), and **54** (117 mg, 0.597 mmol). Once dissolved solid tetramethylchloroformamidinium hexafluorophosphate (335 mg, 1.19 mmol) was added all at once and the reaction was stirred overnight. Once complete the reaction was added to a separatory funnel containing Et_2O (150 mL) and H_2O (150 mL), and extracted 2 x 100 mL Et_2O. The combined organic extracts were washed with saturated brine (250 mL), dried with $MgSO_4$, filtered, and concentrated. The crude material was purified via column chromatography using 1:2 EtOAc:Hexanes to afford pure **55** (311 mg, 87 % yield).

^{1}H NMR (400 MHz, $CDCl_3$) δ=7.28 (d, *J* = 8.0 Hz, 2H), 6.86 (d, *J* = 8.0 Hz, 2H), 5.37 (br s, 1H), 4.56 (m, 2H), 4.21 (m, 4H), 3.93 (m, 1H), 3.79 (s, 3H), 3.67 (s,

2H), 2.85 (m, 1H), 2.36 (m, 1H), 1.01 (m, 2H), 0.87 (s, 9H), 0.84 (s, 3H), 0.06 (s, 3H), 0.04 (s, 9H). ^{13}C NMR (100 MHz, $CDCl_3$) δ = 171.6, 168.3, 159.7, 157.7, 130.1, 129.3, 117.9, 72.2, 70.4, 69.3, 67.2, 64.4, 62.0 55.4, 51.8, 37.2, 30.8, 26.3, 22.5, 1.7, -1.8. HRMS (Q-ToF): *m/z* calc for $C_{28}H_{48}N_2O_8NaSi_2$ [M + Na] 619.2847; found 619.2850.

References

1. Miller, E.D.; Kauffman, C.A.; Jensen, P.R.; Fenical, W. *J. Org. Chem.* **2007**, *72*, 323-330.

2. Makino, K.; Jiang, H.; Suzuki, T.; Hamada, Y. *Tetrahedron: Asymmetry* **2006**, 17,1644–1649.

3. Ushiyama, R.; Yonezawa, Y.; Shin, C. *Chem. Lett.* **2001**, 11, 1172–1173.

4. Kamenecka, T. M.; Danishefsky, S. J. Chem. A. Eur J. 2001, 7, 41–63.

5. Depew, K. M.; Kamenecka, T. M.; Danishefsky, S. J. *Tetrahedron Lett.* **2000**, 41, 289–292.

6. Kamenecka, T. M.; Danishefsky, S. J. *Angew. Chem., Int. Ed.* **1998**, 37, 2995–2998.

7. Hale, K. J.; Jogiya, N.; Manaviazar, S. *Tetrahedron Lett.* **1998**, 39, 7163–7166.

8. Hassall, C. H.; Ramachandran, K. L. *Heterocycles* **1977**, 7, 119–122.

9. Shipe, W. D.; Yang, F.; Zhao, Z.; Wolkenberg, S. E.; Nolt, M. B.; Lindsley, C. W. *Heterocycles* **2006**, 70, 665–689.

10. Daniels, R. N.; Kim, K.; Lewis, J. A.; Lebois, E. P.; Muchalski, H.; Lindsley, C. W. *Tetrahedron Lett.* **2008**, 49, 305–310.

11. Blakemore, P.R.; Cole, W.J.; Kocienski, P.J.; Morley, A. *Synlett*, **1998**, 26-28.

12. Blakemore, P.R.; Ho, D.K.H.; Nap, W.M. *Org. Biomol. Chem.*, **2005**, 3, 1365-1368.

13. Pospisil, J.; Marko, I.E. *Org. Lett.*, **2006**, 8, 5983-5986.

14. Li, W.; Gan, J.; Ma, D. *Angew. Chem. Int. Ed.,* **2009**, 48, 8891-8895.

15. Cavelier, F.; Enjalbal, C. *Tet. Lett.*, **1996**, 37, 5131-5134.

16. Oelke, A. J.; France, D.J.; Hofmann, T.; Wuitschik, G.; Ley, S.V. *Angew. Chem. Int. Ed.*, **2010**, 49, 1-5.

17. Toye J.; Ghosez, L. *J. Am. Chem. Soc.*, 97, **1975**, 2276.

18. All tables and portions of text previously published are used with consent from the publisher.